

DESIGN METHODS FOR PLANAR AND SPATIAL DEPLOYABLE  
STRUCTURES

A THESIS SUBMITTED TO  
THE GRADUATE SCHOOL OF NATURAL AND APPLIED SCIENCES  
OF  
MIDDLE EAST TECHNICAL UNIVERSITY

BY

GÖKHAN KİPER

IN PARTIAL FULFILLMENT OF THE REQUIREMENTS  
FOR  
THE DEGREE OF DOCTOR OF PHILOSOPHY  
IN  
MECHANICAL ENGINEERING

AUGUST 2011

Approval of the thesis:

**DESIGN METHODS FOR PLANAR AND SPATIAL DEPLOYABLE  
STRUCTURES**

submitted by **GÖKHAN KİPER** in partial fulfillment of the requirements for  
the degree of **Doctor of Philosophy in Mechanical Engineering Department,**  
**Middle East Technical University** by,

Prof. Dr. Canan Özgen \_\_\_\_\_  
Dean, Graduate School of **Natural and Applied Sciences**

Prof. Dr. Suha Oral \_\_\_\_\_  
Head of Department, **Mechanical Engineering**

Prof. Dr. Eres Söylemez \_\_\_\_\_  
Supervisor, **Mechanical Engineering Dept., METU**

**Examining Committee Members:**

Prof. Dr. Mehmet Çalışkan \_\_\_\_\_  
Dept. of Mechanical Engineering, METU

Prof. Dr. Eres Söylemez \_\_\_\_\_  
Dept. of Mechanical Engineering, METU

Prof. Dr. Mustafa Kemal Özgören \_\_\_\_\_  
Dept. of Mechanical Engineering, METU

Assoc. Prof. Dr. Ali Ulaş Özgür Kişisel \_\_\_\_\_  
Dept. of Mathematics, METU-NCC

Dr. Volkan Parlaktaş \_\_\_\_\_  
Dept. of Mechanical Engineering, Hacettepe University

**Date:** 12.08.2011

**I hereby declare that all information in this document has been obtained and presented in accordance with academic rules and ethical conduct. I also declare that, as required by these rules and conduct, I have fully cited and referenced all material and results that are not original to this work.**

Name, Last name : Gökhan Kiper

Signature :

# **ABSTRACT**

## **DESIGN METHODS FOR PLANAR AND SPATIAL DEPLOYABLE STRUCTURES**

Kiper, Gökhan

Ph.D., Mechanical Engineering Department

Supervisor : Prof. Dr. Eres Söylemez

August 2011, 146 pages

This thesis study addresses the problem of overconstraint via introduction of conformal polyhedral linkages comprising revolute joints only and investigation of special geometric properties for the mobility of such overconstrained linkages. These linkages are of particular interest as deployable structures. First, planar case is issued and conditions for assembling irregular conformal polygonal linkages composed of regular and angulated scissor elements are derived. These planar assemblies are implemented into faces of polyhedral shapes and radially intersecting planes to obtain two different kind of polyhedral linkages. Rest of the thesis work relates to spatial linkages. Identical isosceles Bennett loops are assembled to obtain regular polygonal linkages and many such linkages are assembled to form polyhedral linkages. Then, Fulleroid-like linkages are presented. After these seemingly independent linkage types, Jitterbug-like linkages are introduced. Based on some observations on present linkages in the literature a definition for Jitterbug-like linkages is given first, and then a set of critical properties of these linkages are revealed. This special type of polyhedral linkages is further

classified as being homothetic and non-homothetic, and geometric conditions to obtain mobile homothetic Jitterbug-like polyhedral linkages are investigated. Homohedral linkages, linkages with polyhedral supports with 3- and 4-valent vertices only, tangential polyhedral linkages are detailed as special cases and the degenerate case where all faces are coplanar is discussed. Two types of modifications on Jitterbug-like linkages are presented by addition of links on the faces and radial planes of Jitterbug-like linkages. Finally, a special class of Jitterbug-like linkages - modified Wren platforms are introduced as potential deployable structures.

Keywords: Deployable Structures, Conformal Polyhedral Linkages, Jitterbug-like Linkages

# ÖZ

## DÜZLEMSEL VE UZAYSAL KATLANABİLİR YAPILAR İÇİN TASARIM YÖNTEMLERİ

Kiper, Gökhan

Doktora, Makina Mühendisliği Bölümü

Tez Yöneticisi: Prof. Dr. Eres Söylemez

Ağustos 2011, 146 sayfa

Bu tez çalışması yalnızca döner eklemler içeren ve fazla kısıtlı olan konformal çokyüzlü mekanizmalarının elde edilebilmesi için gerekli geometrik koşulların araştırılarak fazla-kısıtlılık probleminin bu mekanizmalar özelinde çözümünü hedeflemektedir. Bu mekanizmalar uygulamada katlanabilir yapılar olarak kullanılabilirler. Öncelikle düzlemsel durum incelenmekte, bayağı ve açılı makas elemanlarından oluşan düzgün olmayan konformal çokgen mekanizmalarını elde etmek için gerekli koşullar çıkarılmıştır. Bu düzlemsel kinematik zincirler çokyüzlü şekillerin yüzlerine ya da radyal olarak kesişen düzlemlere yerleştirilip montaj yapılarak iki tip çokyüzlü mekanizması elde edilmiştir. Tez çalışmasının geri kalanı uzaysal mekanizmalar üzerinedir. İlk önce özdeş eşkenar Bennett devreleri birbirlerine monte edilerek düzgün çokgen mekanizmaları ve bu şekildeki pek çok kinematik zincir birleştirilerek çokyüzlü mekanizmaları elde edilmiştir. Daha sonra Fulleroid-tipi mekanizmalar sunulmuştur. Bu özgün mekanizmalardan sonra Jitterbug-tipi mekanizmalar işlenmiştir. Literatürde mevcut mekanizmalar üzerine bazı

gözlemler temel alınarak Jitterbug-tipi mekanizmalar için bir tanım verildikten sonra bu tip mekanizmaların bazı önemli özellikleri çıkarılmıştır. Bu özel tip çokyüzlü mekanizmaları homotetik ve homotetik olmayan olarak iki sınıfa ayrılmış ve homotetik Jitterbug-tipi çokyüzlü mekanizmaları elde etmek için gerekli geometrik koşullar araştırılmıştır. Homohedral mekanizmalar, her köşesinde 3 veya her köşesinde 4 yüz birleşen çokyüzlü geometrisine sahip mekanizmalar ve teğetsel çokyüzlü mekanizmaları özel durumlar olarak ayrıntılı olarak incelenmiş ve dejenere durum olarak tüm yüzlerin bir düzlemde olduğu durum tartışılmıştır. Jitterbug-tipi mekanizmalardan yüzlere ve radyal düzlemlere uzuv eklenmesi şeklinde iki çeşit modifikasyon ile elde edilen yeni mekanizmalar sunulmuştur. Son olarak özel bir Jitterbug-tipi sınıfı olan değiştirilmiş Wren platformları potansiyel katlanabilir yapılar olarak önerilmiştir.

Anahtar kelimeler: Katlanabilir Yapılar, Konformal Çokyüzlü Mekanizmaları, Jitterbug-tipi Mekanizmalar

## **ACKNOWLEDGMENTS**

The author is most sincerely grateful to his supervisor Prof. Dr. Eres Söylemez for being such a great example of a fine engineer, for being available whenever needed sparing all his resources and his fatherly sympathy.

The author also would like to gratefully thank Prof. Dr. Bahram Ravani of University of California Davis, Prof. Dr. Chintien Huang of National Cheng Kung University and all Advanced Highway Maintenance and Construction Technology Research Center staff at University of California Davis for their hospitality and guidance during the sabbatical period in 2010; Assoc. Prof. Dr. A. U. Özgür Kişisel of Middle East Technical University (METU), Northern Cyprus Campus and Prof. Dr. Kemal Özgören of METU for their guidance as members of thesis progress committee; Prof. Dr. Karl Wohllhart and Prof. Dr. Otto Röschel of Graz University of Technology, Prof. Dr. Manfred Husty, Asst. Prof. Dr. Hans-Peter Schröcker and Dr. Martin Pfurner of University of Innsbruck and Prof. Dr. Hellmuth Stachel of Vienna University of Technology for their valuable council; and finally all staff of Department of Mechanical Engineering of METU for their support and encouragement.

The financial support supplied by the Scientific and Technological Research Council of Turkey and METU for the doctoral education and by the Council of Higher Education for the sabbatical period in University of California Davis is gratefully acknowledged.



## TABLE OF CONTENTS

ABSTRACT .....	iv
ÖZ .....	vi
ACKNOWLEDGMENTS .....	viii
TABLE OF CONTENTS .....	ix
LIST OF FIGURES .....	xiii
CHAPTER	
1. INTRODUCTION .....	1
1.1 Overconstrained Linkages .....	3
1.2 Conformal Polyhedral Linkages .....	5
2. IRREGULAR POLYGONAL AND POLYHEDRAL LINKAGES COMPRISING REGULAR AND ANGULATED SCISSOR ELEMENTS .....	9
2.1 The Cardan Motion and Angulated Elements .....	13
2.2 Assembling Angulated Elements for Polygonal Deployment .....	15
2.3 Addition of Regular Scissor Elements .....	18
2.4 Polyhedral Linkages .....	19
3. POLYHEDRAL LINKAGES SYNTHESIZED USING CARDAN MOTION ALONG RADIAL AXES .....	22
4. REGULAR POLYHEDRAL AND REGULAR SPHERICAL POLYHEDRAL LINKAGES COMPRISING BENNETT LOOPS ...	32



7. MODIFICATIONS ON JITTERBUG-LIKE LINKAGES .....	92
7.1 Addition of Links on the Faces of Jitterbug-Like Linkages .....	92
7.1.1 Cardan Motion Associated with the Polygonal Links .....	93
7.1.2 Attaching Links to Jitterbug-Like Linkages - Examples ..	95
7.1.3 Obtaining New Linkages by Removing Some Links and Joints .....	100
7.2 Addition of Links on Radial Planes of Jitterbug-Like Linkages ..	104
7.2.1 An Observation .....	104
7.2.2 Relating the Cardan Motion With Elliptic Paths of Polygonal Links .....	106
7.2.3 Polyhedral Linkages .....	109
8. MODIFIED WREN PLATFORMS .....	116
8.1 Self Motions of Parallel Manipulators and Wren Platforms .....	116
8.2 3-UPU Parallel Manipulators .....	118
8.3 Jitterbug-Like Linkages .....	119
8.4 Modifications on the Verheyen Platform .....	120
8.4.1 Cylindrical Platforms .....	120
8.4.2 General Parallel Leg Configuration .....	122
8.4.3 Conical Platforms .....	123
8.4.4 Other Joint Configurations .....	125
8.5 Use of Modified Wren Platforms as Deployable Structures .....	125
9. CONCLUSIONS .....	127
REFERENCES .....	129

APPENDIX

A. Glossary .....	139
CURRICULUM VITAE .....	146

## LIST OF FIGURES

### FIGURES

Figure 1.1	The parallelogram mechanism .....	4
Figure 1.2	The Heureka Octahedron .....	7
Figure 2.1	a) Translational (regular) scissor element and b) the lazy tong mechanism in two configurations .....	10
Figure 2.2	a) Polar scissor element and b) an assembly in two configurations .....	10
Figure 2.3	a) Angulated scissor element and b) an assembly in two configurations .....	11
Figure 2.4	a) The elliptic trammel of Archimedes and b) the two gears of Geronimo Cardano .....	13
Figure 2.5	a) Three points on a moving Cardan circle and b) two such moving planes coupled .....	15
Figure 2.6	a) A quadrilateral and b) its contracted version .....	16
Figure 2.7	A quadrilateral polygonal assembly at its two limiting configurations .....	17
Figure 2.8	Quadrilateral dilation with regular and angulated elements .....	18
Figure 2.9	Additional link for vertex figures .....	19
Figure 2.10	An irregular hexahedral linkage .....	20
Figure 2.11	A deployable tent .....	21
Figure 3.1	An angulated element pair to magnify a triangle ABC .....	22
Figure 3.2	A triangular dissection for the radial magnification of a cube .....	23

Figure 3.3	A cube being magnified .....	24
Figure 3.4	A tetrahedral linkage in two limit configurations .....	25
Figure 3.5	An octahedral linkage in two limit configurations .....	25
Figure 3.6	A dodecahedral linkage in two limit configurations .....	26
Figure 3.7	An icosahedral linkage in two limit configurations .....	26
Figure 3.8	a) Hoberman's (1990) truncated icosahedral linkage in 3 phases and b) Wohlhart's (2004) cubic zig-zag linkage in 2 phases .....	27
Figure 3.9	Another triangular dissection for the radial magnification of a cube .....	28
Figure 3.10	a) Cubic skeleton b) Cube c) Octahedron d) Octahedral skeleton .....	29
Figure 3.11	5 phases of a tetrahedral linkage .....	30
Figure 3.12	4 phases of dodecahedral/icosahedral linkage .....	31
Figure 4.1	The Bennett Loop .....	33
Figure 4.2	A triangular assembly of Bennett loops .....	34
Figure 4.3	An octahedral linkage – in expanded and folded positions .....	36
Figure 4.4	A tetrahedral linkage – in expanded and folded positions .....	37
Figure 4.5	A tetrahedral linkage comprising Bricard loops .....	38
Figure 4.6	Cubic linkage – in expanded position and one of the dofs used ...	39
Figure 4.7	Cuboctahedral linkage – in expanded and folded positions .....	40
Figure 5.1	The Fulleroid in motion .....	43
Figure 5.2	Some cumulations of a cube with unit edge length: A concave icositetrahedron, the cube, the tetrakis hexahedron, the rhombic dodecahedron and another concave icositetrahedron .....	44

Figure 5.3	A concave icositetrahedral linkage (obtained by cumulating the cube inwards by 1/4th of the edge length) .....	45
Figure 5.4	A cubic linkage .....	45
Figure 5.5	A tetrakis hexahedral linkage (obtained by cumulating the cube outwards by 1/4th of the edge length) .....	46
Figure 5.6	A concave icositetrahedral linkage (obtained by cumulating the cube outwards by $1/\sqrt{2}$ <sup>th</sup> of the edge length) .....	46
Figure 5.7	A rhombohedral linkage that has faces with $\sqrt{2}:1$ diagonal ratio .	47
Figure 5.8	A symmetrical spatial 8R closed chain .....	48
Figure 5.9	An octahedral linkage .....	49
Figure 5.10	An octagonal dipyramidal linkage .....	50
Figure 5.11	A stella octangula linkage .....	51
Figure 6.1	Two of Verheyen's (1989) dipolygonids comprising a) 4 double faces (also issued by Stachel (1994) as the Heureka Polyhedron with tetrahedral motion) and b) 6 double faces with overlapping link pairs .....	53
Figure 6.2	a) An octahedral linkage (Röschel, 1996a), b) a cuboctahedral linkage (Verheyen, 1989; Röschel, 1995) and their supporting polyhedra .....	54
Figure 6.3	a) A tetrahedral (Wohlhart, 2001b) and b) a cubic (Kiper, 2009b) linkage with multiple links in a face .....	58
Figure 6.4	a) An offset element and b) a dipolygonid of Verheyen (1989) re-issued as an expandable virus model by Kovács, Tarnai, Fowler and Guest (2004a) .....	58
Figure 6.5	Part of the neighborhood of a vertex (three adjacent faces) and part of the spherical indicatrix (two spherical links) associated with the spatial loop (dashed regions) around this vertex .....	60

Figure 6.6 a) An octahedron with the spherical indicatrices of its vertices, b) The spherical assembly of indicatrices .....	64
Figure 6.7 A polygonal link and its supporting polygon in dilation .....	66
Figure 6.8 Snub disphenoidal linkage, its supporting polyhedron and IRAs of triangular links .....	69
Figure 6.9 Hypothetical CRRC linkage for two adjacent polygonal links ...	71
Figure 6.10 An n-valent vertex figure cut along an edge .....	72
Figure 6.11 Two adjacent polygonal links .....	74
Figure 6.12 A double 3-valent vertex cut along an edge and expanded to the plane and 6 links around it – a) maximal configuration, b) arbitrary configuration .....	80
Figure 6.13 A 3-valent vertex and a loop around it at maximal configuration .	81
Figure 6.14 A tetrahedral linkage with ISA guides .....	82
Figure 6.15 An insphere and two planes of faces tangent to it .....	84
Figure 6.16 A tetrakis hexahedral linkage with ISA guides .....	86
Figure 6.17 A 4-valent vertex and associated parts of the polygonal links around the vertex .....	87
Figure 7.1 An 8R loop around a 4-valent vertex .....	93
Figure 7.2 A double slider mechanism .....	94
Figure 7.3 The Heureka Octahedron with extra links .....	96
Figure 7.4 Tetrahedral dipolygonid with extra links .....	97
Figure 7.5 Cubic dipolygonid with extra links .....	98
Figure 7.6 Linkage obtained from a tetrakis hexahedron .....	99
Figure 7.7 A rhombohedral linkage .....	101



Figure 7.8 A square pyramidal cap linkage .....	101
Figure 7.9 A tetrahedral linkage .....	102
Figure 7.10 A tetrahedral cap linkage .....	103
Figure 7.11 Another tetrahedral cap linkage .....	103
Figure 7.12 The motion of relevant parts of two adjacent polygonal links ....	105
Figure 7.13 A double slider mechanism with a crank attached .....	106
Figure 7.14 The Heureka Octahedron with extra coupler links and cranks ...	110
Figure 7.15 The Heureka Octahedron with extra coupler links .....	111
Figure 7.16 Modified tetrahedral linkage .....	112
Figure 7.17 Modified cubic linkage .....	113
Figure 7.18 Modified tetrakis icositetrahedral linkage .....	114
Figure 7.19 Modified tetrakis icositetrahedral linkage with 24 links removed .....	115
Figure 8.1 a) Single dof mode b) Singular configuration c) Two-dof mode of a 5-leg Wren platform .....	117
Figure 8.2 One of Verheyen's (1989) dihedral dipolygonids .....	119
Figure 8.3 Construction of a cylindrical platform with joint intersections on congruent circles .....	121
Figure 8.4 The translatory motion of a spatial parallelogram mechanism (the joint axes on the platform/base are parallel to the view) .....	123
Figure 8.5 A conical platform .....	124
Figure 8.6 A deployable mast with square polygonal links .....	126

# CHAPTER 1

## INTRODUCTION

The motivation of this thesis study is mostly theoretical: to develop some of understanding on the mysterious mobility of the so-called *overconstrained linkages*. Simply, these linkages are assemblies which are only mobile provided that some special geometric conditions are satisfied. Although there has been vast research on the subject, quite general results on synthesis of these linkages are not yet present. This study also does not address the whole problem, but merely tries to attack a small portion of it.

Among many other fields, these linkages are commonly utilized as *deployable structures* which, by name, imply a contradiction: mobile structures! A deployable structure is a mobile assembly which, as oppose to common applications, does not include motion as an aim, but just to attain certain different configurations at different service conditions - mostly due to compact storage/transfer requirements. So they are designed to serve as structures, but mobility is necessary for the configuration change.

As statically indeterminate structures are generally preferred over determinate ones for their rigidity, usually overconstrained linkages are preferred over simply constrained ones for deployable structure designs. This study aims to attack the design of overconstrained linkages problem in terms of deployable structures. Although most of the presented material provides broader results than just for deployable structures, it should be emphasized that all of the problems were constructed keeping the deployable structures in mind.

Similarly, although in most sections overconstrainedness is not mentioned at all, the subject linkages are always overconstrained.

When design of structures is of concern, the main contributors are civil engineers and architects. Naturally there is a lack of profession for these disciplines when it is required to mobilize structures. So mechanical engineers have been and are still trying to help deployable structure designers regarding kinematics aspects. This study is a part of this effort.

Still as a particular portion of the problem, only specific types of deployable structures are kept in focus. First of all, only the deployable structures with - theoretically - rigid links and joints are considered. For the sake of further simplicity, only geometries with linear boundaries are dealt with – corresponding planar linkages are called *polygonal linkages* and spatial linkages are called *polyhedral linkages*. Finally as a further subclass, assemblies with pivots only are taken into consideration. Despite these specializations such assemblies constitute most of the deployable structures present in mankind's life.

In the remaining sections of this chapter, some related studies on the problem are presented: In Section 1.1 is a brief review of overconstrained linkages and in Section 1.2 is about polyhedral linkages. Chapters 2 and 3 are built upon the studies of Kiper (2006): Chapter 2 introduces a methodology to deploy irregular polygonal and polyhedral shapes; Chapter 3 is application of the method in (Kiper, 2006) to radial planes in order to obtain polyhedral linkages. Chapters 4 and 5 are rather independent from the rest of the thesis: Chapter 4 is on how to assemble Bennett linkages to obtain polyhedral linkages; Chapter 5 is on a heuristic method to obtain new linkages from a specific polyhedral linkage. Chapter 6 bears the core material of the thesis – it introduces Jitterbug-

like linkages, presents some of their properties and finally states a series of theorems about Homothetic Jitterbug-like linkages. Chapters 7 and 8 are mainly on application of planar methods of (Kiper, 2006) to the Jitterbug-like linkages of Chapter 6. Chapter 9 deals with Jitterbug-like linkages that can be used as parallel platforms. The last chapter is for conclusions and discussions. A glossary is given in Appendix A for definitions of some terms appearing in the text that may be unfamiliar to the reader.

## 1.1 Overconstrained Linkages<sup>1</sup>

Determining the degrees of freedom (dof) is the very first step in analyzing a mechanism. There are several formulations for determination of dof of mechanisms. Gogu (2008) lists about 36 different formulations starting with Chebychev, Sylvester, Grübler and so on. Today, the most well known and thought formula are known as the Chebychev-Grübler-Kutzbach (CGK) formula:

$$M = \lambda(\ell - j - 1) + \sum f_i$$

where  $\lambda$  is dof of space,  $\ell$  is the number links,  $j$  is the number of joints and  $\sum f_i$  is the connectivity sum for which each  $f_i$  represents the dof of  $i^{\text{th}}$  joint. This formula does not take metric properties into account and does not work for some mechanisms which satisfy special geometric conditions. Accordingly, Hervé (1978) classifies mechanisms into three groups: trivial, exceptional and paradoxical. Trivial mechanisms satisfy the CGK formula and the other two

---

<sup>1</sup> Although the terms mechanism and linkage can be used interchangeably according to some authors, for example Waldron & Kinzel (2004), generally a linkage is a kinematic chain with lower kinematic pairs only (see ex. Hunt (1979)). This second definition is adopted in this thesis.

types do not due to special metric conditions. In this study, exceptional and paradoxical mechanisms are not distinguished, but any mechanism that does not satisfy the CGK formula is classified as an overconstrained mechanism.

The first overconstrained linkage in literature is the parallelogram mechanism by De Roberval - 1669 as mentioned in Gogu (2008). The parallelogram mechanism consists of a fixed and a floating link which are similar and at least two identical cranks connecting these two (Fig. 1.1.). When there are more than two cranks CGK formula gives non-positive dof, while the actual dof is 1.

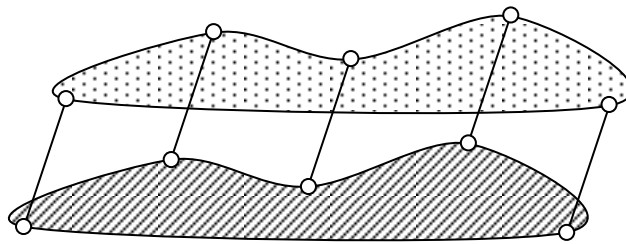


**Figure 1.1** The parallelogram mechanism

Planar overconstrained linkages do not make much of an interest in the related literature. The significant single loop spatial overconstrained linkages are due to Sarrus (1853), Bricard (1897), Delassus (1900, 1902, 1922), Bennett (1903), Myard (1931), Goldberg (1943), Altmann (1954), Dimernberg and Yoslovich (1966), Waldron (1967, 1968, 1969, 1979), Schatz (1975), Baker (1978), Wohlhart (1987, 1991), Dietmaier (1995), Mavroidis and Roth (1995), Fang and Tsai (2004), Pfulner (2009).

Recently many multi-loop overconstrained linkages were devised, mainly regarding two fields – parallel robots and polyhedral linkages. Polyhedral linkages are thoroughly investigated in the following section, but references for parallel robots related studies are made whenever necessary.

## 1.2 Conformal Polyhedral Linkages<sup>2</sup>

Just as a thorough understanding in plane kinematics necessitates a good knowledge on polygons and circles, in order to study spatial kinematics, one needs to master the geometry of polyhedra and the sphere. The passage from spatial rigid structures to mobile ones lies in the question of which polyhedra are rigid and which are movable. First results on this matter are due to Bricard (1987), Bennett (1911) and Goldberg (1942), who defines a polyhedral linkage as a space linkage made entirely of rigid flat plates hinged together. As indicated by Bricard (1987), these studies address the answer to the question “Do there exist polyhedra with invariant faces that are susceptible to an infinite family of transformations that only alter solid angles and dihedrals?”. Recent studies show that there are also mobile assemblies resembling polyhedral shapes where the dihedral and planar angles are preserved. Altogether, these assemblies are called polyhedral linkages.

More precisely, *polyhedral linkages* are used for spatial deployment, where a certain polyhedral shape is to be preserved or a transformation between some polyhedral shapes is required. That is, the links and joints of the linkage enclose a finite volume with planar boundaries - a *supporting polyhedron*. The

---

<sup>2</sup> The introductory part of this section is included (Kiper, 2010a).

supporting polyhedron continuously changes its size/shape via an n-parameter transformation for an n-dof polyhedral linkage. This section is mainly devoted to polyhedral linkages for which dihedral and planar angles are preserved during the shape transformation of the supporting polyhedron. This kind of linkages will be called *conformal polyhedral linkages*.

A conformal transformation applicable to linkages is first described by Buckminster Fuller in 1948 (Fuller, Krausse & Lichtenstein, 1999, p. 32) and the discovered mobile assembly is named as the *Jitterbug*. As described by Fuller (1975), the Jitterbug is a model constructed with 24 struts which constitute 8 triangles able to move with respect to each other. The connections are such that the assembly goes through a single dof transformation. Originally introduced as a conceptual system, the motion of the Jitterbug described in Fig. 460.08 of Synergetics of Fuller (1975) was brought to life as a mobile sculpture in a research exhibition in Zürich and became to known as the Heureka Octahedron (Stachel, 1994).

The Heureka Octahedron comprises 8 ternary, 12 binary links and 24 revolute joints. Although such an assembly generally has  $6(20 - 24 - 1) + 24 = -6$  dofs, this assembly is mobile with single dof. The 3 revolute joint axes of a ternary link are parallel and equidistant while the 2 joint axes of a binary link are intersecting. When the linkage is its most compact form, it resembles a regular octahedron and during the motion the centers of the triangular links remain on the three-fold symmetry axes of a regular octahedron (Figure 1.2). At any configuration, the planes of the triangular faces bound an octahedral region, hence as the linkage expands/contracts, a dilation of an octahedron is realized. The binary links are used to preserve the dihedral angle along the edges of the bounded octahedron.

Although became famous in the Zürich expo in 1991, using revolute joints for the Jitterbug was the idea of Dennis Dreher in 1974 (Edmondson, 2007, p. 192). Many Jitterbug-like linkages were discovered afterwards and Verheyen (1989) classified the so-called dipolygonoids which consist of equilateral polygonal links sliding along and rotating about fixed axes in space, just like the Jitterbug. These axes all intersect at a common point.

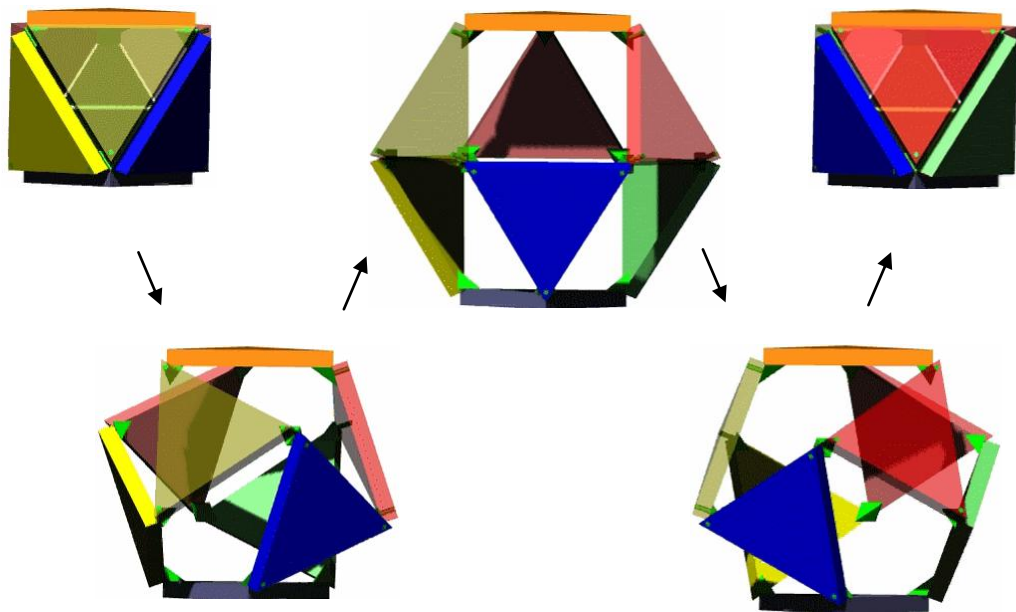


**Figure 1.2** The Heureka octahedron

Next attempt to generalize these linkages was by Röschel (1995, 1996a, 1996b, 2001), who coupled Darboux motions - a motion for which all point paths are planar - to synthesize not necessarily regular Jitterbug-like assemblies.



Röschel's studies are of special importance because the main material of this thesis work is built on top of these works.

Röschel's (1996a, 1996b, 2001) method to construct Jitterbug-like linkages starts by defining a planar equiform motion (see Bottema (1979), p. 455-480) and then reflecting this motion to some nonparallel planes. In the second paper of the 3-paper series, Röschel (1996a) applies this method to octahedra which inscribe a sphere and in the third paper (2001) the method is applied such that neighboring equiform motion centers are on a circle. In Chapter 6 theorems are presented which generalize these findings of Röschel.

Other Jitterbug-like polyhedral linkages were discovered by Wohlhart (1993, 1994, 1995). Some other types of conformal polyhedral linkages were presented by Agrawal, Kumar and Yim (2002), Kovács, Tarnai, Guest and Fowler (2004b), Wohlhart (1999, 2001a, 2001b, 2004a, 2004b, 2005, 2008), Gosselin and Gagnon-Lachance (2006) and Kiper, et al. (2007, 2008, 2009b, 2010b, 2010c, 2011a).

## CHAPTER 2

### IRREGULAR POLYGONAL AND POLYHEDRAL LINKAGES COMPRISING REGULAR AND ANGULATED SCISSOR ELEMENTS<sup>1</sup>

The first mechanism that comes into mind for deployable structures is a scissor mechanism. Scissor mechanisms have been widely used for several applications that require uni-dimensional or planar expansion/contraction. A general analysis of such mechanisms is given in (Langbecker, 1999).

For regular scissor mechanisms, the intermediate links have three collinear hinges and two of such elements are joined at the mid joint such that the resulting regular (or translational) scissor element is symmetric with respect to the horizontal (Figure 2.1a). A series of regular scissor elements (Figure 2.1b) form a lazy tong mechanism or Nuremberg scissors (Dijksman, 1976, p. 20).

When the element is symmetric with respect to the vertical instead of the horizontal the so-called polar scissor element is obtained (Figure 2.2). See (Langbecker, 1999; Kokawa, 1997; Akgün, Gantes, Kalochairetis & Kiper, 2010) for assemblies of such elements.

The links in translational and polar elements are mentioned to be identical and this is the case in general, however, it is also possible to use non-identical links as addressed in (Langbecker, 1999) and (Gantes & Konitopoulou, 2004).

---

<sup>1</sup> The main content of this chapter is published by Kiper and Söylemez (2010c).

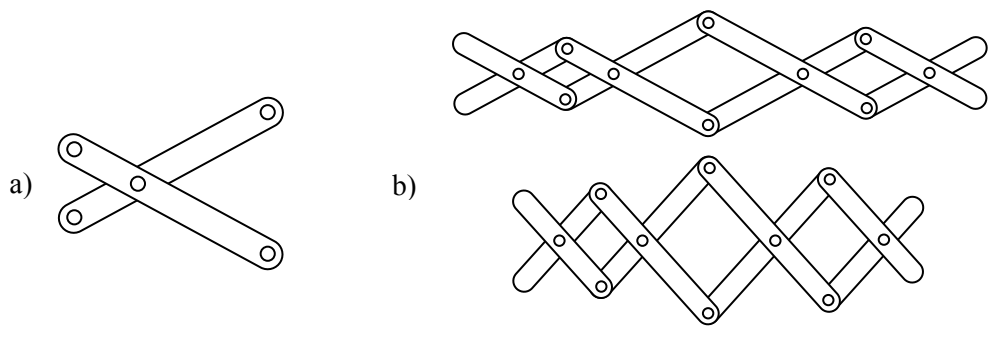


**Figure 2.1** a) Translational (regular) scissor element and b) the lazy tong mechanism in two configurations

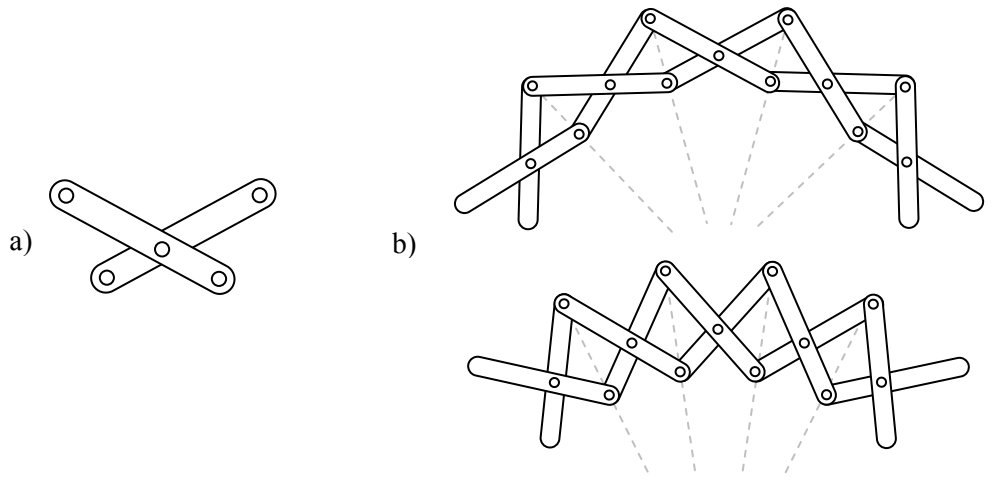


**Figure 2.2** a) Polar scissor element and b) an assembly in two configurations

When the hinges are not collinear, one can obtain deployment along intersecting lines without changing the angle between the lines provided that some special geometric dimensions are imposed. These bended links are called angulated elements and were introduced by an American inventor, Charles Hoberman (1990) (Figure 2.3). The beauty of the invention is in that the angulated elements can be assembled radially to obtain circular or spherical deployment. Hoberman's angulated elements were analyzed and generalized by You and Pellegrino (1997) and Patel and Ananthasuresh. Wohlhart (2000) and Mao, Luo and You (2009) have shown that Hoberman's linkages are some special cases of generalized Kempe linkages (Kempe, 1878).

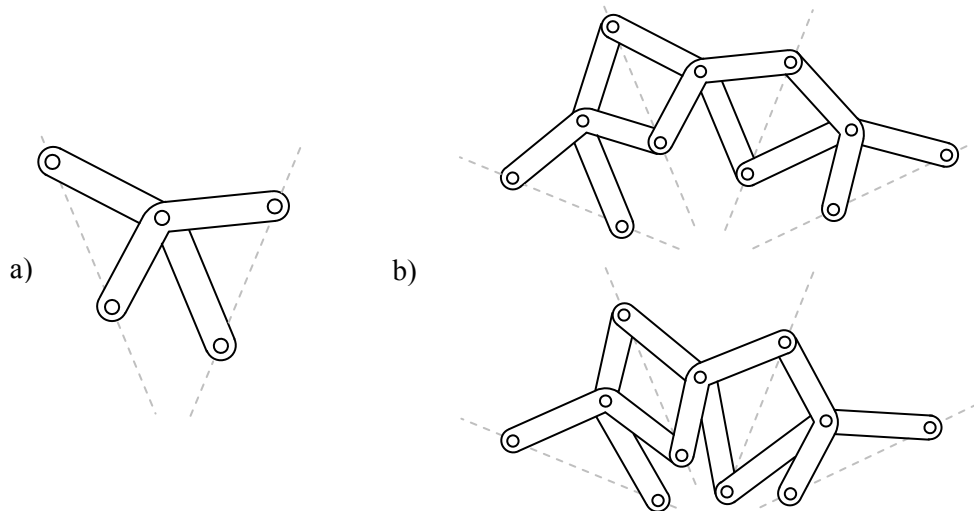


**Figure 2.3** a) Angulated scissor element and b) an assembly in two configurations

Kiper, Söylemez and Kişisel (2008) have proved that the ring assemblies comprising angulated elements can be constructed using Cardan motion (see Bottema & Roth, 1979, pp. 346-348). The key point is that all the joints in such an assembly move along linear trajectories and the motion of the links turn out to be the Cardan motion.

In some applications it is desired to deploy polygonal shapes keeping the angles and side length proportions of the polygon invariant. This is a dilative transformation (Coxeter & Greitzer, 1967, sec. 4.7). In most cases, the shape is radial symmetric. Several designs for non-symmetric cases were employed so far, however the transformations are usually not dilative. Kiper, et al. (2008) claimed that if one intends to deploy a polygonal shape with cranks attached to angulated elements, the polygon has to be a cyclic polygon, i.e. a polygon with a circumcircle. Here is a correction to that result: rather than being cyclic, the polygon has to be a tangential polygon, i.e. a polygon with an incircle. An inscribed circle is necessary if all the cranks are to be joined at a common hinge. However, if cranks are omitted and just angulated elements are used, any polygonal shape can be deployed dilatively, as shown in Section 2.1.

The basic shape becomes more realizable if both regular and angulated elements are used for the dilation of irregular polygons and even any kind of connected planar graph, as presented by Liao and Li (2005). However, in (Liao & Li) it is not formally proved that the transformation is dilative. In this chapter the solution is presented by use of the Cardan motion.

## 2.1 The Cardan Motion and Angulated Elements

The use of the so-called elliptical trammel – a double slider mechanism – attributed to Archimedes has been used to draw ellipses since ancient times (Figure 2.4a). In the 16<sup>th</sup> century it was the Italian mathematician Gerolamo Cardano to notice that elliptic motion can also be obtained using an internal planetary gear pair of 2:1 ratio (Figure 2.4b) (Dörrie, 1965, secs. 47-48). Today, it is known that the motion of the coupler link of the trammel and the planet gear of the latter are identical if  $|AB| = 2|OC|$  (Figure 2.4) and this motion is called the Cardan motion.

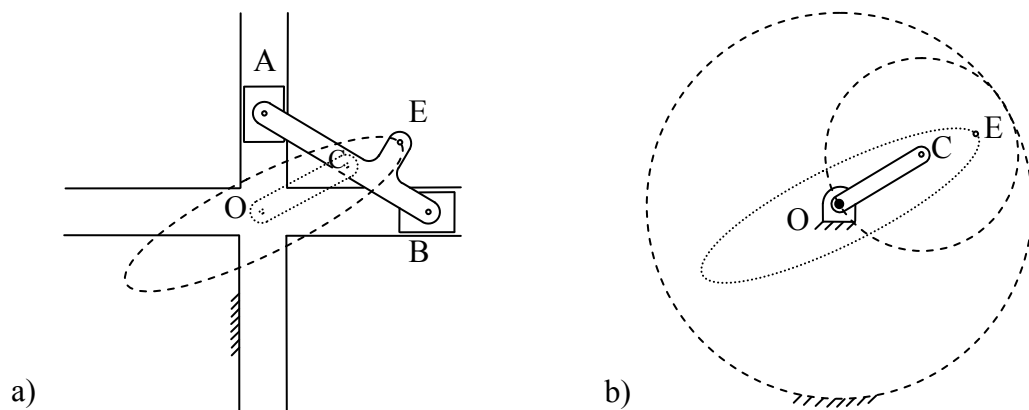


**Figure 2.4** a) The elliptic trammel of Archimedes with a possible crank attached and b) the two gears of Geronimo Cardano

Cardan motion is a special hypocycloid motion (Hilbert & Cohn-Vossen, 1990, p. 277) in which the moving centrode has half the diameter of the fixed centrode. The point trajectories are in general ellipses. As a special case the center of the moving centrode follows a circular path and as the degenerate case all points on the moving centrode move on straight lines all passing through the center of the fixed centrode (Bottema & Roth, 1979, pp. 346-348). Hence Cardan motion is one of the exact straight line motion generation motions.

The very same motion can also be obtained as the motion of the coupler link of an inline isosceles slider crank mechanism (mechanism OCA or OCB in Figure 2.4a) and this mechanism was used in (Kiper, et al., 2008) to obtain some polygonal deployable structures. In this study the idea is generalized for all polygonal shapes.

Consider three points on a moving Cardan circle and their straight line paths (Figure 2.5a). In (Kiper, et al., 2008), the midpoint is chosen to be equidistant to the other two but here its location is arbitrary. Without loss of generality, choose the initial configuration such that the path of the midpoint is on the diameter of the moving centrode. These three points can be connected to each other to obtain a triangle. Next consider the motion of two moving planes, one rotated in one sense and the other in the other sense by the same amount (Figure 2.5b). As seen in the figure, these two motions have two common points: the center of the fixed centrode and analogous midpoints. Joining the two homologous triangles at the midpoints an angulated element is obtained.

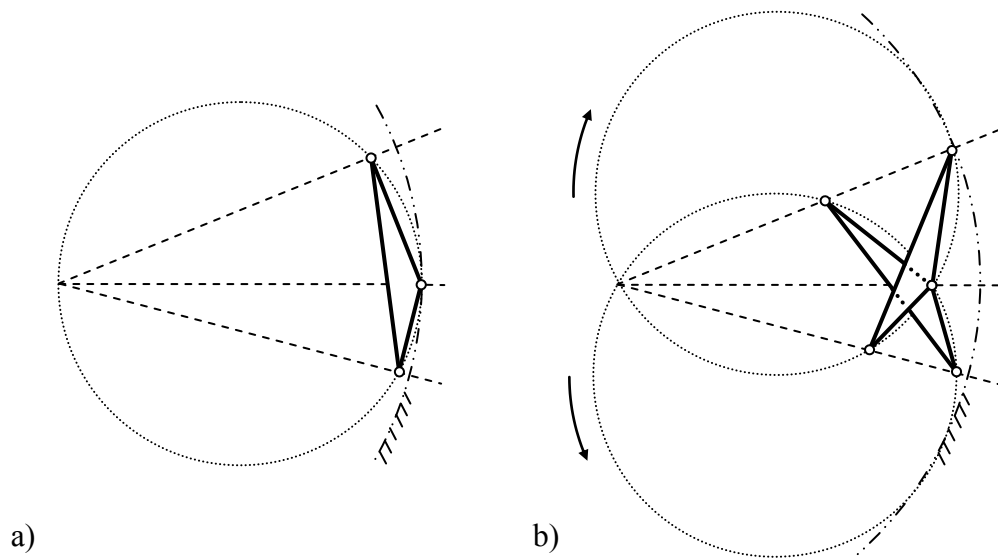


**Figure 2.5** a) Three points on a moving Cardan circle and b) two such moving planes coupled

## 2.2 Assembling Angulated Elements for Polygonal Deployment

Consider a polygon of arbitrary dimensions. Bisect the sides. Through each triplet of points comprising a vertex and the two neighboring bisection points there passes a circle (Figure 2.6a). Considering these triplets as the three points of Figure 2.5a, angulated elements can be formed and the polygonal shape can be scaled as in Figure 2.5b.



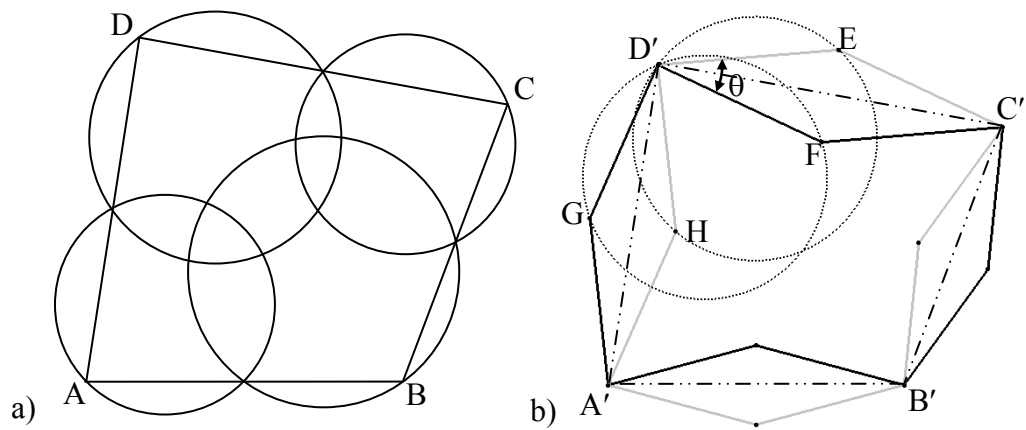


**Figure 2.6** a) A quadrilateral and b) its contracted version

For an  $n$  sided polygon such an assembly comprises  $2n$  links and  $3n$  joints. According to (CGK) mobility criterion this linkage has  $3(2n-3n-1)+3n = -3$  dof, however the assembly is mobile and furthermore the motion is such that the polygon obtained by connecting the angulated element mid joints is always the same polygon with different scale. A constructional proof is presented for that the mobility is unity and that the motion is a dilative one: Given a polygonal shape construct the angulated elements as explained above. Next consider a scaled version of the polygon by a scale  $k < 1$ . It is possible to attach rhombi to each side with rhombi (as  $D'EC'F$  in Figure 2.6b) side lengths being half of the corresponding original polygon side length. The sides of the scaled polygon bisect two opposite angles of corresponding rhombi. The amount of these bisected angles, say  $\theta$ , are all the same for all rhombi and are determined by the scaling ratio  $k$ :  $k = \cos(\theta/2)$ . So the angle between an outer rhombus side at a corner (such as side  $D'E$  at corner  $D'$ ) and an inner side of the neighboring rhombus at the same corner (side  $D'H$ ) is equal to the polygonal

angle at that corner ( $\angle ED'H = \angle A'D'C'$ ) and hence these two rhombus sides constitute a link of the angulated element at this corner.

Notice that there is no restriction on the polygonal geometry in this methodology. The linear paths of the midpoints of the sides, in general, do not meet at a common point. The condition for the guides to meet is that the polygon has an inscribing circle.

When the links are assembled in two layers as in Figure 2.7, the thicknesses of the links limit the deployability. Deployability can be increased by using more layers of assembly to avoid link collisions.

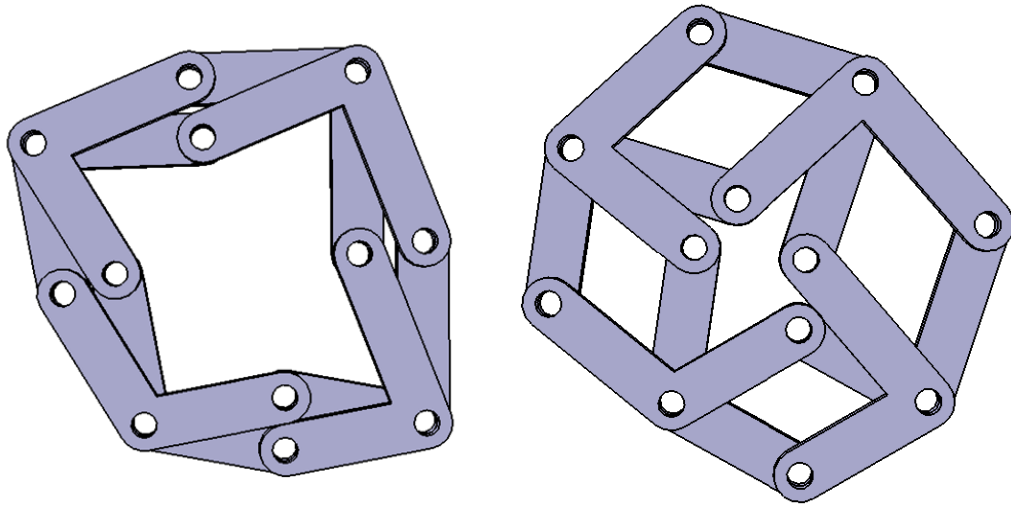


**Figure 2.7** A quadrilateral polygonal assembly at its two limiting configurations

### 2.3 Addition of Regular Scissor Elements

Regular scissor elements can be used along sides to make the assembly look more alike its base polygon. Care must be taken in adding regular scissor elements for the sides to ensure that the deployment is dilative. To do this, the link lengths of the regular elements should be selected such that they comprise rhombi, as also mentioned in (Liao & Li, 2005). In Figure 2.8, regular scissor elements are added for the quadrilateral of Figures 2.6-7. Four layers of assembly are used and the deployability is quite satisfactory.

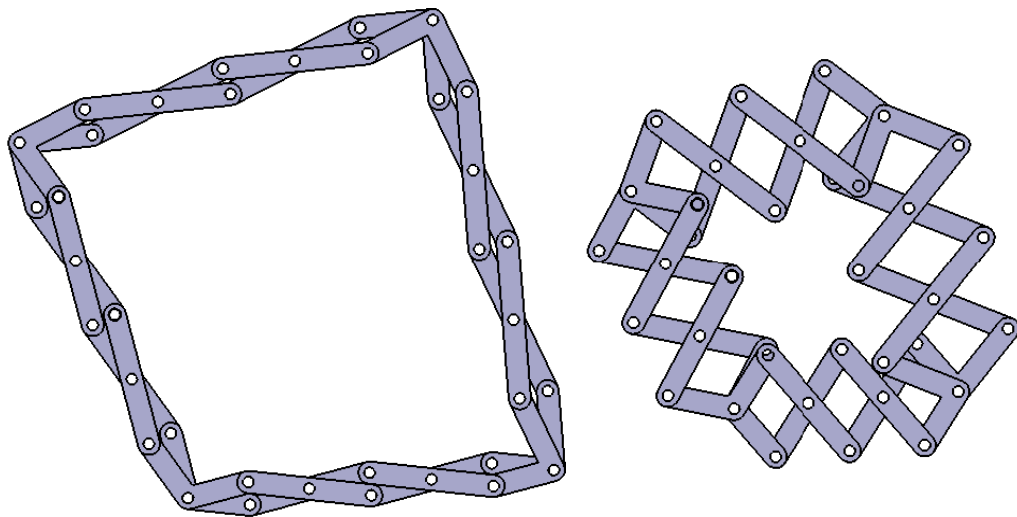


**Figure 2.8** Quadrilateral dilation with regular and angulated elements

## 2.4 Polyhedral Linkages

Several polygonal linkages synthesized as explained above can be assembled to construct polyhedral linkages. For this purpose additional links which are used for preserving the vertex figures should be employed (Figure 2.9). Such an assembly for a hexahedron is presented in Figure 2.10.

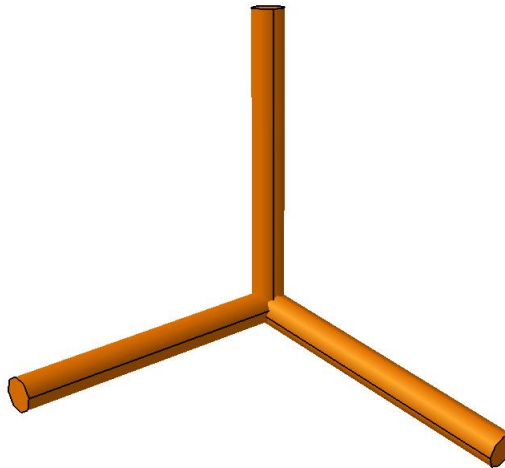


**Figure 2.9** Additional link for vertex figures

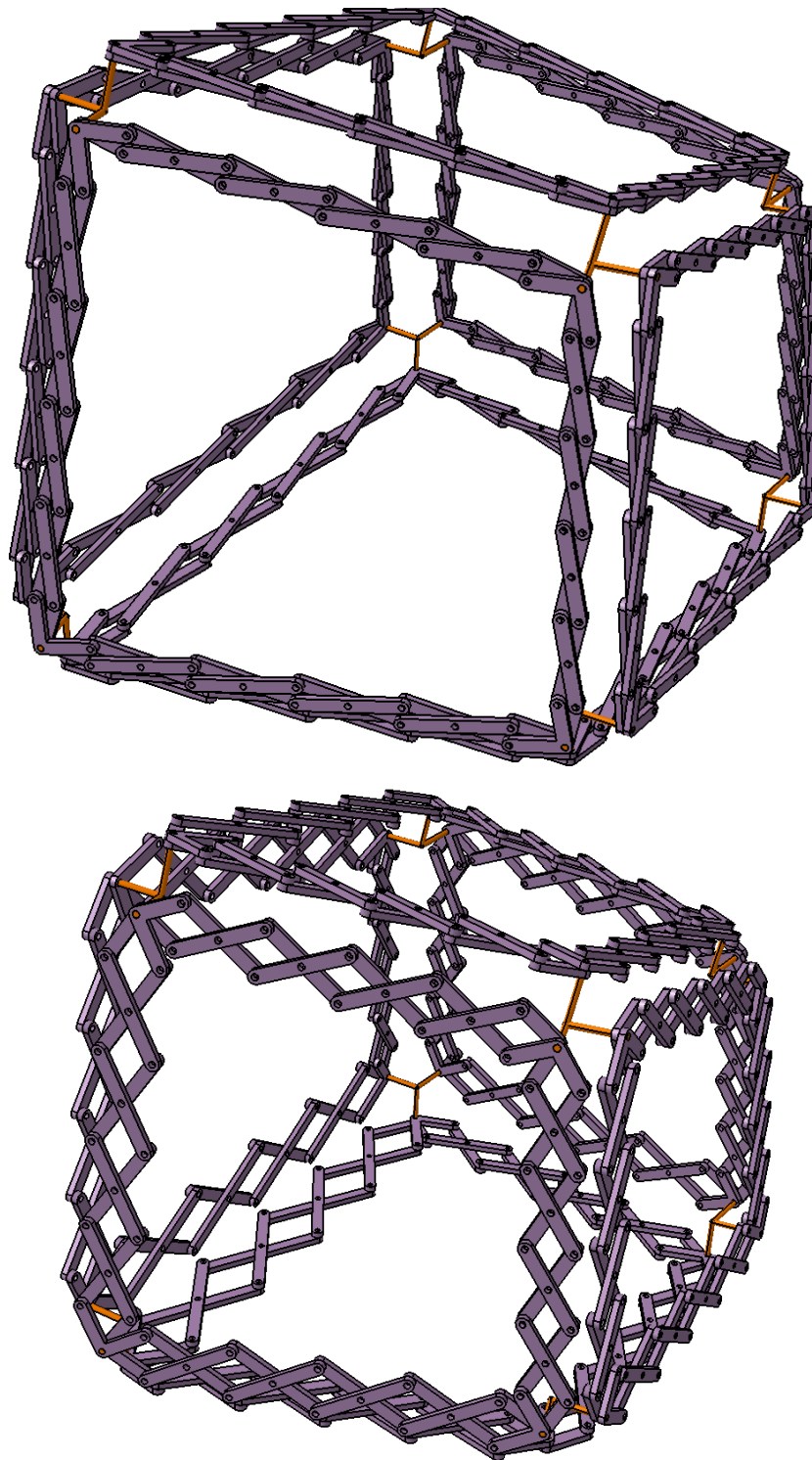


**Figure 2.10** An irregular hexahedral linkage

It is also possible to apply the method to any flat surface and assemble planar linkage groups with the additional links for the vertex figures illustrated in Figure 2.9. A deployable tent skeleton is presented in Figure 2.11.

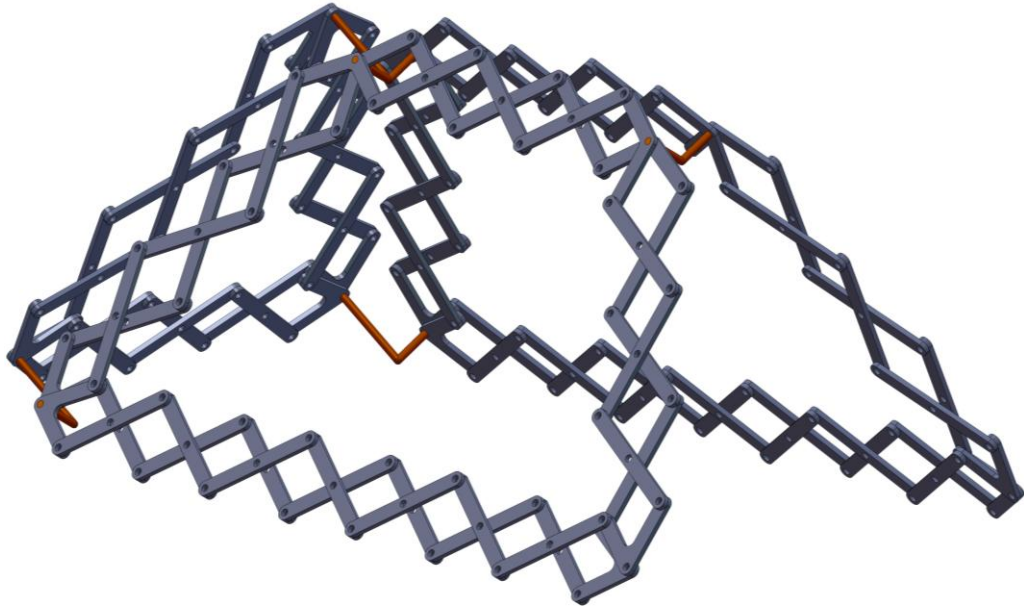


**Figure 2.11** A deployable tent skeleton

Another method to deploy polyhedral shapes using scissor elements is presented by Wohlhart (2004b). In this study of Wohlhart scissor elements are employed along edges of polyhedral shapes rather than sides of polygons.

## CHAPTER 3

### POLYHEDRAL LINKAGES SYNTHESIZED USING CARDAN MOTION ALONG RADIAL AXES<sup>1</sup>

The method of obtaining linkages in this chapter again makes use of the Cardan motion. As mentioned in Chapter 2, Cardan motion can be realized by means of the angulated elements. Some certain special dimensions are possible in order for an angulated element pair to track two intersecting straight lines (You & Pellegrino, 1997), however to obtain similarity the elements must be isosceles, the bend angle and the angle between the lines being tracked must be supplementary angles as noted by Kiper, Söylemez & Kişisel (2008) (Figure 3.1).

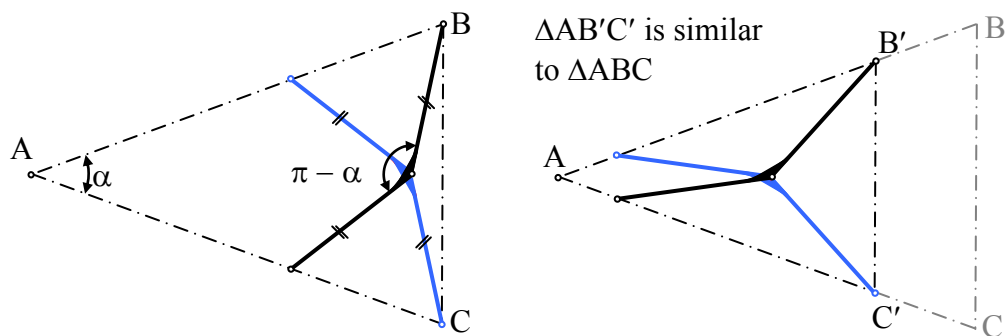


**Figure 3.1** An angulated element pair to magnify a triangle ABC

<sup>1</sup> The main content of this chapter is published by Kiper, Söylemez and Kişisel (2007).

In (Kiper, et al., 2008), these mechanisms were used to magnify an isosceles triangle. Many such linkages are assembled to form cyclic polygons, which can finally assemble to form a polyhedral shape. Here, the triangle-magnifying linkages are used to obtain a magnification of polyhedral shapes along radial axes.

Consider an inner point in a polyhedral shape. Connecting this point to the vertices, one obtains  $e$  many triangles, where  $e$  is the number of edges. These triangles, hence the whole polyhedral shape can be magnified using isosceles angled elements. In order to avoid interference of skew revolute joint axes, an offset along the lines connecting the magnification center to the vertices must be introduced (Figure 3.2). Depending on the design, the amount of offset can take any value.

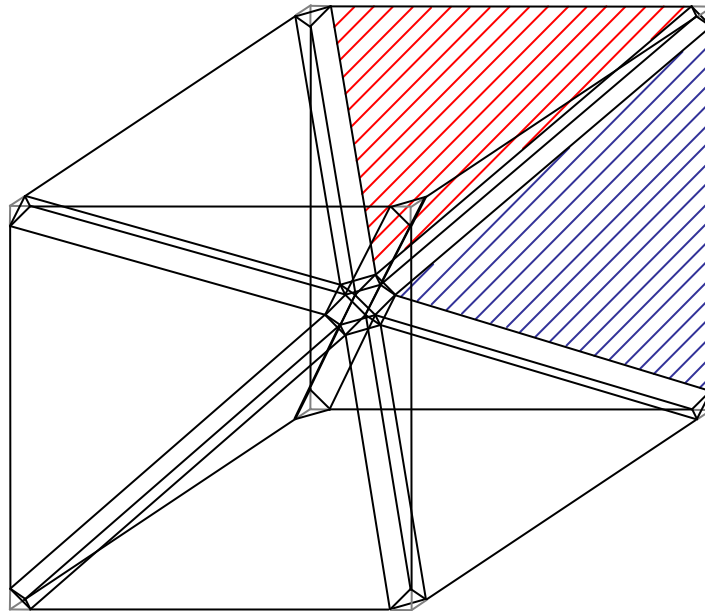


**Figure 3.2** A triangular dissection for the radial magnification of a cube



Since the triangular dissections must all be isosceles, all the vertices must be equidistant to the magnification center. Hence, only spherical polyhedra, i.e. the polyhedra with all vertices on a sphere, can be magnified using the linkages proposed. Using the most symmetric spherical polyhedra, i.e. the Platonic solids, cubic, tetrahedral, octahedral, dodecahedral and icosahedral linkages synthesized accordingly are illustrated in Figures 3.3-7. Notice that there are Sarrus loops (an overconstrained linkage with 2 sets of 3 parallel revolute joint axes) (Sarrus, 1853) at each vertex.

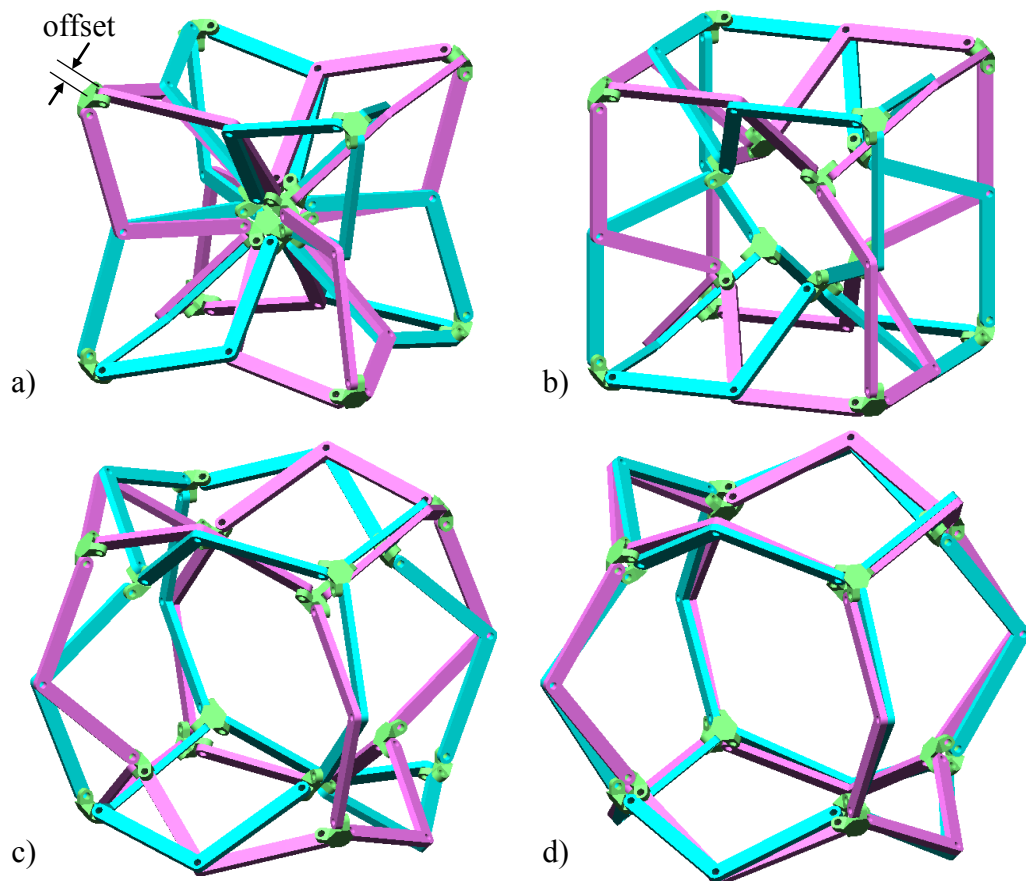


**Figure 3.3** A cube being magnified

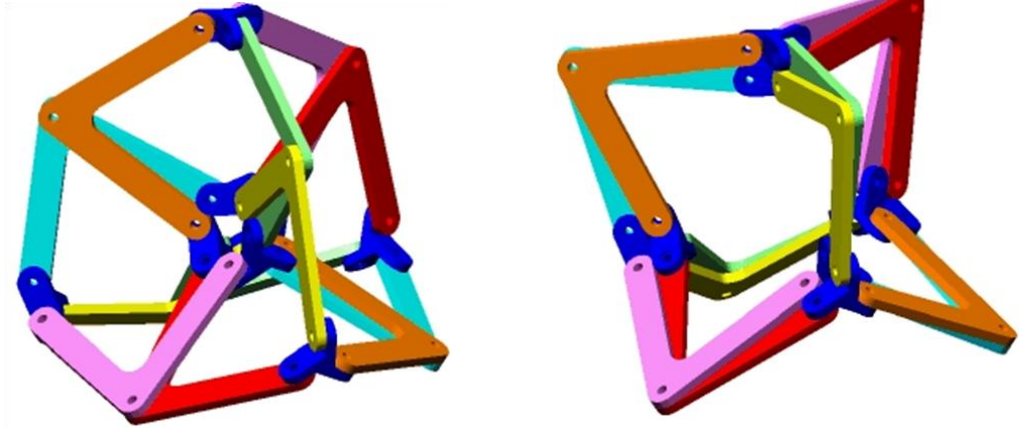


**Figure 3.4** A tetrahedral linkage in two limit configurations

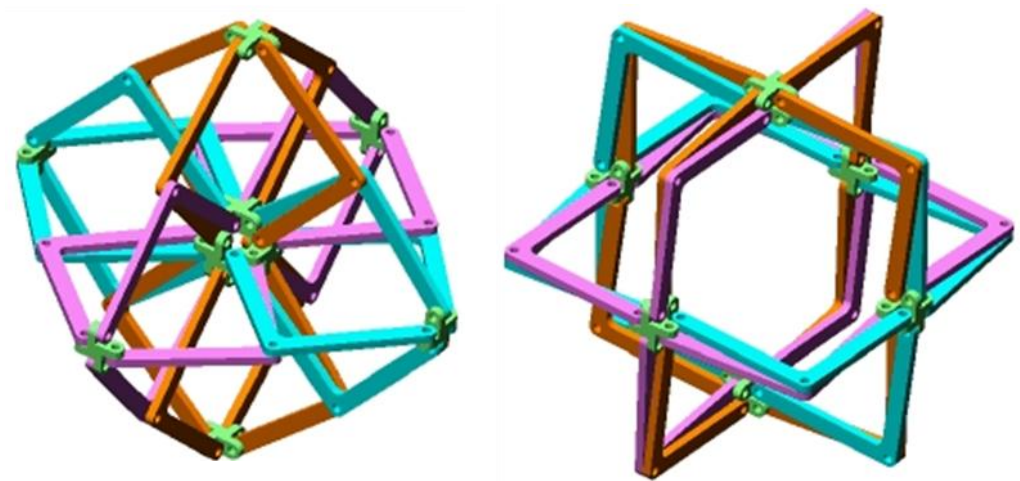


**Figure 3.5** An octahedral linkage in two limit configurations

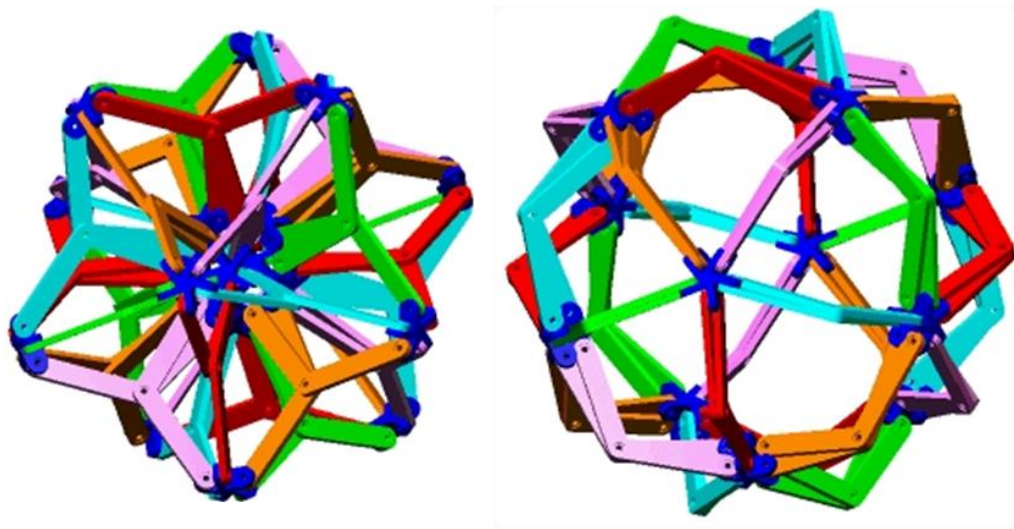


**Figure 3.6** A dodecahedral linkage in two limit configurations

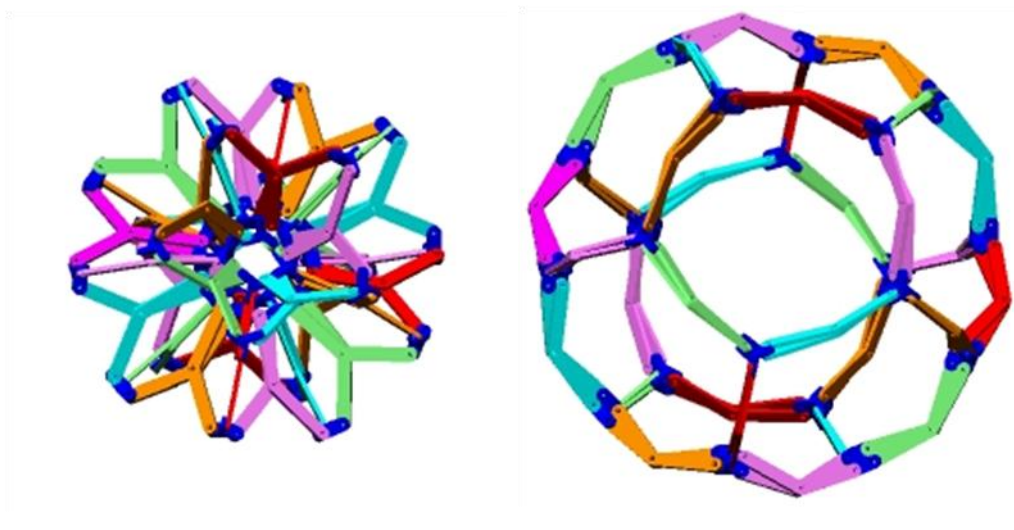


**Figure 3.7** An icosahedral linkage in two limit configurations

The total ratio of magnification is very small for single pair of angulated elements. One may add ordinary scissor elements in order to increase the ratio of magnification, as was done by Hoberman (1990) (Figure 3.8a) with his famous toy Hoberman Sphere<sup>®</sup> (1995) and Wohlhart (2004) (Figure 3.8b) and also utilized in Chapter 2.

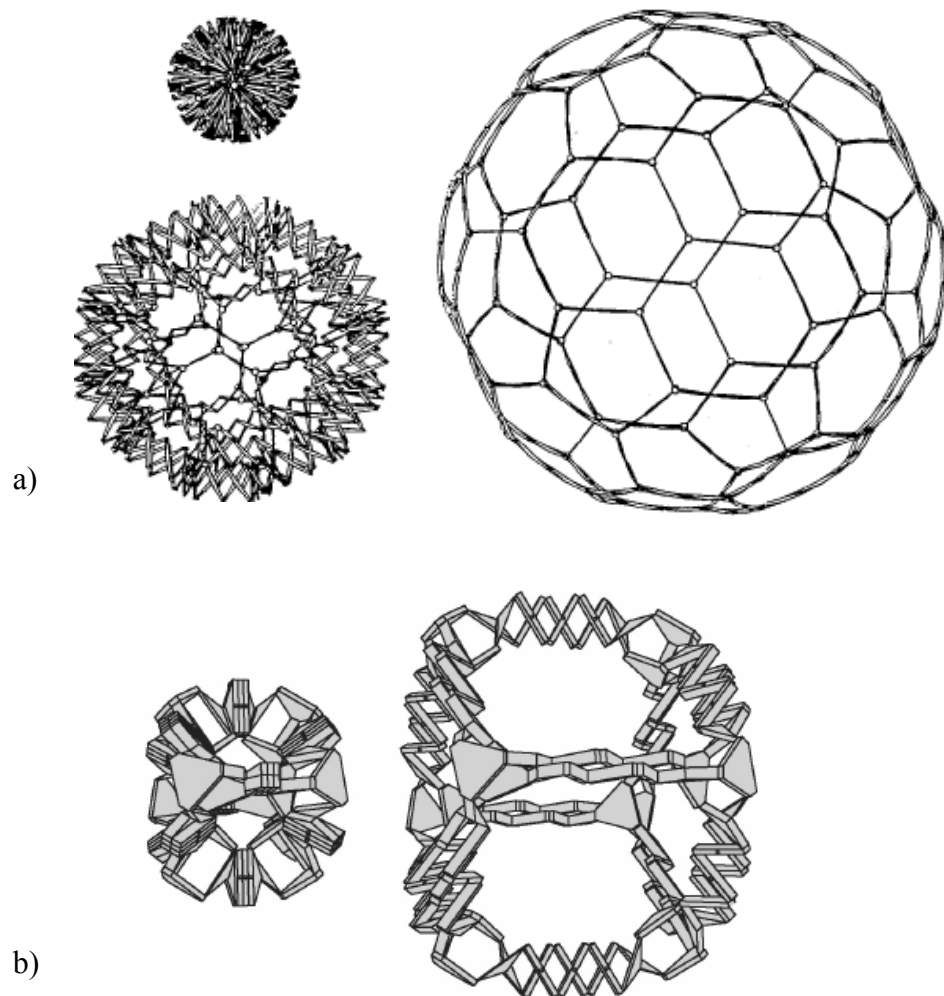


**Figure 3.8** a) Hoberman's (1990) truncated icosahedral linkage in 3 phases and b) Wohlhart's (2004) cubic zig-zag linkage in 2 phases

Alternatively, one may dissect the polyhedral shape of interest such that the circumcenter of the polyhedron, a vertex and the circumcenter of a face form a triangle (Figure 3.9 – triangles AOB, BOC, etc.). Notice that the triangular dissections will be intersecting each other along the line connecting the circumcenter of the polyhedron and the circumcenter of a face. Hence a constraint along an intersection line makes it possible to reduce the degree-of-freedom of the triangular linkage. So, binary links can be used instead of angulated elements, removing the need to have an isosceles triangle. Indeed, then these binary links move as double slides, which are also well known to realize the Cardan motion.

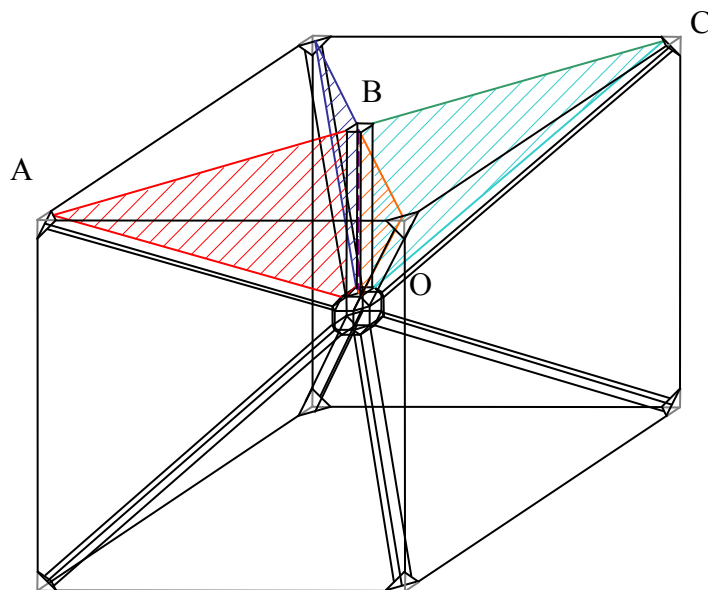


**Figure 3.9** Another triangular dissection for the radial magnification of a cube

When proper connections are implemented between the binary links, it happens to be that the shape the linkage encloses varies between a family of polyhedra which belong to the same symmetry group. Because of this fact, there are two minimal and two maximal configurations, which are dual (Most simply dual polyhedra are obtained by interchanging faces and vertices) of each other. Cubic/octahedral, tetrahedral (self dual) and dodecahedral/icosahedral linkages are illustrated in Figures 3.10-12.

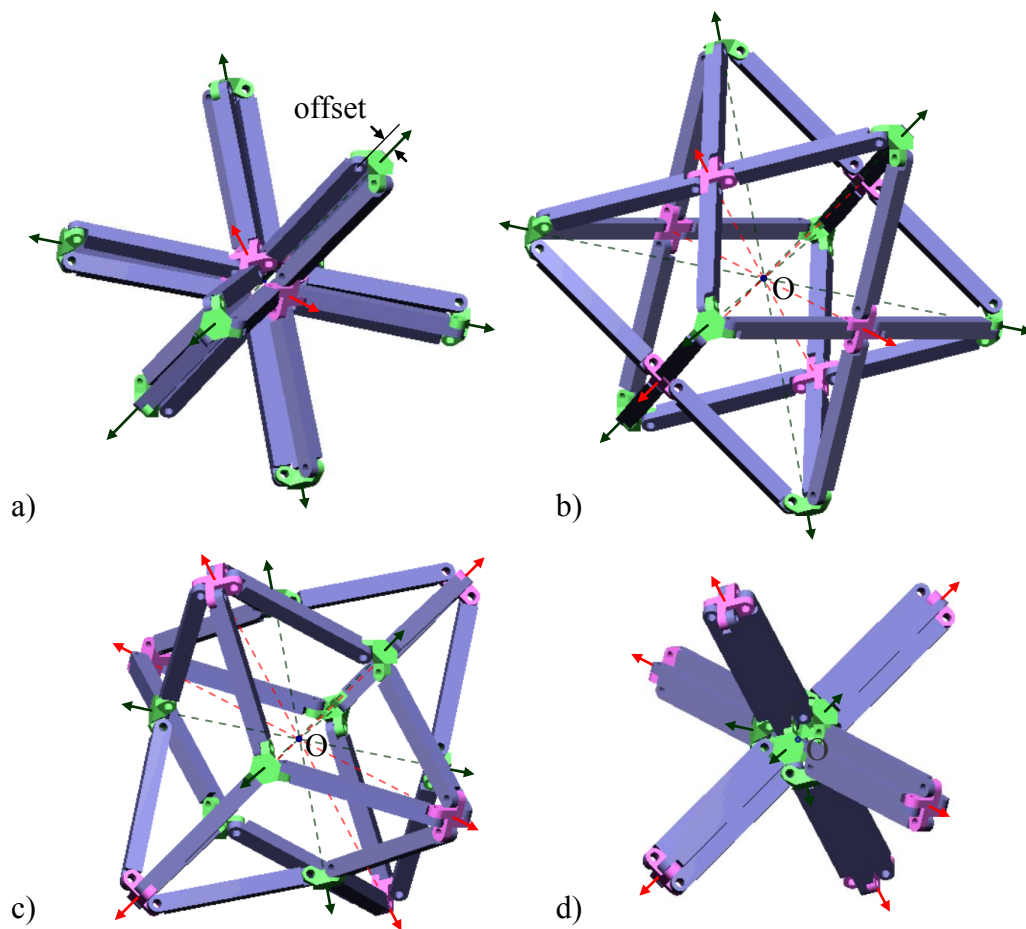


**Figure 3.10** a) Cubic skeleton b) Cube c) Octahedron d) Octahedral skeleton



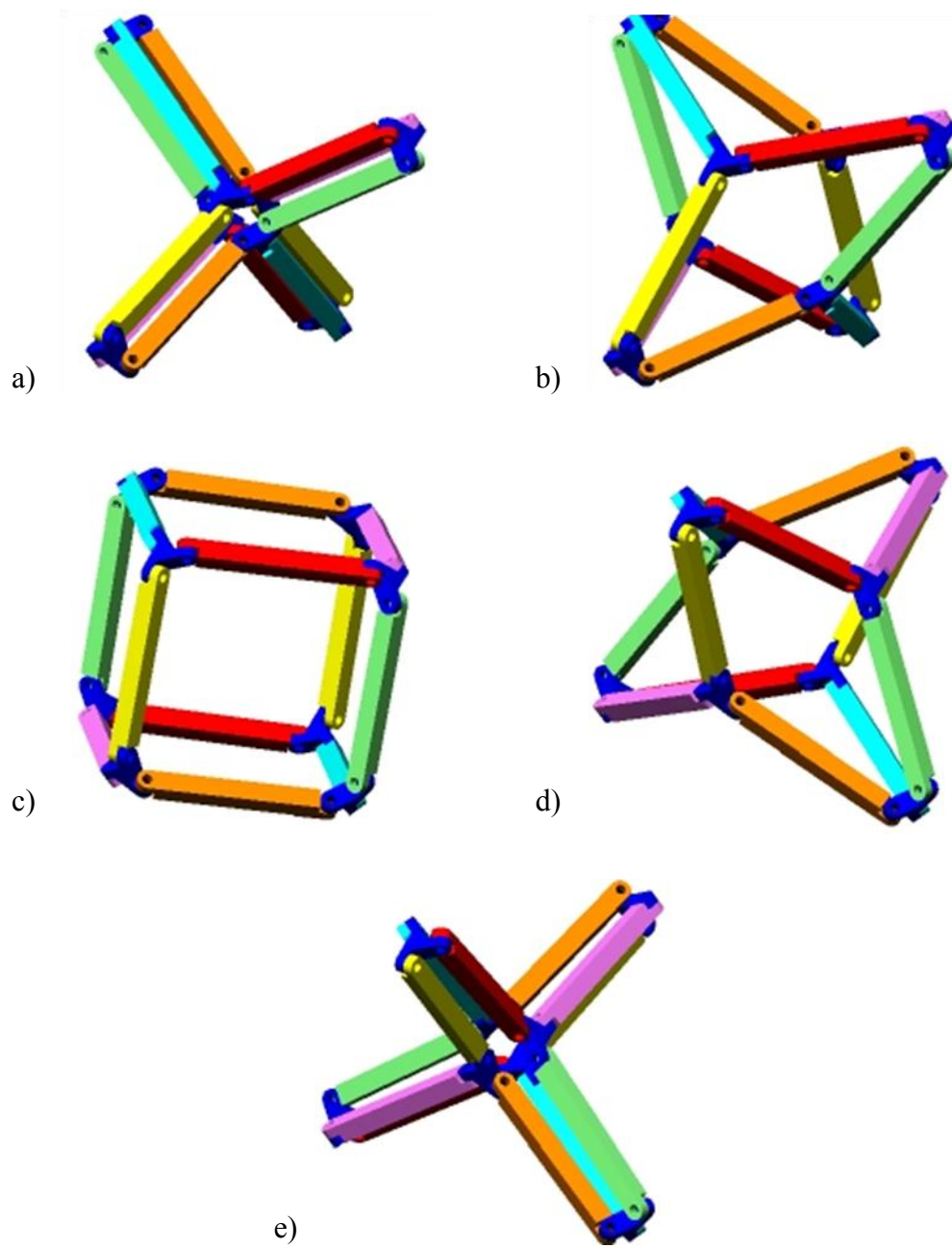


**Figure 3.11** 5 phases of a tetrahedral linkage

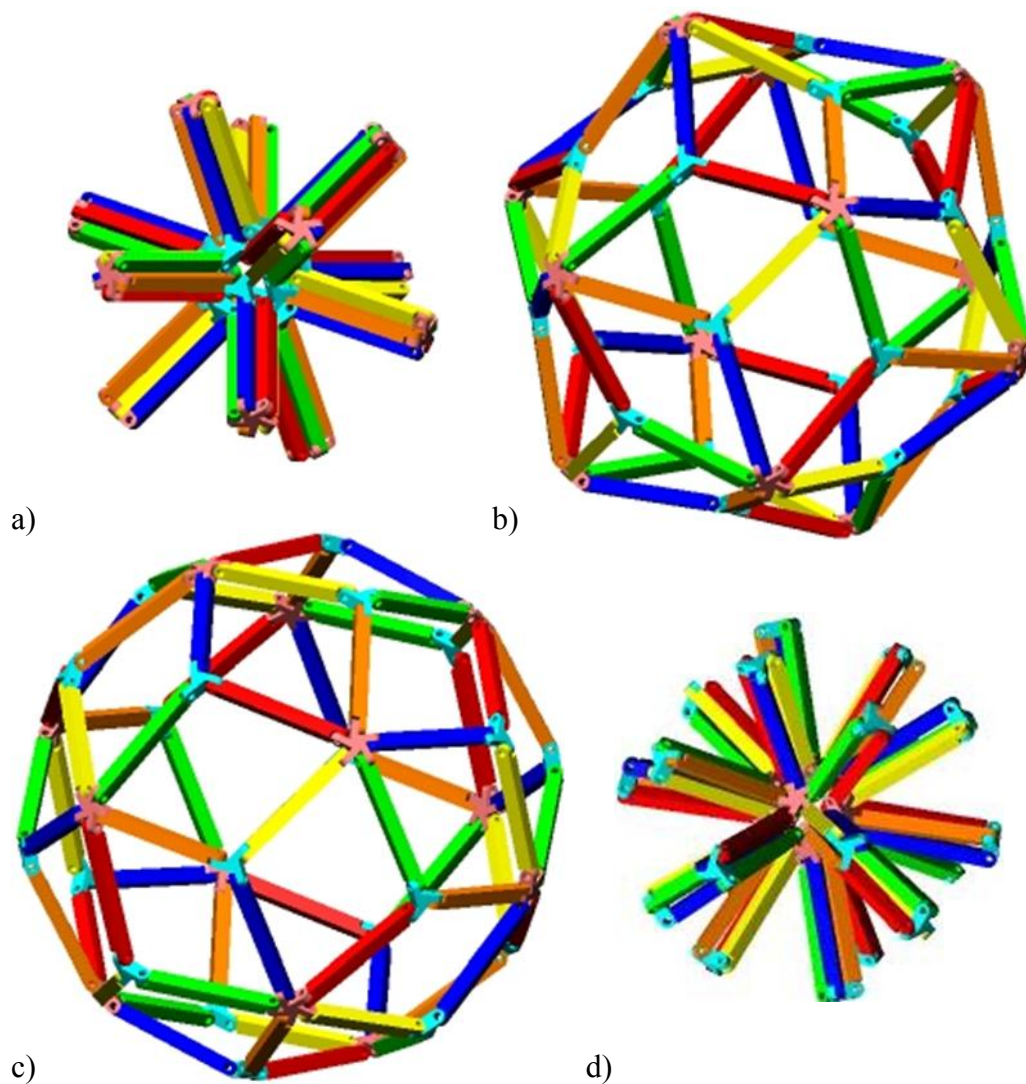


**Figure 3.12** 4 phases of a tetrahedral linkage

This type of linkages was also presented by Wohlhart (1995) and Hoberman (2004a). Hoberman's (2004b) famous toy Switch Pitch<sup>®</sup> has the kinematic structure of the tetrahedral linkage in Figure 3.11.



## CHAPTER 4

### REGULAR POLYGONAL AND REGULAR SPHERICAL POLYHEDRAL LINKAGES COMPRISING BENNETT LOOPS<sup>1</sup>

Kiper, Söylemez, Kişisel (2008) have observed that some linkages in the literature are obtained by systematically removing some links from a highly overconstrained linkage. That is, for that planar family of linkages, the most general case was the most overconstrained one. In this chapter, anticipating the same fact in the spatial case, polyhedral linkages comprising single loop spatial overconstrained chains is with revolute joints only are sought. As the simplest of such loops is given by Bennett (1903), his linkage with 4 revolute joints is the basic module.

Using the Denavit- Hartenberg (1955) notation, the Bennett loop is given by the following relations (Bennett, 1903) (Figure 4.1): Link lengths and twist angles are such that

$$a_{12} = a_{34} = a \quad \text{and} \quad a_{23} = a_{41} = b \quad (4.1)$$

$$\alpha_{12} = \alpha_{34} = \alpha \quad \text{and} \quad \alpha_{23} = \alpha_{41} = \beta \quad (4.2)$$

which satisfy

---

<sup>1</sup> The main content of this chapter is published by Kiper and Söylemez (2009b).

$$a/\sin\alpha = b/\sin\beta \quad (4.3)$$

and the offsets between the common perpendiculars along all the hinge axes are zero. Throughout the motion, the linkage is symmetric about a line  $z$  which perpendicularly bisects the diagonals connecting the nonconsecutive hinges. For simplicity, one of the special cases noted by Bennett (1914) is used: Let the link lengths be equal, i.e.  $a = b$ , and hence by equation 4.3, consecutive twist angles add up to  $\pi$ . Then, the linkage is said to be equilateral.

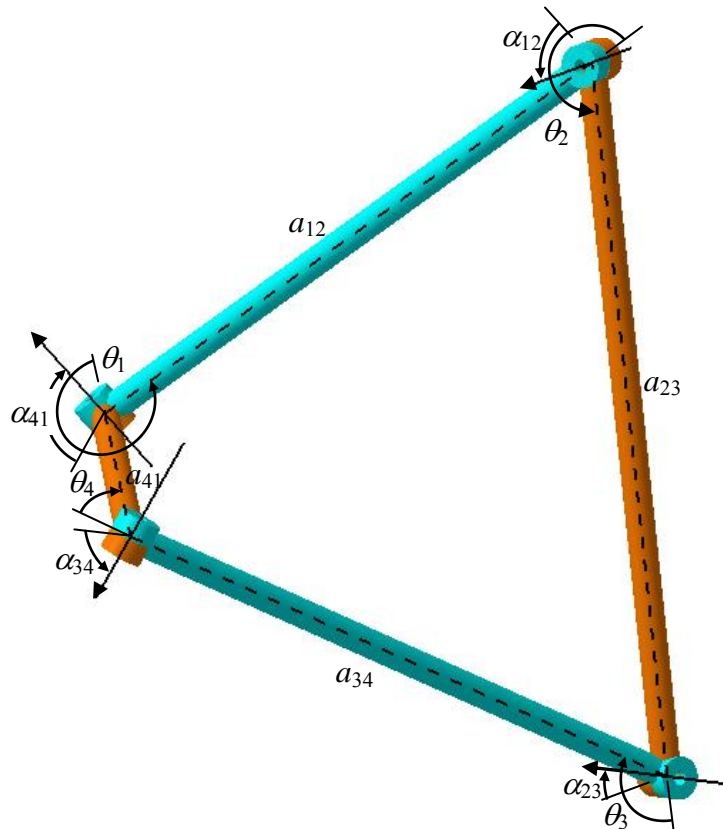


**Figure 4.1** The Bennett loop

When two identical equilateral Bennett loops are superposed along congruent hinges as in Figure 4.2 this common hinge axis  $a-a$  intersects the opposite hinges  $b-b$  and  $c-c$ . If a third Bennett loop is assembled in the same way, the connected hinge and the opposite one for this loop will also intersect the other hinges at the same intersection point. Notice that the intersection point  $O$  of these axes can be used as a dilation center of a polygonal region as the diagonal lengths are altered.

A remarkable notice about Figure 4.2 is that this linkage can also be seen as the assembly of two general plane-symmetric type Bricard (1897) six-link loops (ADBGCH and AEBFCI).

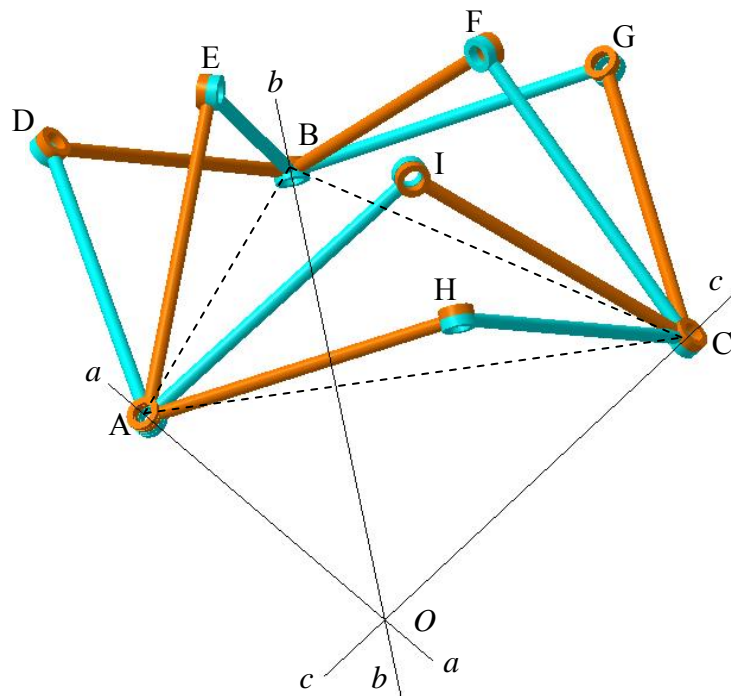


**Figure 4.2** A triangular assembly of Bennett loops

If three identical loops are assembled, since three hinge axes are common for neighboring loops, the diagonals AB, BC and CA will have the same length. Given this diagonal length, the isosceles triangles AOB, BOC and COA can be assembled uniquely such that the equal sides and the apex O coincide. Hence the assembly is fixed by a single input, i.e. the diagonal length, hence the resulting linkage has single dof. When four Bennett loops are assembled as explained, for a given diagonal length the isosceles triangles will form a spherical four-bar linkage, so the assembly has 2 dofs. In general, a serial assembly of  $n$  Bennett loops has  $n - 2$  dofs. But when these polygonal loops are assembled, the resulting polyhedral linkage may have single dof.

The polygonal loops can be assembled to obtain polyhedral linkages. The loops could be connected at A, B, C, ... of Figure 4.2 by spherical joints, but physically this results in collision of links, so some intermediate links should be employed. Although A, B, C, ... are coplanar, the orientations of hinge axes will rotate as the dilation is realized, so these hinge axes should be connected to the intermediate links via revolute joints. An octahedral linkage assembled and simulated accordingly is illustrated in Figure 4.3. The links of the Bennett loops coincide in Figure 4.3, but these collisions may be avoided as illustrated with the tetrahedral linkage in Figure 4.4. If the twist angles are increased up to  $90^\circ$  the dyads of the Bennett loops merge to get trihedral symmetric Bricard (1897) loops and a prettier polyhedral linkage is obtained (Figure 4.5).

The octahedral and tetrahedral linkages each have single dof, but in case of a cubic linkage the dof is 3 because of the special condition that there are three pairs of parallel faces and so the three pairs of opposite polygonal linkage groups are independently movable (Figure 4.6). The cuboctahedral linkage is presented as an example of a non-Platonic regular shape in Figure 4.7.

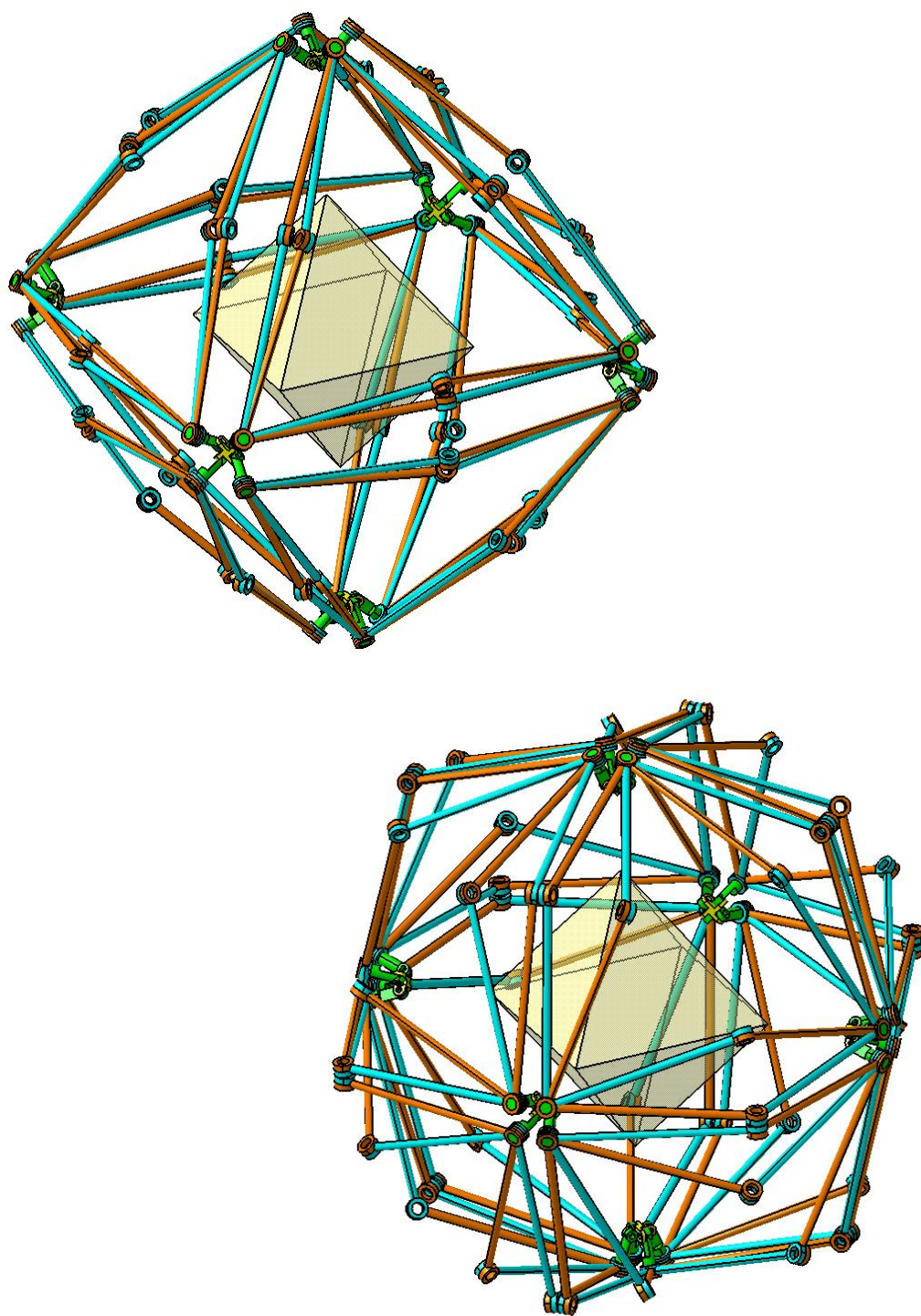


**Figure 4.3** An octahedral linkage – in expanded and folded positions

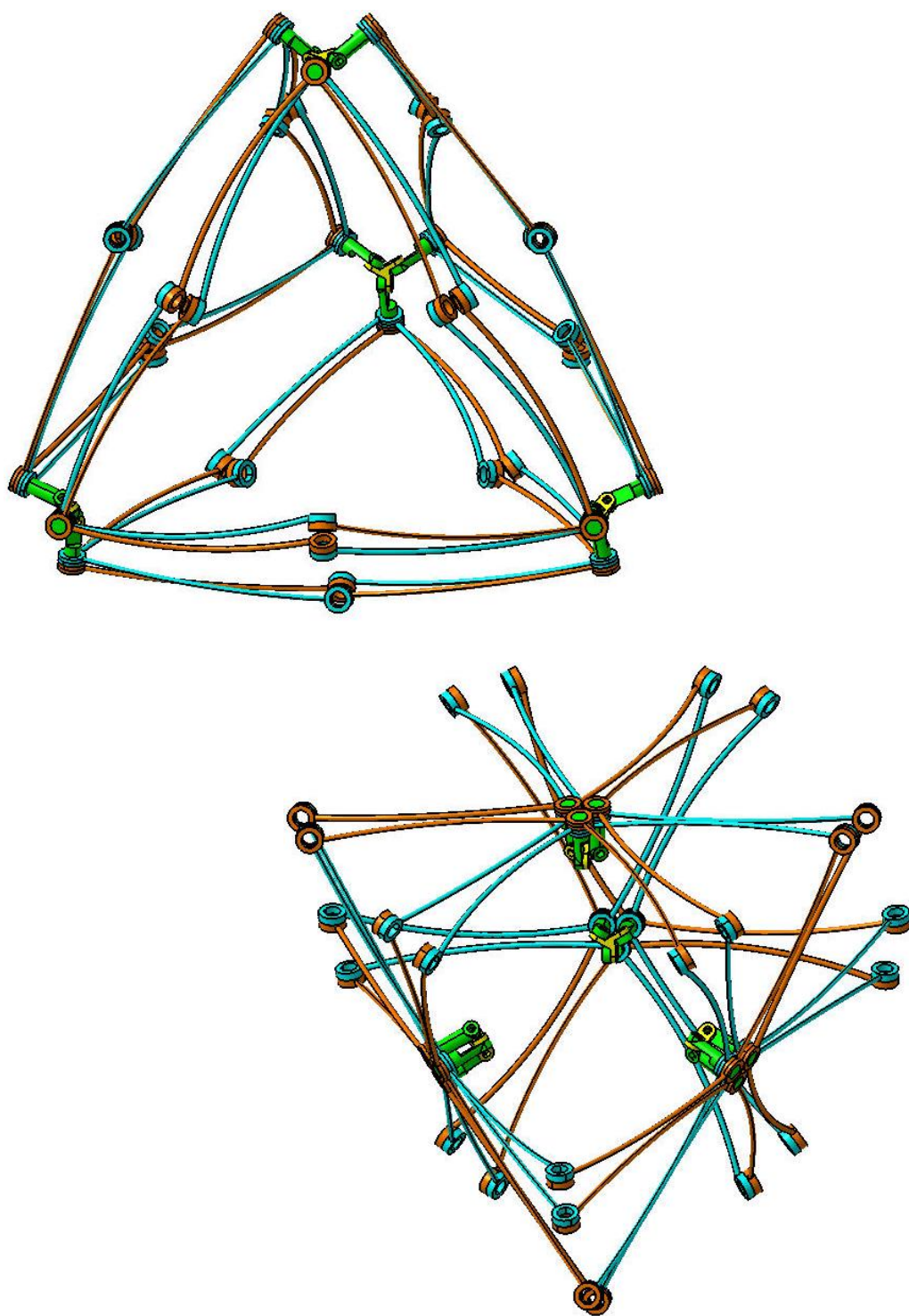


**Figure 4.4** A tetrahedral linkage – in expanded and folded positions

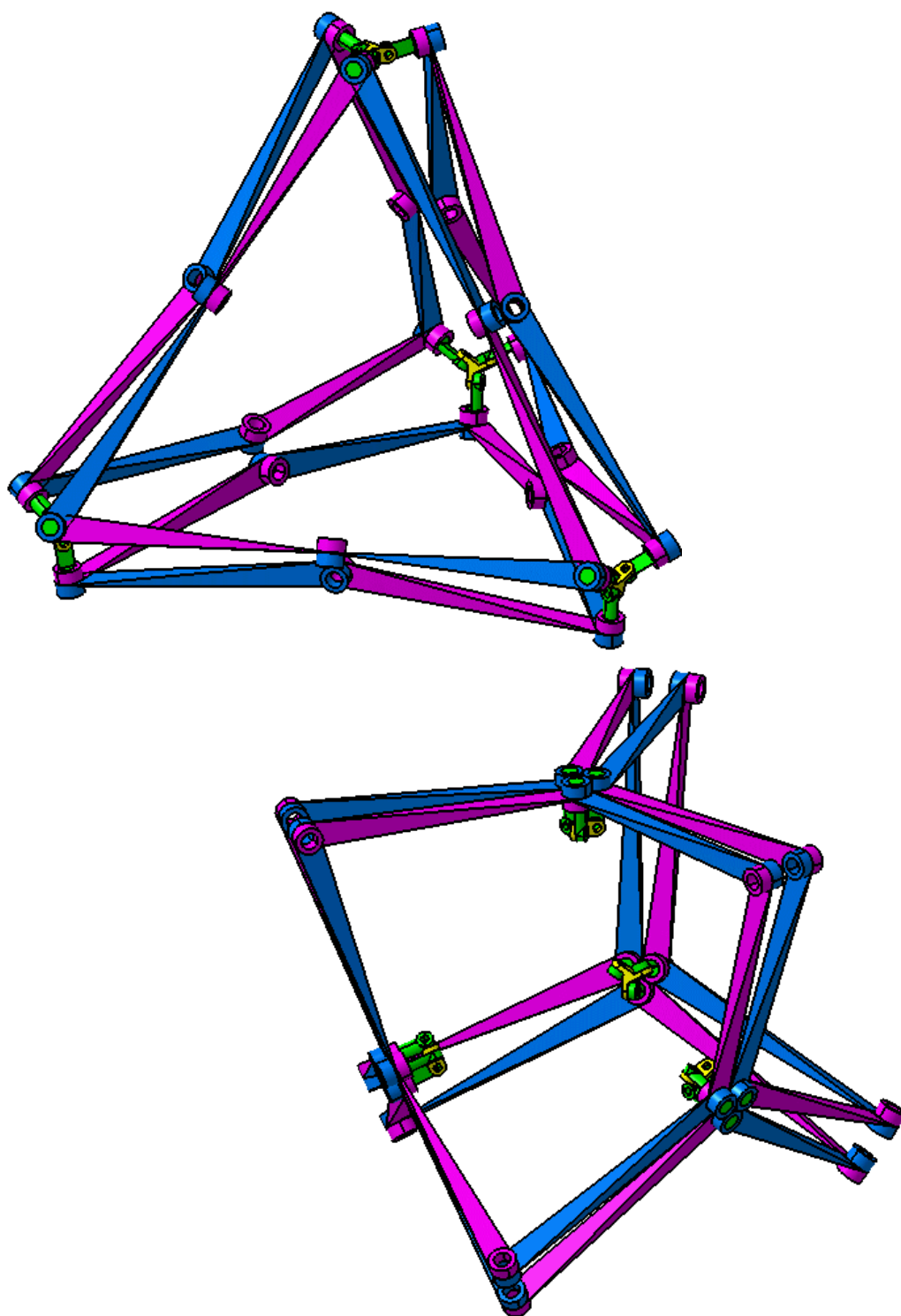


**Figure 4.5** A tetrahedral linkage comprising Bricard loops



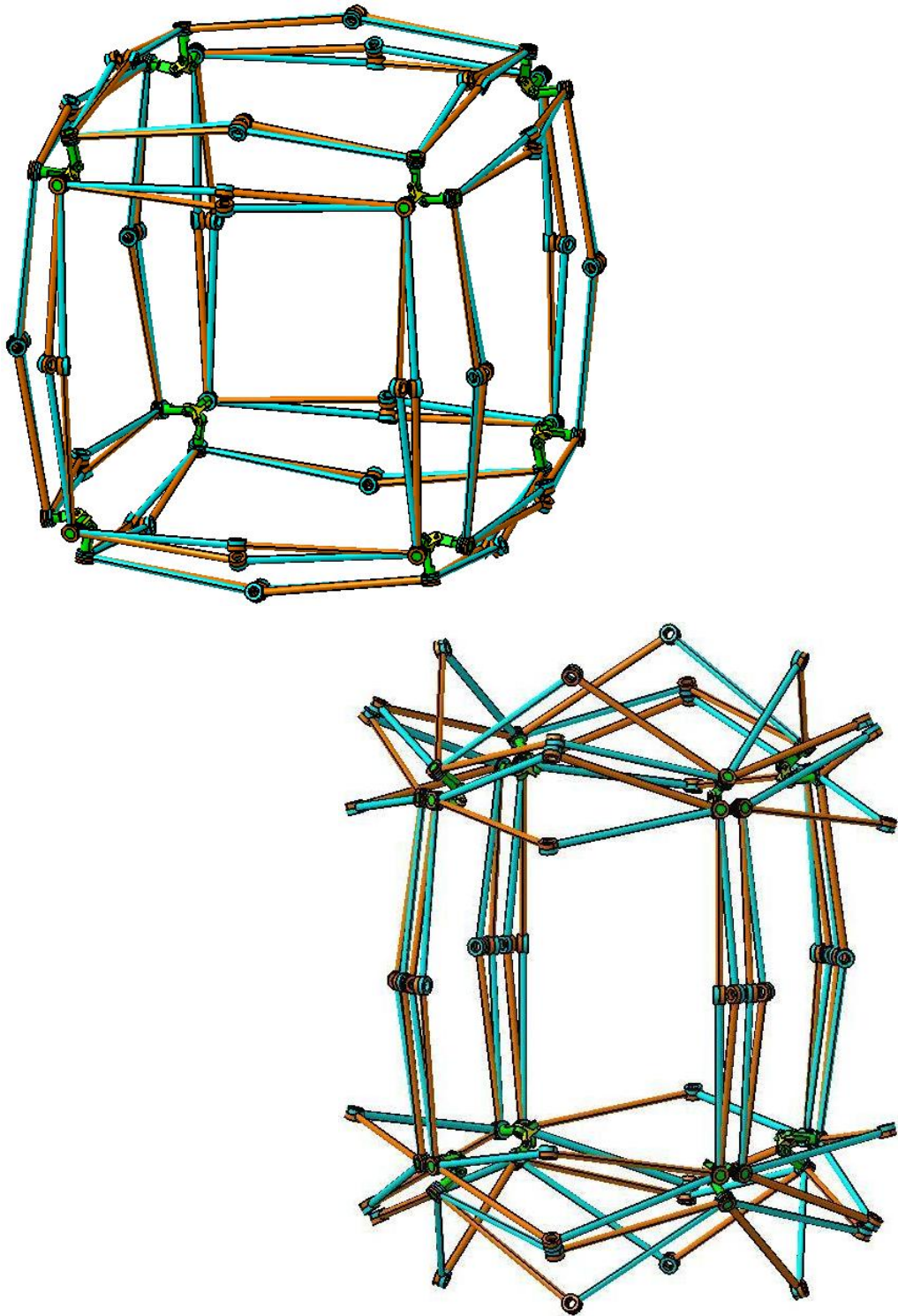


**Figure 4.6** Cubic linkage – in expanded position and one of the dofs used



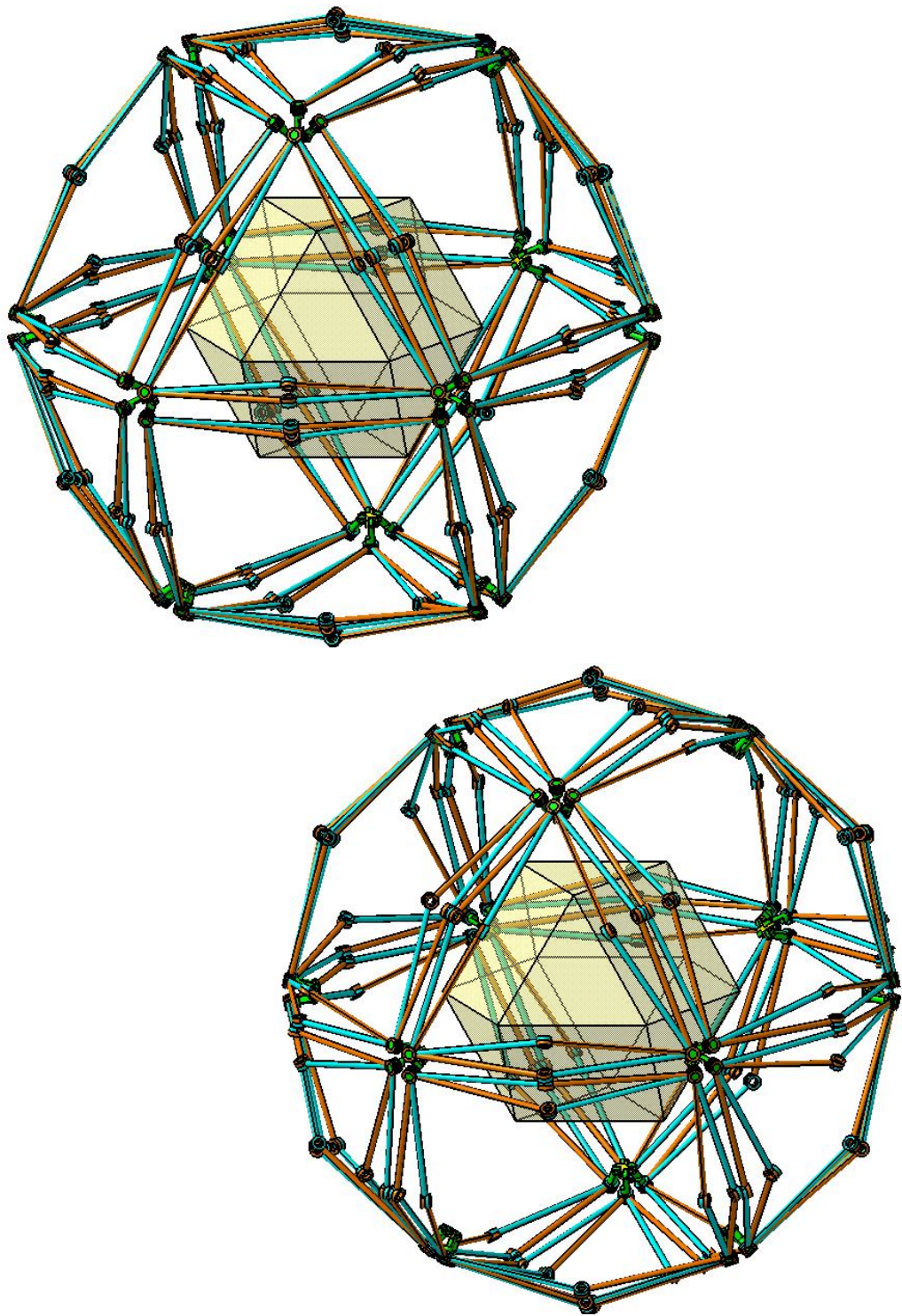


**Figure 4.7** Cuboctahedral linkage – in expanded and folded positions

Expansion ratio of the polyhedral linkages presented here are quite small when compared to the other linkages in literature. The expansion ratio is evaluated with considering the dilation of the reference polyhedral shape, ignoring the link portions outside this polyhedral boundary. If the mechanism is actuated from a revolute joint of a Bennett loop that is not connected to the other loops, then the length of the diagonal opposite to this joint will be, by cosine theorem,  $\sqrt{2a^2 - 2a^2 \cos \theta}$ , where  $a$  is link length and  $\theta$  is the angle between the links which construct a triangle with the diagonal of interest. Let the angles at expanded and folded configuration be  $\theta_e$  and  $\theta_f$ . Then the expansion ratio is given by  $\sqrt{(1 - \cos \theta_e) / (1 - \cos \theta_f)}$ . Note that  $\theta_e$  and  $\theta_f$  depend on the selection of twist angles and the dimensioning of links. For the specific twist angles ( $70.53^\circ$  and  $109.47^\circ$ ) and dimensioning (joint thickness to link length ratio 0.03 and joint diameter to link length ratio 0.06) used in the examples, the expansion ratio evaluated for the tetrahedron is 1.864, for the octahedron is 1.146, and for the cuboctahedron is 1.036.

A subject of discussion is whether this type of construction can be used with non-equilateral Bennett loops to obtain polygonal dilation. This is not possible, because the nonconsecutive hinge axes do not meet in this case. Alternatively, equilateral, but non-identical Bennett loops may be assembled. In Figure 4.2, the Bennett loops are identical. When three arbitrary non-identical equilateral Bennett loops are assembled, still a single degree-of-freedom linkage is obtained, however, the relative motion of A, B and C of Figure 4.2 does not necessarily result in an equiform motion.

## CHAPTER 5

### FULLEROID-LIKE LINKAGES<sup>1</sup>

This chapter is devoted to a heuristic method in synthesis of polyhedral linkages. The method starts with an existing polyhedral linkage exposing some symmetry and makes use of the symmetry axes to obtain new linkages. One of Wohlhart's (1995) linkages, the Fulleroid is used for illustration of the method.

#### 5.1 The Fulleroid

The Fulleroid is a highly overconstrained single dof linkage. The linkage has 24 ternary and 24 binary links connected by a total number of 60 revolute joints (Figure 5.1). There are 6 loops comprising 4 binary and 4 ternary links and 6 loops comprising 3 binary, 6 ternary links and 3 revolute joints. In all configurations, the linkage is bounded by a rhombic dodecahedral shape of varying scale. Although this enclosing polyhedral shape has 12 faces, the geometry described will be considered to be a 24-faced polyhedron, 12 pairs of faces being coplanar. The reason for this way of thinking will be apparent in the following paragraphs.

---

<sup>1</sup> The main content of this chapter is published by Kiper (2009a).

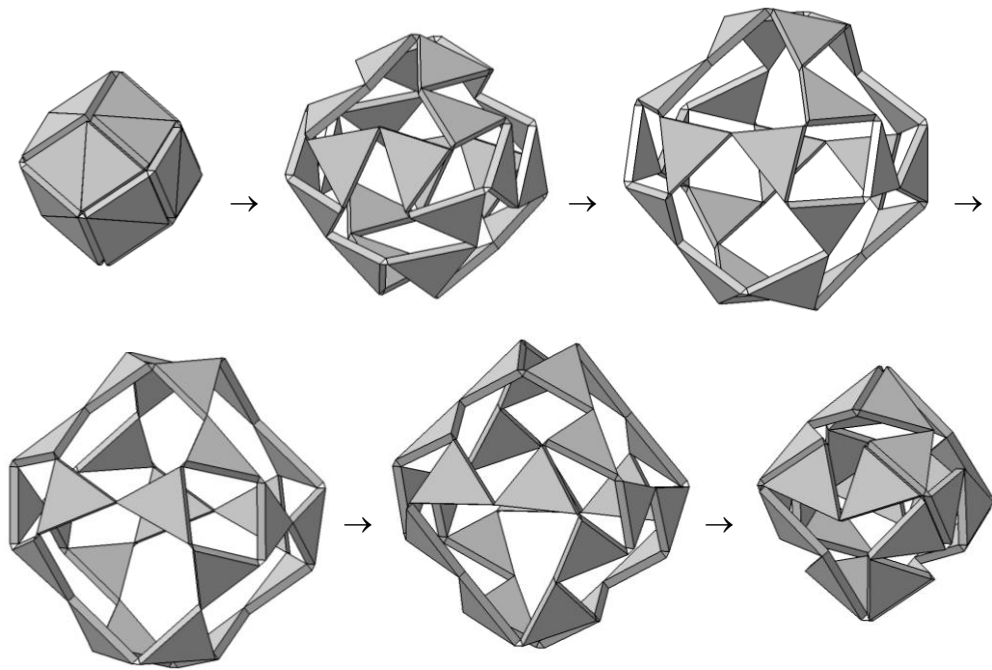


**Figure 5.1** The Fulleroid in motion

## 5.2 Icositrahedral Linkages

As a first question, what if binary links are inserted into the revolute joints joining the ternary links of the Fulleroid and ternary link dimensions are changed accordingly? That is, what if the 24-faced polyhedron, i.e. the icositrahedron, had no coplanar faces while it had the same group of symmetries (the octahedral group)? The infinite family of polyhedra described by the cumulation series of the cube satisfy these conditions. The cumulation series of the cube is illustrated in Figure 5.2.

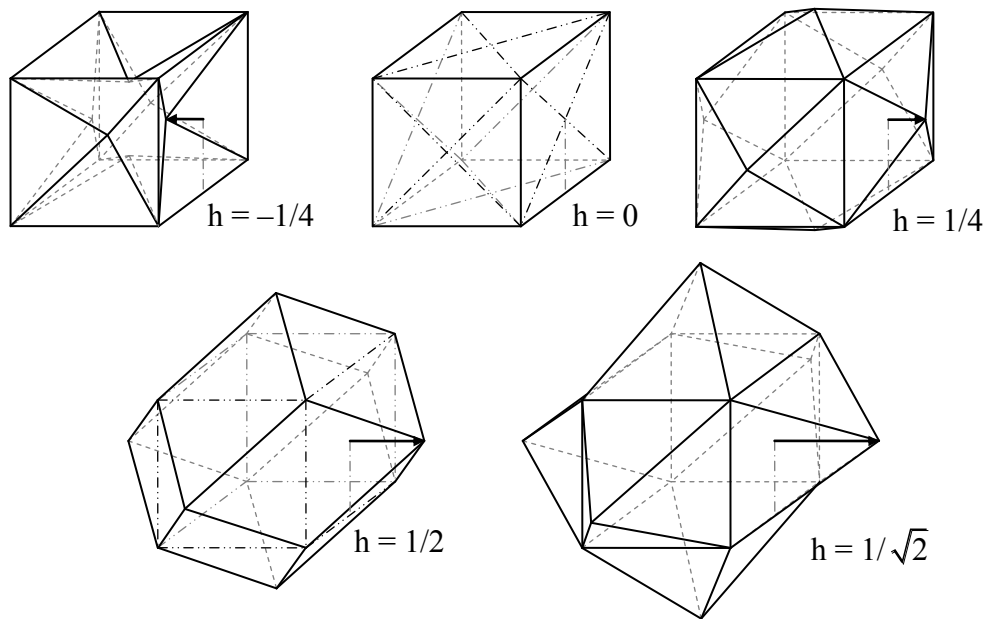


**Figure 5.2** Some cumulations of a cube with unit edge length: A concave icositetrahedron, the cube, the tetrakis hexahedron, the rhombic dodecahedron and another concave icositetrahedron;  $h$ : cumulation depth.

If the faces of these cumulations are connected by dihedral angle preserving links, the resulting linkages are movable with single dof (Figures 5.3-6). The mobility checks were performed by running a kinematic simulation in Catia V5.R19<sup>®</sup> DMU Kinematics module. The cubic linkage of Figure 5.4 was further issued by Röschel (2010). For a physical model of a concave linkage the thickness dimensioning should be done carefully, because overlapping occurs when simple prism-shaped links are used. Note that the concave linkage in Figure 5.6 is fully closed in both limit configurations.

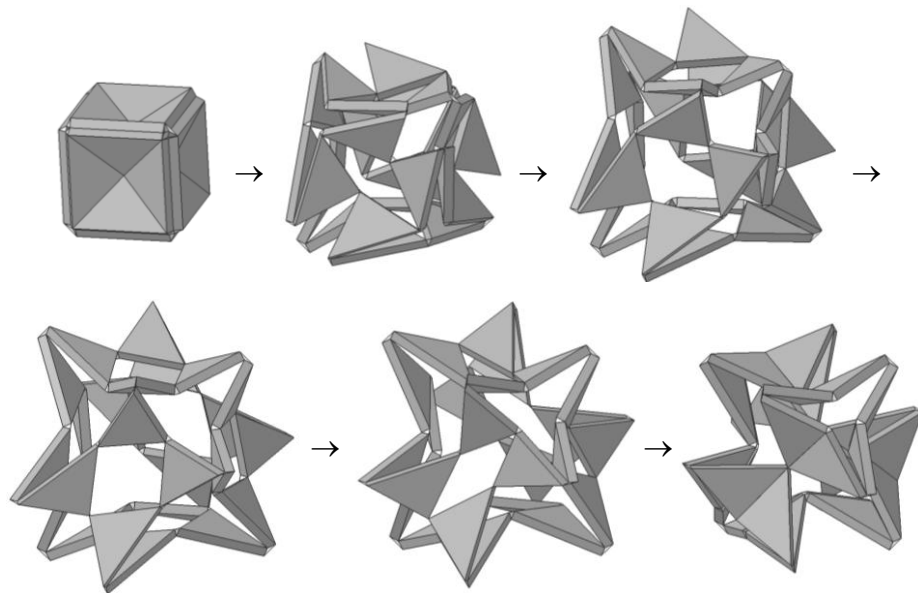


**Figure 5.3** A concave icositetrahedral linkage (obtained by cumulating the cube inwards by 1/4th of the edge length)

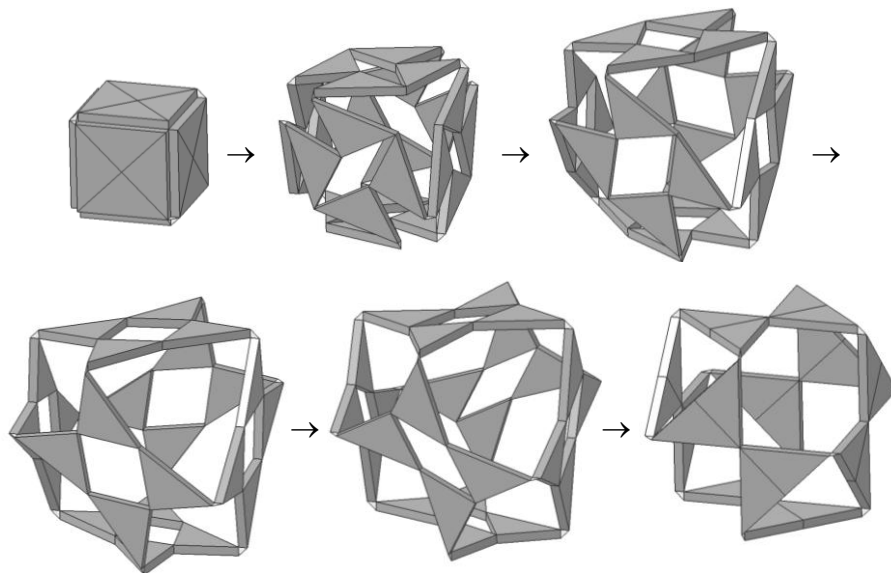


**Figure 5.4** A cubic linkage

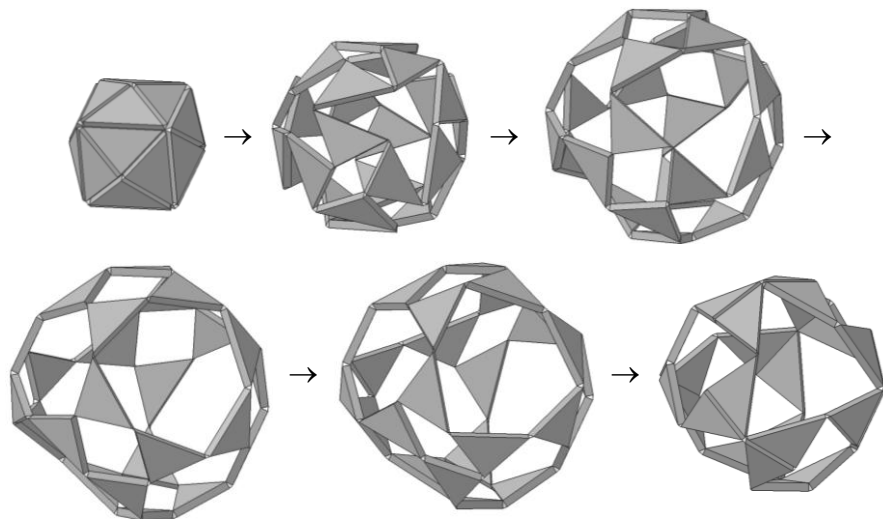


**Figure 5.5** A tetrakis hexahedral linkage (obtained by cumulating the cube outwards by  $1/4^{\text{th}}$  of the edge length)

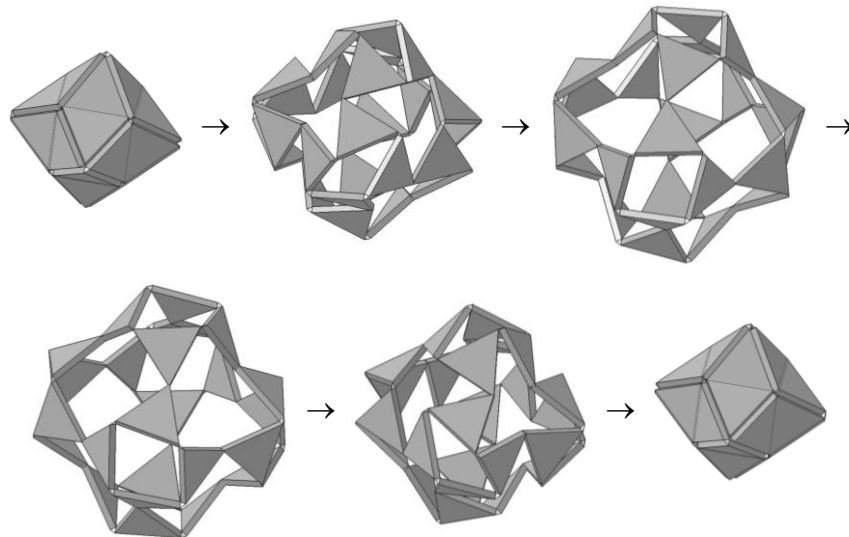


**Figure 5.6** A concave icositetrahedral linkage (obtained by cumulating the cube outwards by  $1/\sqrt{2}^{\text{th}}$  of the edge length)

### 5.3 Rhombohedral Linkages

Next question is what if the cube is distorted such that a rhombohedron is obtained. Another icositetrahedral linkage is obtained if three of the binary links (out of twelve) of the cubic linkage are removed (Figure 5.7). Note that the expansion is not uniform in this linkage, i.e. not all of the faces perform similar expansion. This is probably because of the non-uniformity of the vertices: at three of the vertices the plane angles are not all equal. This linkage, maybe, should not be considered in the same class with the previous ones, but it is a quite notable spatial linkage. Due to the tripod-like appearance of the final phase of the linkage it shall be named as the tripodohedral linkage.

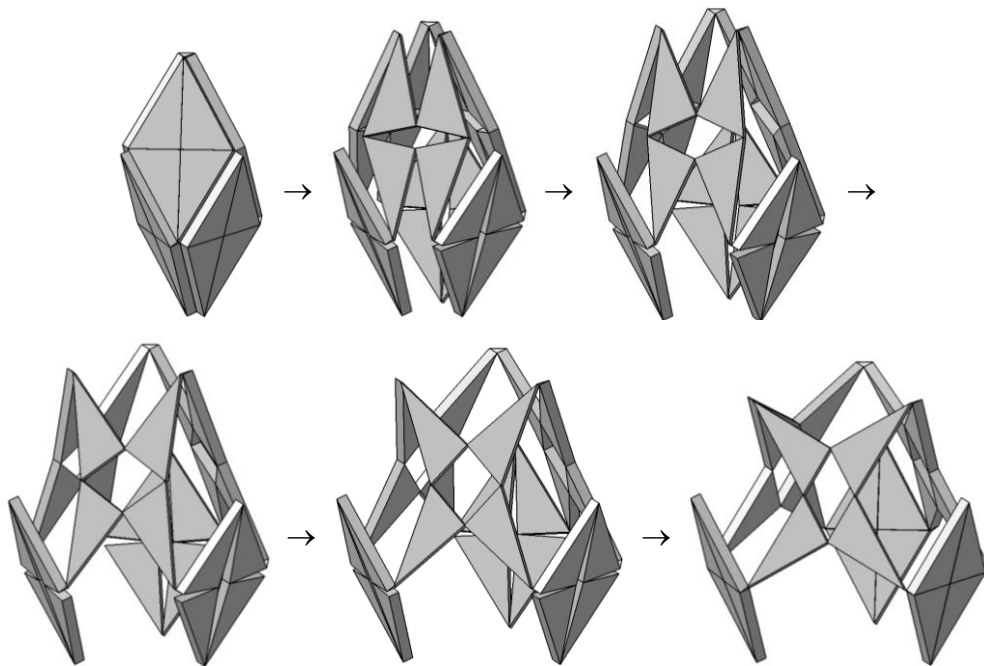


**Figure 5.7** A rhombohedral linkage that has faces with  $\sqrt{2}:1$  diagonal ratio



## 5.4 Dipyramidal and Stellated Linkages

In the Fulleroid (Figure 5.1), tetrakis hexahedral linkage (Figure 5.5) and the concave icositetrahedral linkages of Figures 5.3 and 5.6, there is an assembly of a certain module, a spatial 8R (8 revolute) closed chain with the following properties: every joint axis is intersecting one of the neighboring axes and is parallel to the other, the four intersection points are separated by the closest distance between the four parallel axes, the distances being equal and two opposite intersecting joint axis pairs have the same angle in between (Figure 5.8). If the intersecting joint pair is called as a V joint (a 2 dof joint with two revolution axes – a gusset as named by Wohlhart (1995)), the linkage can be described as a 4V equilateral closed chain. Note that in the degenerate case,  $\alpha$  and/or  $\beta$  may be zero, in which case a VRVR or a 4R chain is obtained. Indeed, the Fulleroid has the VRVR chains and the cubic linkage has the 4R chains.

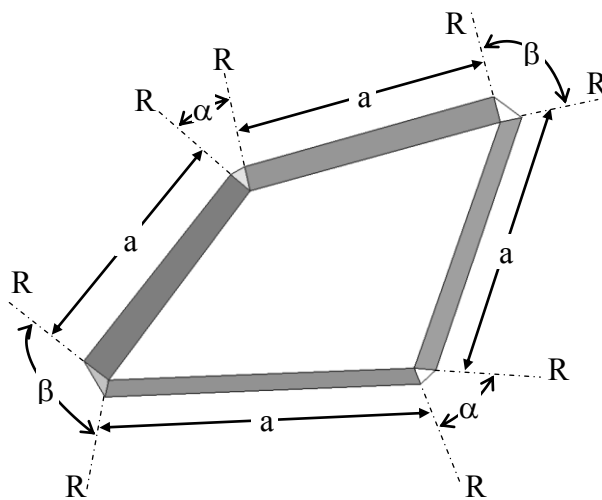


**Figure 5.8** A symmetrical spatial 8R closed chain

If one of the links of this linkage is fixed, the resulting mechanism has 2 dof. If four of these linkages are assembled to construct a loop using some more V and/or R joints, special design parameters are necessary to have mobility (See Chapter 6). Note that the 4V linkage can only be employed at 4-valent vertices (vertices at which four faces meet).

Using these 4V chains as modules, dipyrramids can be mobilized. For  $\alpha = \beta = 2\arctan(1/\sqrt{2}) = 70.53^\circ$ , if the six of the 4V linkages are assembled such that neighboring three equilateral links form a triangle, the Jitterbug (Fuller, 1975) is obtained. Some other dipolygonoids of Verheyen (1989) may also be synthesized this way (ex: cuboctahedral linkage  $8\{3\}+6\{4\}|54^\circ44'08''$ ).

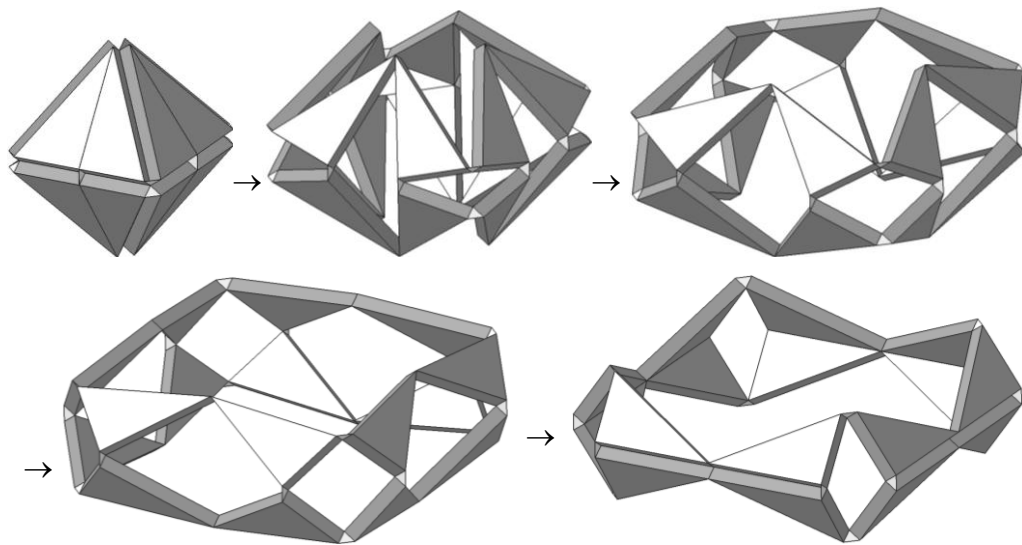


**Figure 5.9** An octahedral linkage

Another way of mobilizing the octahedron is to dissect each face into two, hence obtaining 16-faced linkages (Figure 5.9). The triangular faces of the polyhedral shape need not be equilateral (Figure 5.10). For these linkages, as the number of the sides of the base polygon increases, the openings about the apexes become larger and a ring-like form is obtained.

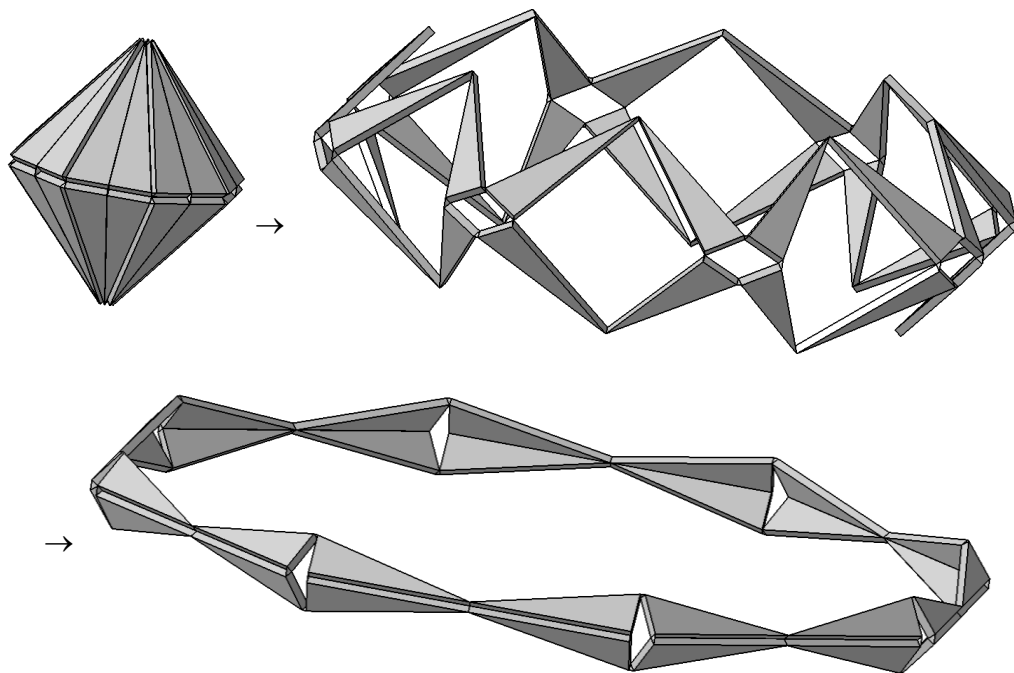


**Figure 5.10** An octagonal dipyramidal linkage

Also, the 4V chains can be used to mobilize stellated polyhedra (Figure 5.11 – VRVR chains are used in this example).

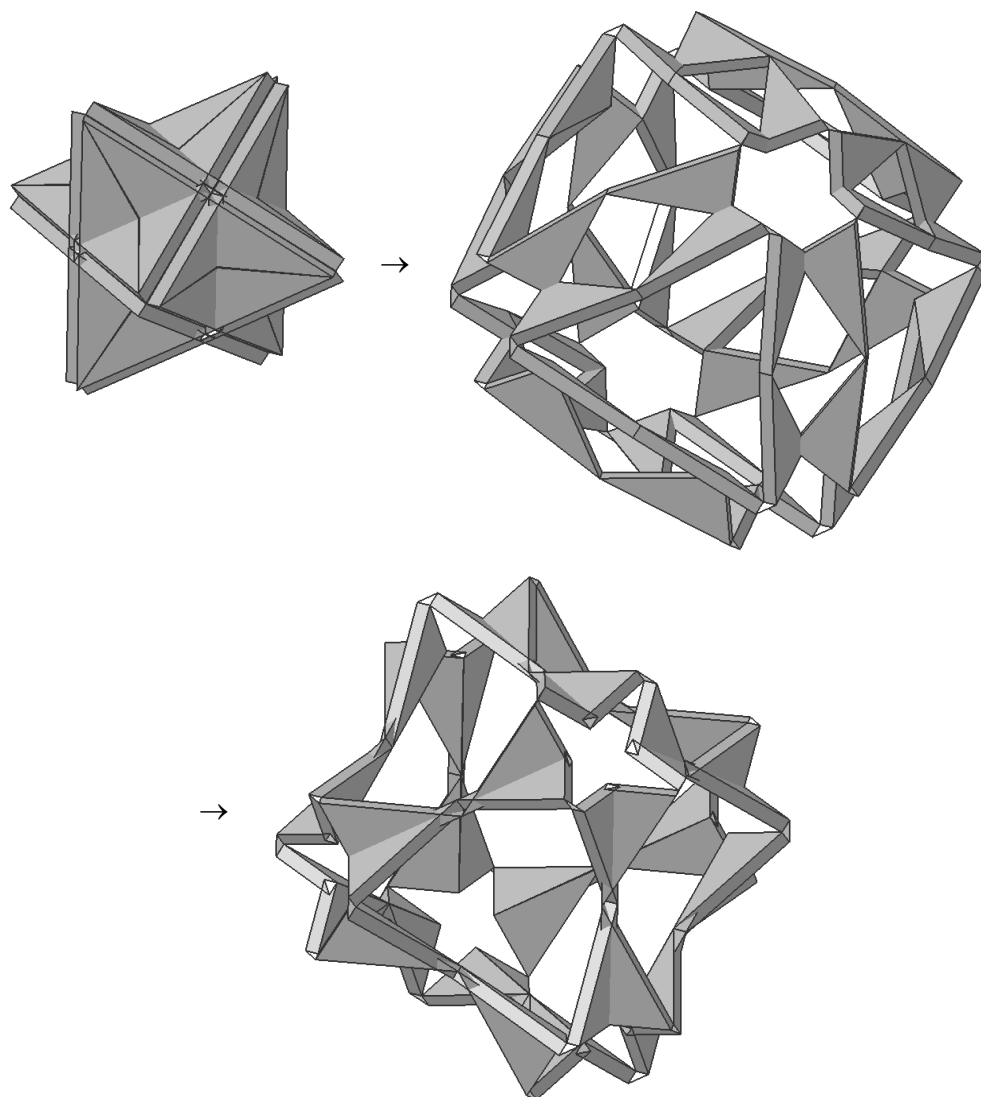


**Figure 5.11** A stella octangula linkage

The linkages synthesized here, except the tripodohedral linkage, are special cases of Röschel's (2001) so-called "unilaterally closed mechanisms". Here unilateral closure means one-side matching of a rectangular planar graph, just like wrapping a plain paper into a cylinder by matching two opposite ends.

## CHAPTER 6

### JITTERBUG-LIKE LINKAGES

Verheyen (1989) and Röschel's (1995, 1996a, 1996b, 2001) approach to synthesize Jitterbug-like polyhedral linkages is to consider the in-plane motion of a polygonal element and transfer this motion spatially by transforming them into neighboring planes. Once the motions are interrelated, the whole structure is mobile bound to certain criteria. As oppose to this approach, in this chapter, the spatial loops that comprise the linkage are examined to reveal some properties of Jitterbug-like linkages.

#### 6.1 Jitterbug-like Linkages<sup>1</sup>

##### 6.1.1 Some Observations and A Formal Definition

For the linkages in Verheyen (1989), Röschel (1995, 1996a, 1996b, 2001) and Wohlhart (1995), in general, there corresponds single link for each face of the polyhedral shape. In some cases though, there are overlapping pairs of links on faces (Figure. 6.1). In some of Verheyen's (1989) and Wohlhart's (1995) linkages there are planar chains on the faces. As illustrated in (Kiper, 2009a), these linkages are in general degenerate cases of a more general family of

---

<sup>1</sup> The main content of this section is published by Kiper (2010a).

linkages, where some of the faces of the polyhedral shape coincide. In all these linkages, a separate face will be considered for each link even if some planes coincide.

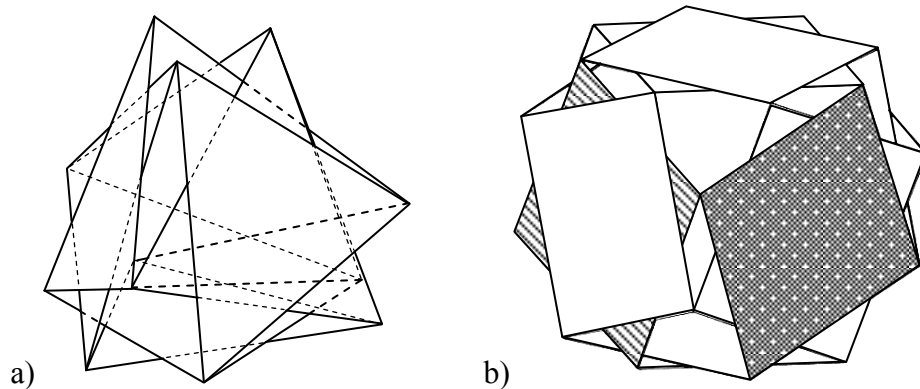


**Figure 6.1** Two of Verheyen's (1989) dipolygonoids comprising a) 4 double faces (also issued by Stachel (1994) as the Heureka Polyhedron with tetrahedral motion) and b) 6 double faces with overlapping link pairs

In general each loop is used to obtain expansion/contraction around a vertex. However, for some cases, the supporting faces do not intersect all at a point, such as the ones demonstrated in Figure 6.2. In this section, such cases are not considered; the focus is on linkages for which each vertex is surrounded by a spatial loop.

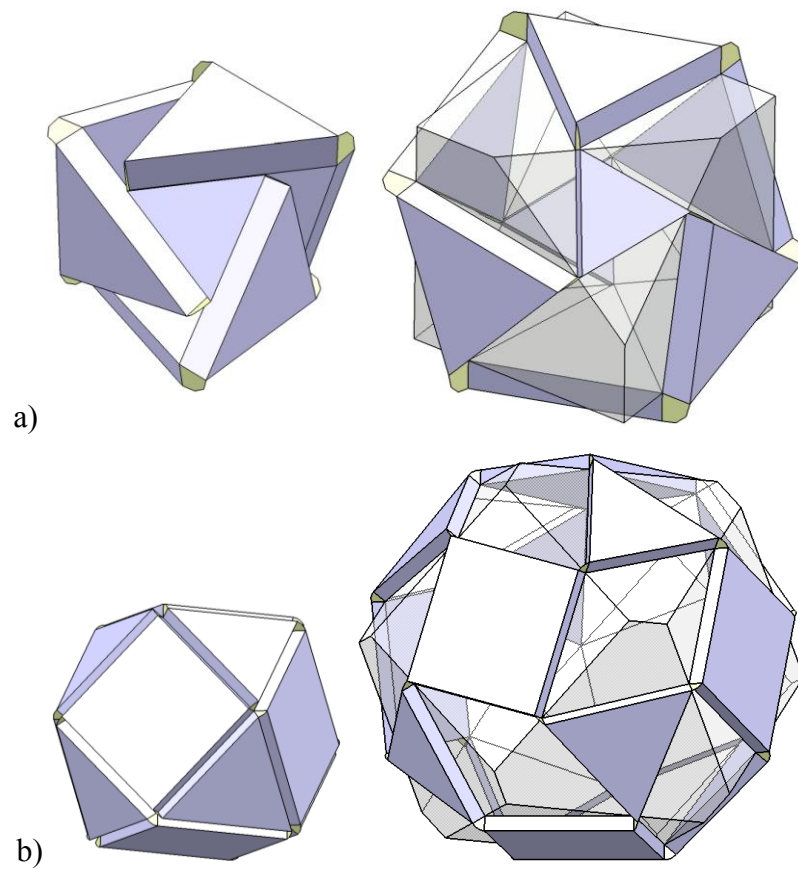


**Figure 6.2** a) An octahedral linkage (Röschel, 1996a), b) a cuboctahedral linkage (Verheyen, 1989; Röschel, 1995) and their supporting polyhedra

Taking a closer look at these linkages, it is seen that adjacent joint axes are either parallel, or intersecting. The small links between the intersecting joint pairs are *dihedral angle preserving* (dap for short) elements. The links between the parallel ones are links on the faces, which can be referred to as the *polygonal links*.

By constructing the supporting polyhedron for many configurations of the octahedral linkage in Figure 6.2a, it is seen that not only the dihedral and planar angles are preserved, but also the conformal transformation is a proper dilation due to the existence of an inscribing sphere (Röschel, 1996b). However, for the cuboctahedral linkage in Figure 6.2b, the square faces and the triangular faces dilate in different proportions, hence the total transformation of the supporting polyhedron is not a dilation. Furthermore, when all planes are intersected, the corners of the triangles are chopped off and hexagons are formed. The hexagons have variable side length ratios. So, the supporting polyhedral shape transformation is not dilative for all Jitterbug-like linkages.

With these observations, a Jitterbug-like linkage can be defined as follows:

**Definition:** Let  $E$  and  $F$  denote the number of edges and faces for a polyhedral shape  $P$ . A Jitterbug-like linkage associated with  $P$  is a mobile assembly with the following properties:

1. There are two types of links: polygonal links and binary (dihedral angle preserving or dap) links.
2. All joints are revolute.
3. No polygonal/dap link is directly connected to another polygonal/dap link.
4. To every face of  $P$  there corresponds one and only one polygonal link ( $\Rightarrow$  Number of polygonal links:  $F$ )
5. The joint axes of a polygonal link are all parallel to each other, while the axes of a dap link intersect each other.
6. The plane of axes of a binary link remains perpendicular to a corresponding edge of  $P$ .



7. Joint axis intersections of dap links around a polygonal link are coplanar and these planes remain parallel to corresponding faces of  $P$ .
8. In any configuration the planes defined by joint axes intersections bound a finite volume, called the supporting polyhedron, and this shape can be obtained from  $P$  by a conformal transformation. The topological shape of the supporting polyhedron is invariant and this topological shape will be named as the base polyhedron.

A wholly representative Jitterbug-like linkage is obtained if the following properties are also satisfied:

9. Number of dap links:  $E$ .
10. To each vertex of  $P$  there corresponds a spatial loop comprising revolute joints twice as many as the corresponding vertex valence.

The latter are named as wholly representative, because in addition to every face corresponding to a face, every edge and vertex is represented by a dap link and a spatial loop, respectively. The Jitterbug is an example of a wholly representative linkage. Two examples of non-wholly representative Jitterbug-like linkages are given in Figure 6.2. The rest of this section issues the wholly representative linkages, only.

### **6.1.2 Some Properties of Suitable Spatial Loops**

In this section, some conditions for suitable polyhedral geometries and some properties of suitable loops are investigated. Since a vertex of a polyhedron is at least 3-valent, the simplest loop shall involve 3 pairs of intersecting or

parallel joint axes. However in most cases odd-valent vertices cannot be used around an odd-valent vertex as mentioned by Wohlhart (1998). The motivation in claiming this is the fact that instantaneous screw axes are fixed and so neighboring polygonal links rotate in opposite senses at all times. The links rotating in opposite senses is generally true; at least there is no counterexample so far. However, when one just concentrates on a spatial loop around a vertex, it is seen that it may be the case where two neighboring polygonal links rotate in the same sense. This is due to the Cardan motion of a polygonal link in its plane of motion. Again, there is no example of such a linkage so far, hence for the time being, it shall be assumed that all vertex valences are even. This issue is cleared for homothetic Jitterbug-like linkages in the next section.

There are also some tricks to design a Jitterbug-like linkage for a polyhedral shape with odd-valent vertices, such as employing multiple links in a face (Figures 6.1 and 6.3), where the 3-valent vertices are converted to 6-valent ones. Another trick is embedding offsets between dap links (Figure 6.4). In this case, the dap links are doubled in number and the dihedral angles are halved. These offset links are nothing but digons and by embedding them the number of edges is doubled, and so are the vertex valences. In each case, eventually, the supporting polyhedral shape is altered.

The two joints of a dap link are generally considered as a single joint and the link is not counted as a link in literature. Wohlhart (1995) uses the terms “double rotary joint” or “gusset”, while Röschel (2001) prefers “spherical double hinges”. Here, for brevity and due to the shape of the links, this 2-dof joint will be called a “V joint”.

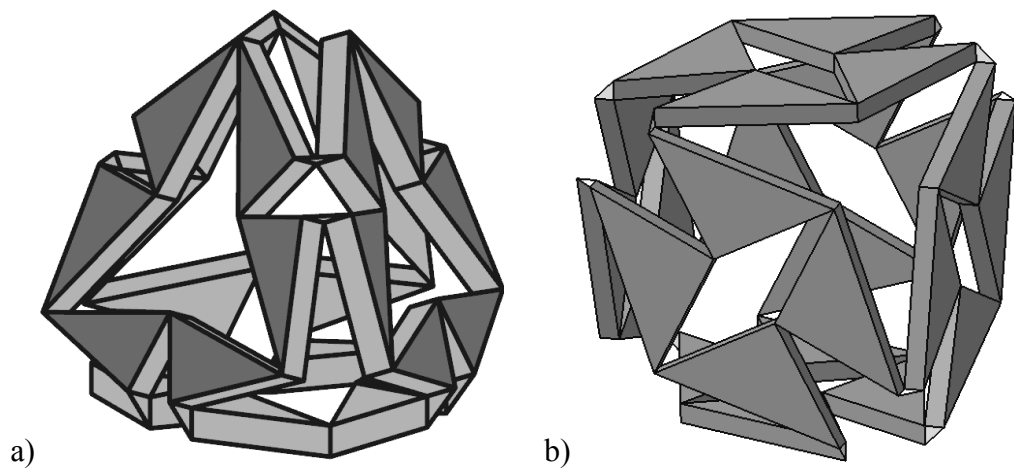


**Figure 6.3** a) A tetrahedral (Wohlhart, 2001b) and b) a cubic (Kiper, 2009b) linkage with multiple links in a face

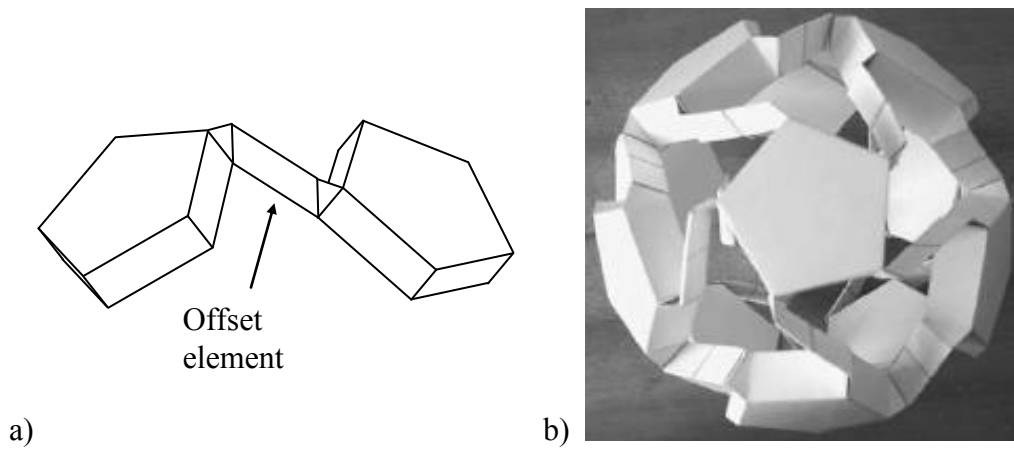


**Figure 6.4** a) An offset element and b) a dipolygonid of Verheyen (1989) re-issued as an expandable virus model by Kovács, Tarnai, Fowler and Guest (2004a)

For most of the linkages in literature, it is seen that generally they contain at least one 4V loop. However, as some counterexamples are already seen (Figures 6.1 and 6.4), there are some linkages with no 4V loops. Still, it can be showed that for the linkages with polyhedral geometries obeying Euler's formula  $V - E + F = 2$  there should be at least one 4V loop ( $V$ ,  $E$ ,  $F$ : number of vertices, edges and faces, respectively). For the proof, assume that the vertex valences are all greater than or equal to six. Then  $F \leq 6V/3$  (equal when all vertices are 6-valent and all faces are triangular) and  $E \geq 3V$  (equal when all vertices are 6-valent). So  $V + F \leq 3V$ , while  $E + 2 \geq 3V + 2 > 3V$ , hence Euler's formula is not satisfied and the assumption about the vertex valences is not valid. Polyhedral shapes involving concurrent faces and digons do not obey Euler's formula, so all vertex valences may be greater than four. Still, in the generic case 4-valent vertices should be expected.

### 6.1.3 The Spherical Indicatrix Associated With the Loops

In its most general meaning, the spherical indicatrix of a ruled surface is obtained by a cone of lines with its vertex at the center of a sphere, each line having a corresponding parallel generator on the surface. The indicatrix is the spherical curve of intersection between this cone and the sphere. It is used to separate rotations and translations in spatial linkages (Hunt, 1978, p.287).

Consider a spatial loop around a vertex such that adjacent joint axes are either parallel, or intersecting. The spherical indicatrix of such a loop does not distinguish between parallel axes. If the sphere is unit, the link lengths of this spherical linkage are " $\pi -$  dihedral angle"s and the angles between the links are " $\pi -$  plane angle"s. Since the joint axes are normal to the faces ( $\mathbf{n}_1, \mathbf{n}_2, \mathbf{n}_3$  in

Figure 6.5), the associated link lengths ( $\delta_{12}$ ,  $\delta_{23}$  in Figure 6.5) being “ $\pi$  – dihedral angle”’s is obvious. For the angles between the links of the spherical linkage, consider three adjacent faces meeting at a common vertex as shown in Figure 6.5. First move the tails of the face normals to the vertex. The angle between  $\delta_{12}$  and  $\delta_{23}$  is the angle between the normals  $\mathbf{b}_{12}$  and  $\mathbf{b}_{23}$  to  $\mathbf{n}_2$  that are in the planes defined by  $\mathbf{n}_1$  &  $\mathbf{n}_2$  and  $\mathbf{n}_2$  &  $\mathbf{n}_3$ , respectively. Then  $\mathbf{b}_{12}$  and  $\mathbf{b}_{23}$  are also normal to the edges  $e_{12}$  and  $e_{23}$ , respectively. The angle between  $\mathbf{b}_{12}$  and  $\mathbf{b}_{23}$ , say  $\beta_2$ , is then supplementary to the plane angle  $\alpha_2$ .

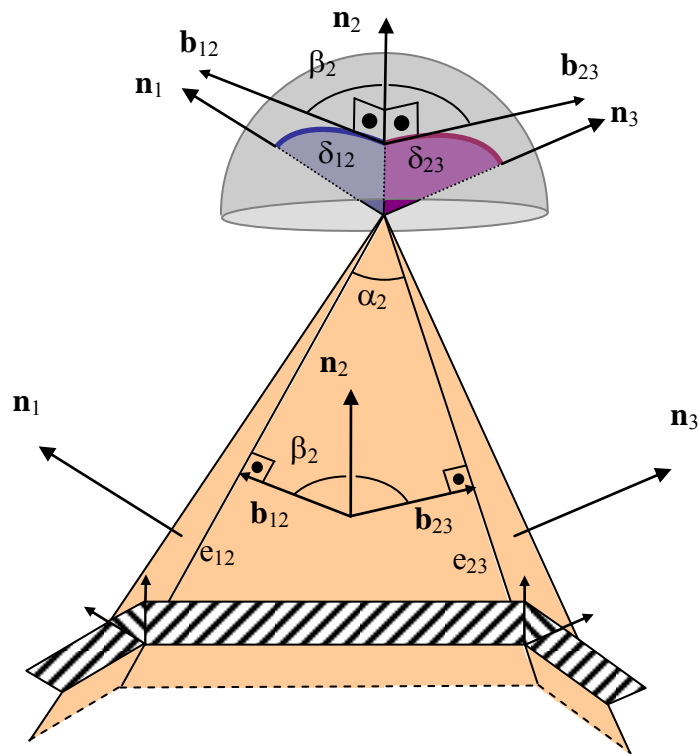


**Figure 6.5** Part of the neighborhood of a vertex (three adjacent faces) and part of the spherical indicatrix (two spherical links) associated with the spatial loop (dashed regions) around this vertex

For a conformal polyhedral linkage, neither the dihedral nor the planar angles should change. So the spherical indicatrix is dictated by the corresponding vertex figure and should remain unchanged during the motion. The side lengths and interior angles of a vertex figure are the planar angles and dihedral angles of the associated vertex, respectively and these angles fully define the spherical indicatrix that is dealt with here. The converse is also true: if the spherical indicatrices of all loops of a polyhedral linkage are fixed during the motion, the linkage should be a conformal polyhedral linkage. But, an assembly constructed for a specific polyhedral shape, such that the spherical indicatrices remain unchanged, may or may not be mobile – mobility is bound to special link dimensions.

If a loop has an immobile spherical indicatrix, it means that the dap links are constrained to move in pure translation with respect to each other. Now, the problem is how to get these constraints. Consider the relative motion of two polygonal links connected to each other via a dap link. The dap link ensures that the angle between the planes of the polygonal links remain constant during the motion. When all links are assembled together to enclose a polyhedral region, one can fix a coordinate system in space such that the instantaneous screw axes of polygonal links do not change their directions with respect to this frame for all times, i.e. the motion is a Schoenflies motion (see Bottema & Roth, 1979, sec. 9.5), as noted by Wohlhart (1997) for the Fulleroid. This fixed frame can be chosen to be attached to any of the links. Röschel (1996b) investigates the case where the motions of the polygonal links are fixed-axis Darboux motions (see Bottema & Roth, 1979, sec. 9.3).

To illustrate, take two such normal directions, say  $\mathbf{n}_1$ ,  $\mathbf{n}_2$  in Figure 6.5. As the directions of  $\mathbf{n}_1$  and  $\mathbf{n}_2$  do not change throughout the motion, the dap link in between realizes a translational motion along the perpendicular to  $\mathbf{n}_1$  and  $\mathbf{n}_2$ ,

i.e. along edge  $e_{12}$ . Of course  $e_{12}$  is not fixed in space and with respect to the fixed frame; the translation is curvilinear (see Verheyen, 1989, p. 208).

Several problems may occur in assembling the links. First of all, given a polyhedral shape, even if the polygonal and dap links are selected properly, the assembly may be immobile. As explained below, the spatial loops cannot be constructed arbitrarily, and even if all the loops are mobile individually, the assembly of the loops, which is a loop of loops, may be immobile. If the assembly is mobile, still it may not be a conformal polyhedral linkage. Also there is no guarantee of obtaining a single linkage. Multi-dof assemblies arise, for instance if diagonal links are used: If 12 digons are added to a regular octahedron and proper dap links are inserted, the resulting linkage has multi-dof (In Verheyen's notation  $12\{2\} + 8\{3\}|35^\circ 15' 52''$  - Figure 14a in (Verheyen, 1989)).

Next, the overconstrainedness of the spatial loops shall be demonstrated. An  $nV$  loop comprises  $2n$  revolute joints and  $2n$  links (disregarding the degenerate case where some axes are coincident). According to CGK formula, in general such a loop possesses  $6(2n - 1) + 5 \cdot 2n = 2n - 6$  dofs. If the special condition that the joint axes are pairwise parallel is not imposed, the spherical indicatrix of such a loop comprises  $2n$  revolute joints and  $2n$  spherical links and has  $3(2n - 1) + 2 \cdot 2n = 2n - 3$  dofs. Constraining the  $2n - 3$  dofs of the spherical indicatrix, the loop has  $2n - 6 - 2n + 3 = -3$  dofs; hence it is a structure unless some special geometric conditions are imposed. The special conditions on the axes are that adjacent joint axes are either parallel, or intersecting. These conditions make the indicatrix an  $n$ -link spherical linkage, instead of a  $2n$ -link one. When the indicatrix has  $n$  links, it has  $n - 3$  dof(s), and so the loop has  $2n - 6 - n + 3 = n - 3$  dof(s). For the  $4V$  loop, with these conditions on the axes only, the loop has single dof, however, still special link dimensions are

necessary to for such a single dof loop to be used around a vertex figure of a Jitterbug-like linkage. Also not all vertex figures may be suitable for such loops around them.

Finally, it will be showed that the spherical indicatrices of the vertices of a polyhedral shape constitute a spherical polyhedron. Consider the convex octahedron and the six spherical indicatrices of its vertices shown in Figure 6.6a. Each indicatrix defines a part of a ball with four disk fractions. To every edge, there corresponds two identical disk fractions, like the dark ones in Figure 6.6a. In total, there are twelve pairs of these disk fractions. Since these identical pairs are parallel to each other, if the ball fractions are assembled by mating the parallel disk fractions, a whole ball is obtained (Figure 6.6b). The octahedron is just an example, but the facts mentioned are generally true for all polyhedral shapes that can be projected to a sphere, because the spherical indicatrix for a vertex figure is the spherical projection of the dual facial figure. The projection does not tell much about the metric properties of the dual face, but just gives combinatorial information (see, ex. Galiliunas & Sharp, 2005).

In summary, the following properties and conditions are conceived for wholly representative Jitterbug-like linkages

- (i) Vertex valences of the base polyhedron are generally (but not necessarily) even.
- (ii) Spherical indicatrix of the linkage is immobile and the link dimensions of the indicatrix of a loop are uniquely given by the associated dihedral and plane angles.
- (iii) If base polyhedron obeys Euler's formula (specifically if it is convex) it contains at least one 4-valent vertex. Furthermore, in this case the



assembly of spherical indicatrices associated with the vertex figures results in a spherical polyhedron.

- (iv) Polygonal links have Schoenflies motion, dap links are in pure translation.
- (v) Due to the conformal transformation, dihedral and plane angles of the supporting polyhedron are the same during the motion, however side lengths vary.

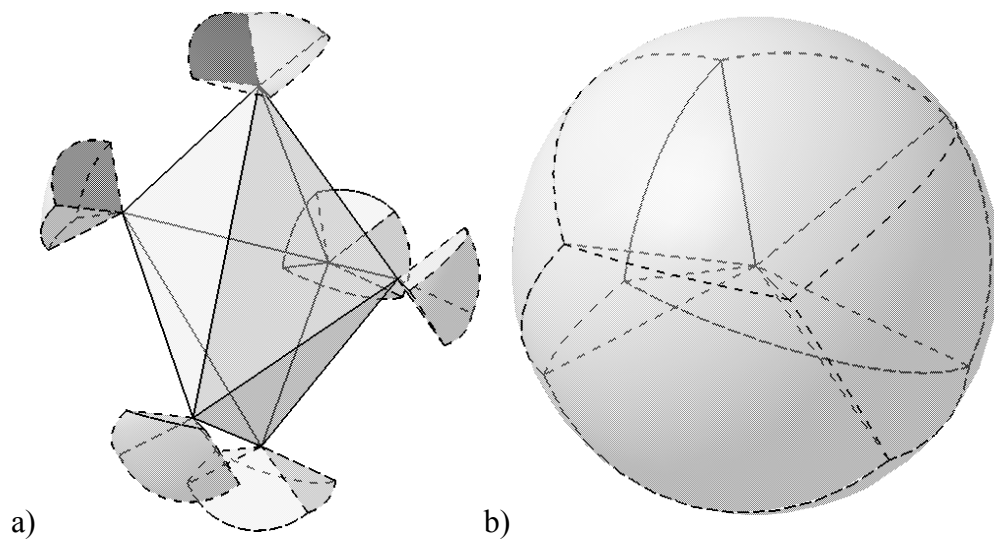


**Figure 6.6** a) An octahedron with the spherical indicatrices of its vertices,  
b) The spherical assembly of indicatrices

## 6.2 Homothetic Jitterbug-like Linkages

If all side lengths of the supporting polyhedron vary proportionally the transformation is a homothety and such linkages shall be called as *homothetic Jitterbug-like linkages*. The Heureka octahedron (Figure 1.2) and the linkage in Figure 6.2a are examples of homothetic linkages, while the linkage in Figure 6.2b is non-homothetic (square and triangular links depart from the polyhedron center at different rates). These facts will be proved in following subsections.

This section deals with the geometric conditions for a homothetic Jitterbug-like linkage. In this section Röschel's (1996, 2001) results are validated using different tools, it is shown in which cases these results are valid and the subject is further developed by new material.

### 6.2.1 Planar Considerations

For a homothetic Jitterbug-like linkage the supporting polyhedron is always similar at any configuration. If the supporting polyhedron goes through a homothetic transformation, so do the faces. In homothety of a polygonal face there is a polygonal link in motion (EFGH in Figure 6.7) and as the link moves the supporting polygon (ABCD in Figure 6.7), boundaries of which are given by the intersections with the neighboring planes of motions, dilates. The problem to be solved is how to locate a polygonal link inside a given a polygonal face so that a dilative motion is achieved.

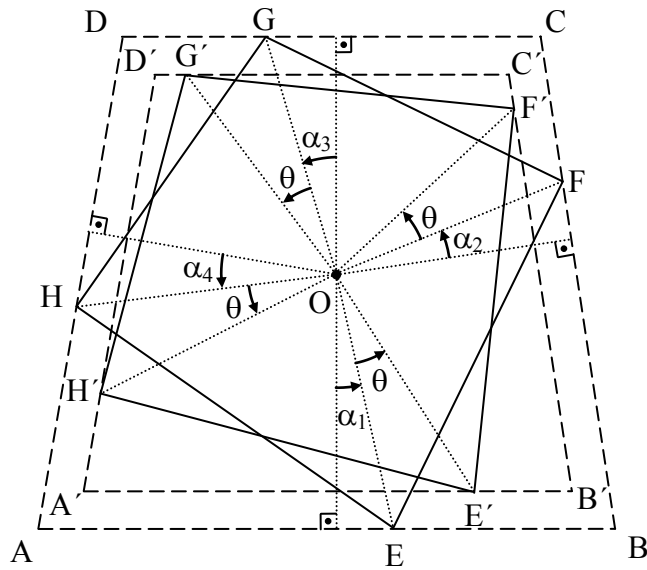


**Figure 6.7** A polygonal link and its supporting polygon in dilation

There is always an invariant point in a homothety unless it is a translation (Coxeter, 1967, p.94). This point is called the homothety center, say  $O$ . Given two similar polygons with parallel corresponding sides the homothety center can be located as the common intersection of lines connecting corresponding vertices (Coxeter, p.94). Assume two configurations of a polygon  $ABCD$  and  $A'B'C'D'$  (the example is a quadrilateral but the construction is valid for any polygon). Place a polygon  $EFGH$  inside  $ABCD$ . A rotated version  $E'F'G'H'$  is sought to be placed inside  $A'B'C'D'$ . Let the amount of rotation be  $\theta$ . Then the angle between the homologous lines  $OE-OE'$ ,  $OF-OF'$ ,  $OG-OG'$  and  $OH-OH'$  are all  $\theta$ . Note that  $O$  is not necessarily the center of rotation for  $EFGH$ , but assume that it is.

**Assumption 1:** Rotation centers of polygonal links are concurrent with associated homothety centers.

The homologous points for O coincide in the two poses. The amount of dilation can be measured by the distance of sides to the homothety center O. Drop perpendiculars from O to the sides of ABCD and let the angles between these perpendiculars and OE, OF, OG, OH be  $\alpha_1, \alpha_2, \alpha_3,$  and  $\alpha_4 \in (-\pi/2, \pi/2),$  respectively. Then

$$\begin{aligned} \cos(\alpha_i)/\cos(\alpha_i + \theta) = \cos(\alpha_j)/\cos(\alpha_j + \theta) &\Rightarrow \cos(\alpha_i)\cos(\alpha_j + \theta) = \cos(\alpha_j)\cos(\alpha_i + \theta) \\ &\Rightarrow \alpha_i = \alpha_j \end{aligned}$$

for  $i, j = 1, 2, 3, 4.$  So given ABCD and O, the corners E, F, G and H cannot be chosen arbitrarily. Once, say E is chosen, F, G and H should be selected such that  $\alpha_1 = \alpha_2 = \alpha_3 = \alpha_4 = \alpha.$  Without loss of generality take  $\alpha = 0,$  or consider the configuration where  $\theta = -\alpha$  as the initial configuration. At this position OE, OF, OG and OH are perpendicular to sides AB, BC, CD and DA, respectively and also the maximum size of ABCD is achieved. So given ABCD one may choose E, F, G and H as the points at the foot of perpendiculars to the sides from an arbitrary inner point O. Therefore, given a polygonal face first a point is selected inside and the foot of the perpendiculars to the sides from this point gives a polygonal link suitable for the purpose. Note that there are  $\infty^2$  possible choices for this inner point.

### 6.2.2 On the Instantaneous Screw Axes and Polyhedral Vertices

While the supporting polyhedron goes through a homothetic transformation there is an invariant point, i.e. the homothety center. Each vertex of the supporting polyhedron dilates with respect to this center with a dilation factor  $k$ . Also every corner of a polygonal face departs from each corresponding facial homothety centers issued in the former section with the same dilation factor  $k$ . So the facial homothety centers dilate with respect to the global homothety center with a dilation factor of  $k$ . If rotation centers of all polygonal links are assumed to be concurrent with the homothety centers of corresponding faces, then the instantaneous screw axes (ISAs) of the polygonal links are too dilated with respect to the global homothety center. The maximal volume of the polyhedral shape is achieved when one of the faces reach its maximum area. Assume that all the faces are maximal simultaneously. Then at this maximal size on every face, the rays from the rotation center to the polygonal link corners meet the polyhedron edges perpendicularly. Hence

**Assumption 2<sup>2</sup>:** At the maximal size of the polyhedral shape, rays from rotation centers to link vertices meet polyhedron edges perpendicularly.

Consider two rays from the rotation centers to the meeting corners of adjacent polygonal links. Through these two rays there passes a plane. At the maximal configuration this plane is perpendicular to the corresponding edge, so is also perpendicular to both of the faces meeting at this edge. Then it includes both of the ISAs, by which one concludes that ISAs of neighboring faces intersect each other.

---

<sup>2</sup> All the results and theorems in the following are valid under Assumptions 1 and 2.

If ISAs of adjacent faces intersect each other, it is natural to ask whether all the ISAs should meet at a common point. This is indeed the case in several known examples, like the Jitterbug and the octahedral linkage in Figure 6.2a, but not true in general. This shall be demonstrated with a counterexample: a snub disphenoidal linkage given in Figure 6.8 (Some ISAs are not drawn long enough but all neighboring axes intersect each other).

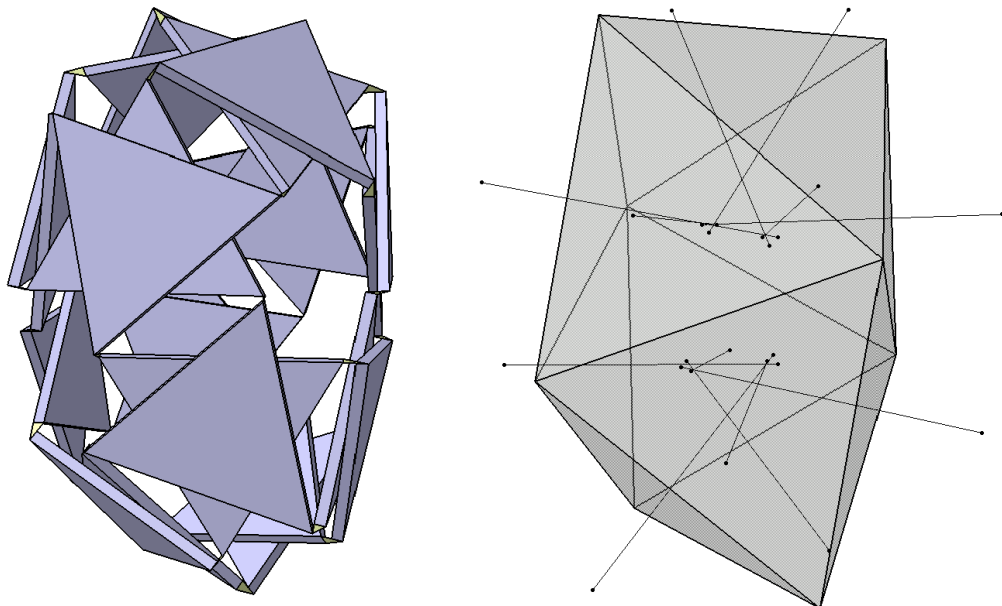


**Figure 6.8** Snub disphenoidal linkage, its supporting polyhedron and ISAs of triangular links

As a special case, if the base polyhedron has an inscribing sphere, all ISAs meet at a point, as investigated by Röschel, 1996. In this case the polygonal links realize Darboux motions with fixed ISAs. However Darboux motions do

not apply for the general case, as again the linkage in Figure 6.8 is a counter-example. When the ISAs are not fixed in space, they dilate with respect to the homothety center, i.e. an ISA stays in a plane. This cannot be a Darboux motion because the axodes are cylinders in Darboux motion (Bottema & Roth, 1979, p. 308).

With Assumption 2 if one link rotates in one sense, it is guaranteed that the neighboring ones rotate in opposite sense, at least in the neighborhood of the maximal configuration. This implies that the polyhedron vertices should have even valence. This fact is mentioned by Röschel (1996, 2001) and Wohlhart (1998), but not rigorously established as it is here. Hence

**Theorem 1:** For a homothetic Jitterbug-like linkage the ISAs of neighboring faces intersect each other. Furthermore, all the vertices of the base polyhedron should have even valence.

As oppose to the result on even valence, notice that the supporting polyhedron in Figure 6.8 has 5-valent vertices. Recall that in the definition for Jitterbug-like polyhedral linkages it is established there corresponds a single polygonal link to each face. There are 24 ternary links for the snub disphenoidal linkage and indeed the supporting polyhedron is not a mere snub disphenoid, but a double snub disphenoid. In a double polyhedron faces overlap pairwise. This is a standard trick to mobilize polyhedra with even valence known since Verheyen (1989).

When ISAs of neighboring faces intersect each other one can think of the motion of two neighboring rays (from rotation centers to concurrent corners of adjacent polygonal links) as the links of a CRRC linkage where the axes of C (cylindrical) joints and also R (revolute) joints intersect and adjacent C and R

axis are parallel. In Figure 6.9  $O_{12}$  and  $O_{23}$  are the homothety centers of neighboring polygonal faces and  $E_2$  is the common corner of the corresponding polygonal links.  $E_{12}$  moves along the intersection of two cylinders along ISAs  $\mathbf{n}_{12}$  and  $\mathbf{n}_{23}$  with radii  $r_{12}$  and  $r_{23}$ . In general two cylinders intersect along a 4<sup>th</sup> order spatial curve. Consider the projection of the intersection curve on the plane of the ISAs ( $xy$  plane in Figure 6.9). The components of any point  $(x, y)$  of this projection curve on  $\mathbf{n}_{12}$  and  $\mathbf{n}_{23}$  give  $s_{12}$  and  $s_{23}$  – the distances of polygonal links/faces to the ISA intersection  $O$ . For a dilative motion  $s_{12}/s_{23}$  should be invariant at all times, which is possible only if  $(x, y)$  is on a line and this is only valid if the trajectory of  $E_2$  is planar. Two cylinders with intersecting axis of revolution intersect along a planar curve only if they have the same radii (Verheyen, 1989, p. 208). So the perpendicular rays meeting at an edge should have the same length.

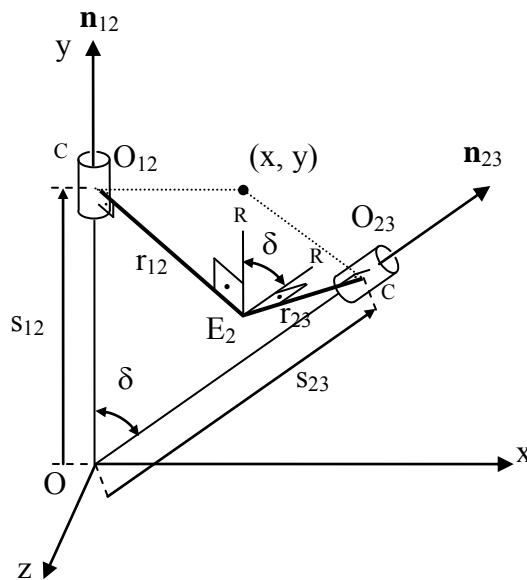


**Figure 6.9** Hypothetical CRRC linkage for two adjacent polygonal links



Consider an  $n$ -valent ( $n$  is even) vertex figure cut along an edge and expanded onto a plane as in Figure 6.10. If the perpendicular rays meeting at an edge have the same length, the plane angles  $\rho_{12}, \rho_{23}, \dots, \rho_{n1}$  at the vertex can be dissected as

$$\rho_{12} = \alpha_1 + \alpha_2, \dots, \rho_{n1} = \alpha_n + \alpha_1.$$

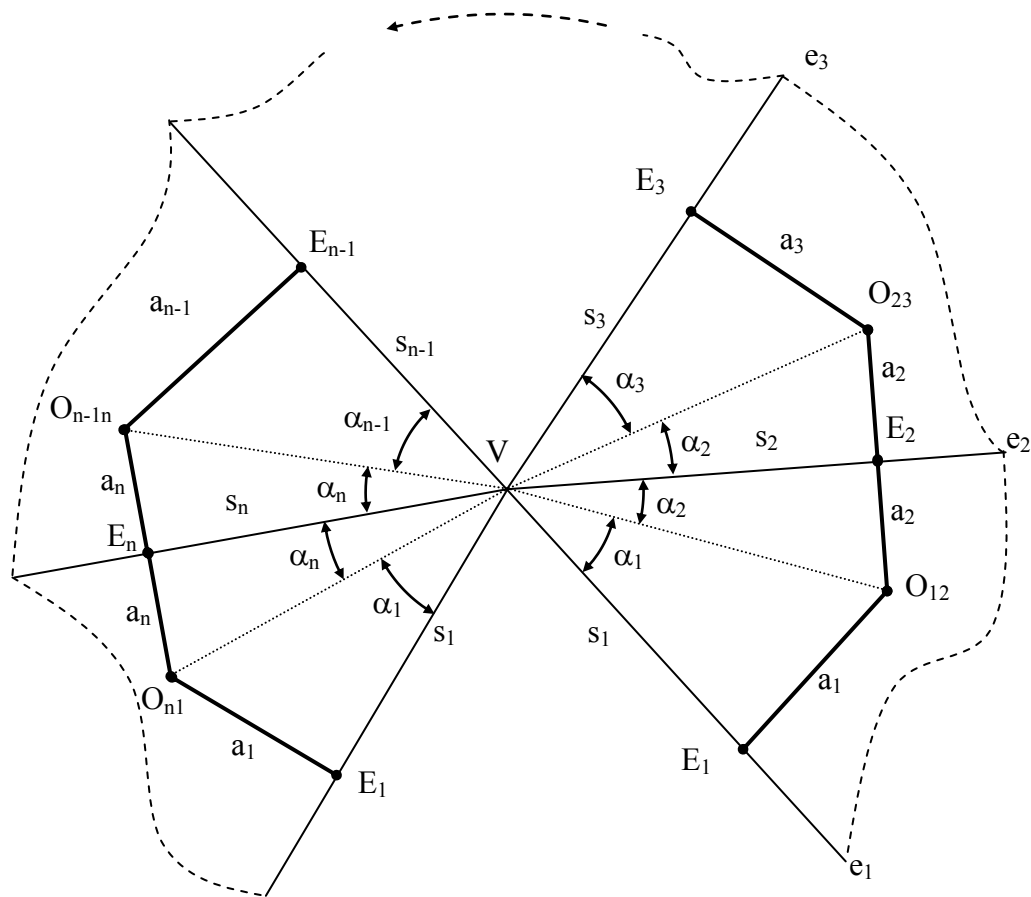


**Figure 6.10** An  $n$ -valent vertex figure cut along an edge

In matrix form these equations read

$$\begin{bmatrix} 1 & 1 & 0 & \cdots & 0 \\ 0 & 1 & 1 & \cdots & 0 \\ \vdots & \vdots & \vdots & \cdots & \vdots \\ 1 & 0 & 0 & \cdots & 1 \end{bmatrix} \begin{bmatrix} \alpha_1 \\ \alpha_2 \\ \vdots \\ \alpha_n \end{bmatrix} = \begin{bmatrix} \rho_{12} \\ \rho_{23} \\ \vdots \\ \rho_{n1} \end{bmatrix}$$

It can be shown by induction that this coefficient matrix has rank  $n - 1$  when the dimension  $n$  is even, so the plane angles  $\rho_{12}, \rho_{23}, \dots, \rho_{n1}$  cannot be arbitrary, but one of them must be depending on the others. This dependence can be expressed as

$$\rho_{12} + \rho_{34} + \dots + \rho_{n-1n} = \rho_{23} + \rho_{45} + \dots + \rho_{n1}. \quad (6.1)$$

This means that not all polyhedral shapes can be used as a supporting polyhedron for a Jitterbug-like linkage (with Assumptions 1 and 2).

This constraint is automatically satisfied if the doubling trick for an odd-valent vertex is used. Consider an  $n$ -valent vertex,  $n$  being odd. The plane angles will be such that  $\rho_{i,i+1} = \rho_{n+i,n+i+1}$  for  $i = 1 \dots n$  ( $2n+1 \equiv 1$ ), so Equation (6.1) is automatically satisfied because  $i^{\text{th}}$  term cancels  $n + i^{\text{th}}$  term.

Homothety centers of neighboring faces being equidistant to the common edge is the same thing Röschel (2001) gets with equiform motions in which he takes mirror symmetries of a planar motion. Röschel (2001) gives an example of constructing such linkages by choosing all rotation centers neighboring a polyhedron vertex on a circle. Is this the only case, or can one get different geometries? This question shall be answered in steps and case based.

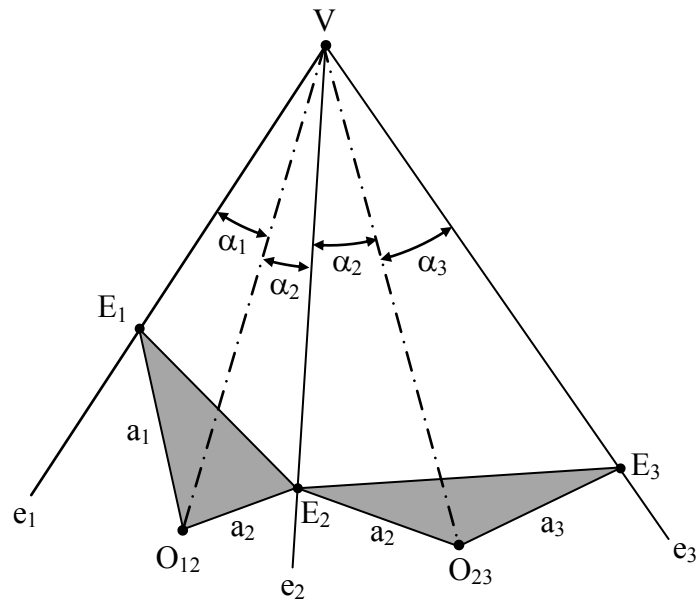


**Figure 6.11** Two adjacent polygonal links

Consider the motion of a corner of a polygonal link, say  $E_2$ , along its corresponding edge, say  $e_2$ . Assuming the notation in Figure 6.11, starting from the maximal configuration, as segment  $E_1E_2$  rotates by an angle  $\theta_{12}$ ,  $E_2E_3$  rotates by angle  $\theta_{23}$  in the opposite sense. The motion along the common edge must comply, so  $a_2\sin\theta_{12} = a_2\sin\theta_{23}$ , hence  $\theta_{12}$  and  $\theta_{23}$  are equal in amount.  $VE_2$  being common,  $E_2O_{12}$  and  $E_2O_{23}$  having the same length and being in symmetric position, by side-angle-side similarity  $|VO_{12}| = |VO_{23}|$  (varying) at all times. This if true for all  $VO_{ij}$ , therefore, the homothety centers on the faces around a vertex are equidistant to the vertex, hence are on a sphere centered at this vertex.

Notice that the motion of a segment  $E_1E_2$  in its plane is Cardan motion with respect to a frame located at  $V$ . The meet of perpendiculars from  $E_1$  and  $E_2$  to their corresponding linear paths should be on the moving Cardan circle, so  $O_{12}$  is on the moving circle. The center of the fixed centrode,  $V$  in this case, is always on the moving centrode. Since triangles  $VE_2O_{12}$  and  $VE_2O_{23}$  are congruent, they have the same size circumscribing circle. Therefore all the Cardan motions associated with the polygonal links are congruent, neighboring ones being in opposite senses. At the maximal configuration, i.e. when  $O_{ij}E_i$  and  $O_{ij}E_j$  are perpendicular to edges  $e_i$  and  $e_j$ ,  $VO_{ij}$  passes through the moving centrode center, hence in this position the fixed centrodes are on the above mentioned sphere centered at  $V$ . As the linkage departs from the maximal configuration the sphere contracts. Hence

**Theorem 2:** A mobile homothetic Jitterbug-like linkage can be obtained if and only if two homothety centers of neighboring faces are in symmetrical position with respect to the common edge.

**Proof:** The necessity of the symmetry condition is demonstrated above. To prove the sufficiency: Assume that one can locate a point  $P_i$  ( $i = 1 \dots F$ ) to each face  $i$  of a polyhedron such that all  $P_i$  are in symmetrical positions with respect to the edges. Choose a maximal size of the base polyhedron and consider the polygonal links constructed by dropping perpendiculars from  $P_i$  to the edges. Since  $P_i$  are symmetric with respect to the edges, the perpendiculars from symmetric  $P_i$  meet at the same point on the corresponding edge. Next consider a contracted version of the base polyhedron by a ratio of  $\cos\theta$ . As demonstrated in the previous section, the polygonal links constructed for the maximal configuration can be located into the new faces by rotating the links by  $\theta$  about  $P_i$ . The sense of rotation of adjacent links is opposite to each other and the links are kept parallel to their original positions by means of the dap

links. Meeting of the polygonal links is guaranteed by the symmetry condition, as explained above via Figure 6.9. This relocation of the links is possible for any angle  $\theta$ , so the assembly is mobile with the motion parameter  $\theta$ . ■

**Corollary 2:** If the homothety centers of any pair of neighboring faces are in symmetrical position with respect to the edge along the faces meet, the homothety centers on the faces around a vertex are equidistant to the vertex and the plane angles around a vertex can be dissected such that Equation (6.1) is satisfied.

**Proof:** Consider two homothety centers  $O_{ij}$  and  $O_{jk}$  on adjacent faces in symmetrical position with respect to edge  $e_j$ . Drop perpendiculars from  $O_{ij}$  and  $O_{jk}$  to  $e_j$  and let the foot be  $E_j$ . Denote one of the vertices of the edge by  $V$ . The triangles  $VE_jO_{ij}$  and  $VE_jO_{jk}$  are congruent due to side-angle-side similarity, so the homothety centers are equidistant to  $V$ . All  $VO_{ij}$  segments around a vertex dissect the associated plane angles as  $\rho_{12} = \alpha_1 + \alpha_2, \dots, \rho_{n1} = \alpha_n + \alpha_1$ , so Equation (6.1) is satisfied. ■

Why the linkage in Figure 6.2b is non-homothetic is now clear: The square and triangular links have the same side length, so they have different ray lengths  $|O_{ij}E_j|$ . Therefore, although Theorem 1 is satisfied for this linkage, Theorem 2 does not hold.

To assemble such loops around vertices to obtain a polyhedral linkage certain conditions are to be satisfied. Consider a base polyhedron with  $F$  many faces,  $E$  many edges and  $V$  many 3-valent vertices. The homothety centers on the faces meeting at a vertex should be equidistant to the corresponding vertex, so consider  $V$  many spheres centered at the vertices such that all spheres for a face intersect at a point, which is the homothety center of that face. The radii of the

spheres are the design parameters. In a face with  $S$  many corners/sides,  $S$  many sphere meeting at a point imposes  $S - 2$  constraints on the radii of the spheres. Then totally there are  $\Sigma(S_i - 2)$  constraints on the radii, where  $S_i$  is the number of the sides of  $i^{\text{th}}$  face and  $i = 1 \dots F$ . Noting that  $\Sigma S_i = 2E$ , number of constraints is  $2E - 2F$ . When the  $V$  parameters are chosen arbitrarily, there still remains  $2E - 2F - V = V - 2\chi$  constraints to be satisfied, where  $\chi$  is the Euler characteristic. Note that  $\chi \leq 2$  (See “Euler characteristic” in the Appendix), so  $V - 2\chi \geq 0$  which implies the overconstraint of the problem.

### 6.2.3 Conditions on the Supporting Polyhedron

As a result of the previous arguments the following theorem is obtained:

**Theorem 3:** A polyhedron can be used as a base polyhedron for a homothetic Jitterbug-like linkage if and only if one can locate spheres centered at vertices of the polyhedron such that on all faces, the associated spheres meet at a common point.

**Proof:** It is already illustrated that locating spheres centered at vertices of the polyhedron such that on all faces the associated spheres meet at a common point is a necessary condition. Now it should be showed that this condition is sufficient. Assume that there exist such  $V$  spheres for a polyhedron. Then the homothety centers should be the point of intersections of the spheres on the faces, which dictates that the homothety centers around a vertex are equidistant to the vertex. Consider two spheres centered at the two ends of an edge  $e_j$ . These two spheres intersect along a circle, which intersects the faces meeting at  $e_j$  at symmetrical points  $O_{ij}$  and  $O_{jk}$  with respect to  $e_j$ . So the homothety centers

are equidistant to  $e_j$ . Because this symmetry situation is valid for all edges meeting at a vertex, the plane angles can be dissected such that (6.1) is satisfied. The result follows by Theorem 2. ■

So the cost of the  $V - 2\chi$  constraints mentioned at the end of previous section is to be paid by selecting base polyhedra that satisfy Theorem 3.

## 6.2.4 Special Cases

### 6.2.4.1 Homohedral Linkages

A homohedron is a polyhedron with congruent faces. Using the information in sections 6.2.1 and 6.2.2 the following theorem can be devised for homohedral linkages:

**Theorem 4:**  $\infty^2$  many homothetic Jitterbug-like linkages can be obtained if the supporting polyhedron is a homohedron.

**Proof:** Two adjacent faces of a homohedron meet along a common edge, hence the faces are necessarily in mirror position with respect to the edge they meet along. Take one of the faces, say  $F$ , and construct a polygonal link by taking an arbitrary point, say  $O_F$ , ( $\infty^2$  many possible choices) inside the face and dropping perpendiculars to the sides. Since all faces and hence all polygonal links are congruent, when assembled the polygonal links and the homothety centers  $O_F$ 's will be in symmetrical position with respect to edges. By Theorem 2 the assembly is mobile. ■

Of many homohedra found in the literature, the isohedra are of special interest. Isohedra are convex polyhedra which look exactly the same no matter which face one looks at (Cromwell 1997, p. 367). All the linkages of Chapter 5 are isohedra, as well as are the Platonic solids, Catalan solids, dipyrramids and trapezohedra. A non isohedral homohedron example is the snub disphenoid, the associated linkage of which is illustrated in Figure 6.8.

#### **6.2.4.2 Polyhedra With 3-Valent Vertices**

3-valent vertices are considered only for double polyhedra and hence actual vertex valence is 6. Considering a 3-valent vertex neighborhood, starting from a point on one of the faces, dropping perpendiculars to the sides and taking mirrors one can locate 6 links to the faces as in Figure 6.12a. When the two ends of the links are bound to their respective linear guides the resulting planar linkage is mobile with single dof due to their Cardan motion (Figure 6.12b).

Although the assembly in Figure 6.12 is mobile, homothety centers cannot be kept arbitrary if Assumption 1 is to be satisfied. So the rotation centers of two links on an overlapping face are forced to be concurrent. Then, in the maximal configuration the corners of the coplanar polygonal links on the faces should coincide, i.e. identical links should be used on overlapping faces.



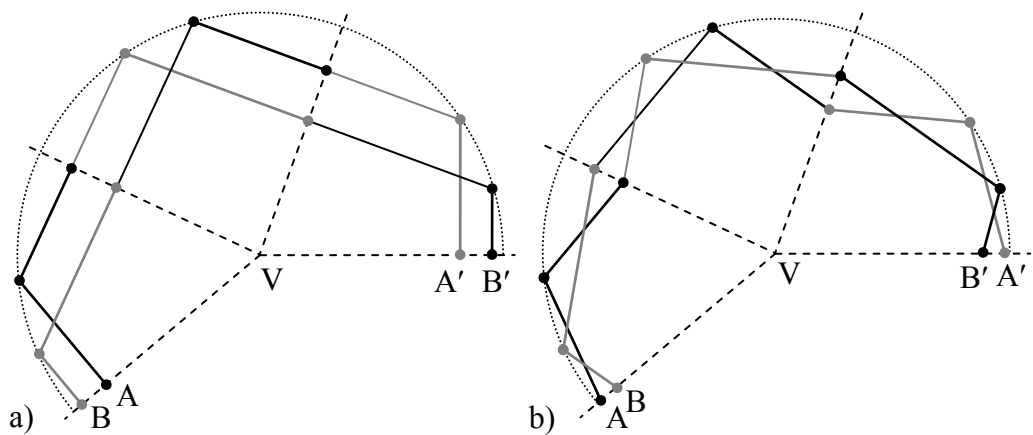


**Figure 6.12** A double 3-valent vertex cut along an edge and expanded to the plane and 6 links around it – a) maximal configuration, b) arbitrary configuration

For 3-valent vertices, there always passes a circle through the 3 homothety centers  $O_{ij}$  around the vertex (Figure 6.13). Since  $O_{ij}$  are equidistant to the vertex  $V$ , the line joining  $V$  and the center of the circle, say  $V'$  is orthogonal to the plane of the circle. So lines  $VO_{ij}$  are on a right cone. Consider the ISAs of polygonal links passing through  $O_{ij}$ . Every ISA should intersect the neighboring one. Consider the plane defined by two of the ISAs. The point of intersection of these two axes with the third one is on this plane, but the third ISA intersects this plane at a single point, so necessarily the three ISAs should meet at a single point. If all the vertices of a polyhedron are 3-valent, then all ISAs meet at a single point, meaning the position of all ISAs with respect to each other are fixed during the motion. In this case, it is guaranteed that the motion of the links are Darboux motions with fixed ISAs.

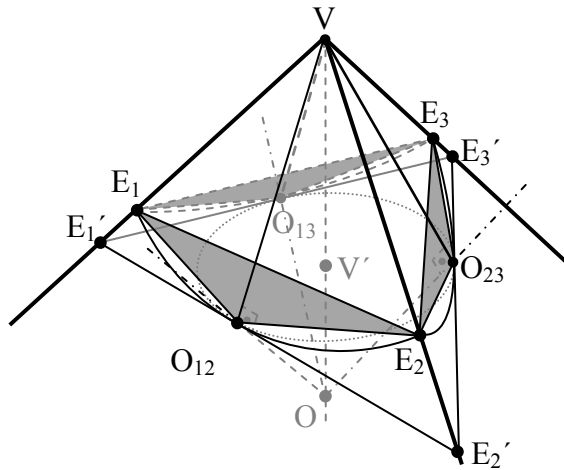


**Figure 6.13** A 3-valent vertex and a loop around it at maximal configuration

One case where ISAs are concurrent is already mentioned: when the base polyhedron has an insphere. Is this the only case? The answer is positive: Denote the point of intersection of the ISAs as  $O$ . Since homothety centers  $O_{ij}$  neighboring a vertex  $V$  are on a right cone,  $\angle OVO_{ij}$  are all equal to the cone angle.  $|VO_{ij}|$  are all equal and  $VO$  is common, so the triangles  $VO_{ij}O$  are congruent implying  $|OO_{ij}|$  are all equal for a vertex  $V$ . Proceeding to adjacent vertices it is seen that  $|OO_{ij}|$  are all equal for all faces, so

**Theorem 5:** If all the vertices of a homothetic Jitterbug-like linkage are 3-valent, the base polyhedron should have an inscribing sphere.

So if a polyhedron has only 3-valent vertices, one cannot find a homothetic linkage satisfying Assumptions 1 and 2 if not all the faces are tangent to an insphere. For example a rectangular prism cannot be used as a base polyhedron unless it is a cube.

For tetrahedra, there is always an insphere, so all tetrahedra is a base polyhedron for a homothetic linkage. Here is an example: Consider the tetrahedron with vertices  $(0, 0, 0)$ ,  $(100, 0, 0)$ ,  $(70, 60, 0)$  and  $(40, 20, 90)$ . It is easy to locate the inscribing sphere by finding the point equidistant to all four faces. Projecting the sphere center on the faces, the homothety centers on the faces are obtained. Dropping the perpendiculars from the facial homothety centers to the edges the polygonal links are obtained. Some configurations of the resulting linkage is given in Figure 6.14.

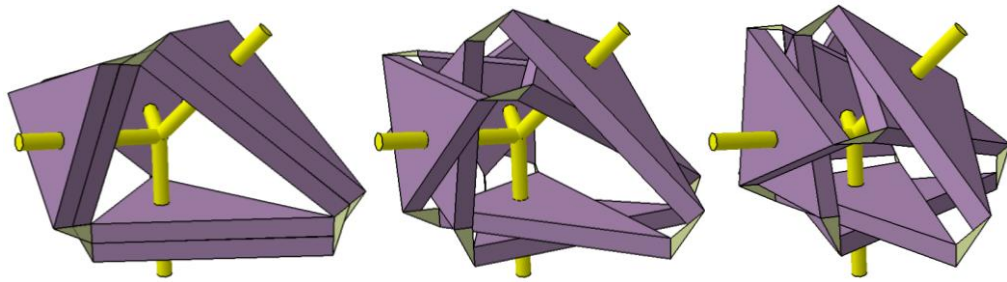


**Figure 6.14** A tetrahedral linkage with ISA guides

Other examples of polyhedra with 3-valent vertices only are prisms, hexahedra, dodecahedra with pentagonal faces and all truncated polyhedra. Of course they can be used provided that there is an inscribed sphere. These example geometries just represent the topology and they can be deformed provided that the faces remain tangent to a sphere; for example the base faces of a prism can

be made non-parallel, or the side faces may be deformed such that the vertices are not on a cylinder.

Also one can include in this class many polyhedra with 3-valent vertices which also have vertices with higher valence. For example (excluding the tetrahedral) all vertices, but one of an  $n$ -gonal pyramid are 3-valent. The ISA of the 3-valent vertices meet at a point hence the remaining vertex with higher valence is irrelevant. All pyramids have an insphere, so they can be used as base polyhedra. Similarly cupolas with inspheres can be used as base polyhedra.

#### 6.2.4.3 Tangential Polyhedral Linkages

The following special case is a generalization of the previous section:

**Theorem 6:** If a polyhedron has an inscribing sphere, it can be used as a base polyhedron for a homothetic Jitterbug-like linkage. In this case if the homothety centers on the faces are chosen as the points of tangencies with the insphere, the ISAs of the polygonal links meet at the sphere center. Conversely if all ISAs of a homothetic Jitterbug-like linkage meet at a point, there is necessarily an inscribing sphere for the supporting polyhedron centered at the meet of the ISAs.

**Proof:** Let a polyhedron have an insphere with center  $O$ . Consider two adjacent faces with points of tangencies  $O_{ij}$  and  $O_{jk}$ , intersecting along edge  $e_j$ , and one of the vertices  $V$  along this edge (Figure 6.15).  $e_j$  meets the plane defined by  $O$ ,  $O_{ij}$  and  $O_{jk}$  perpendicularly. Drop perpendiculars from  $O_{ij}$  and

$O_{jk}$  which both meet  $e_j$  at  $E_j$ .  $|OO_{ij}| = |OO_{jk}|$  and  $OO_{ij}$  and  $OO_{jk}$  are perpendicular to  $O_{ij}E_j$  and  $O_{jk}E_j$ , respectively, so  $OO_{ij}E_jO_{jk}$  is a kite and  $|O_{ij}E_j| = |O_{jk}E_j|$ .  $O_{ij}E_j$  and  $O_{jk}E_j$  being perpendicular to  $e_j$  and  $VE_j$  being common side,  $O_{ij}E_jV$  and  $O_{jk}E_jV$  are congruent, hence  $|VO_{ij}| = |VO_{jk}|$  and  $\angle E_jVO_{ij} = \angle E_jVO_{jk}$ . Similar analysis is valid for all edges and adjacent homothety centers  $O_{ij}$ , so Theorem 2 holds and the polyhedron can be used as a base polyhedron for homothetic Jitterbug-like linkages.

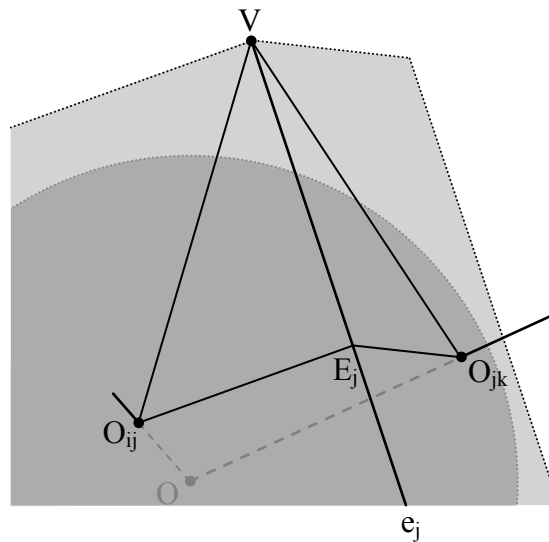


**Figure 6.15** An insphere and two planes of faces tangent to it

Next assume that all ISAs of a homothetic Jitterbug-like linkage meet at a point  $O$ . Choose the homothety center of the supporting polyhedron as the meet of the ISAs and hence fix the ISAs. Consider an edge  $e_j$ , one of the vertices  $V$  on this edge and the two neighboring homothety centers  $O_{ij}$  and  $O_{jk}$  on the faces.

Corollary 2 demands  $|VO_{ij}| = |VO_{jk}|$ .  $VO_{ij}$  and  $VO_{jk}$  are perpendicular to  $OO_{ij}$  and  $OO_{jk}$ , respectively, and  $VO$  is common, so  $VOO_{ij}$  and  $VOO_{jk}$  are congruent, hence  $|OO_{ij}| = |OO_{jk}|$ . This is valid for all edges, so the homothety centers on the faces are equidistant to the polyhedron homothety center  $O$  and are on a sphere. Also the faces are perpendicular to the ISAs, hence are tangent to the sphere. ■

Homothetic linkages with base polyhedra that have inscribed spheres are also issued by Röschel (1996). It is here shown that the construction method given by Röschel (1996) is the only way to obtain homothetic Jitterbug-like linkages with fixed ISAs.

As the most symmetric cases, Platonic solids and the Archimedean duals, i.e. the Catalan solids have insphere. As an example, a tetrakis hexahedral linkage with the ISAs shown as guides is given in Figure 6.16. In this linkage, the homothety centers on the faces are chosen as the points of tangencies with the insphere. Note that since tetrakis hexahedron is an isohedron any point on a face can be used as the homothety center by Theorem 3. An example is presented in Figure 5.5 for which the very same supporting polyhedron, the tetrakis hexahedron is used and the ISAs are not fixed throughout the motion.

It is still possible to obtain homothetic linkages if there is no inscribed sphere, as the fruitful example of Figure 6.8 demonstrates.

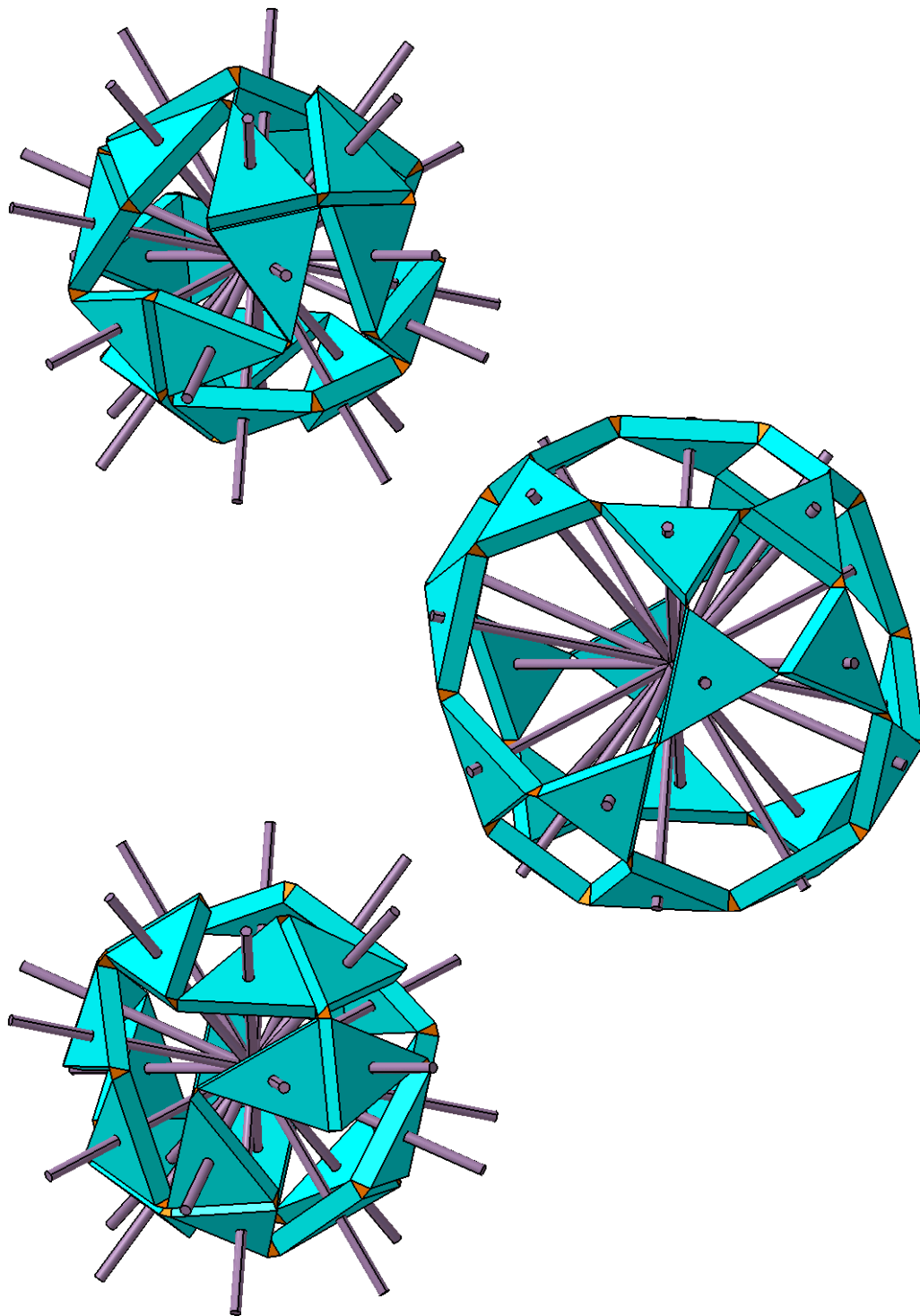


**Figure 6.16** A tetrakis hexahedral linkage with ISA guides

### 6.2.4.4 Polyhedra With 4-Valent Vertices

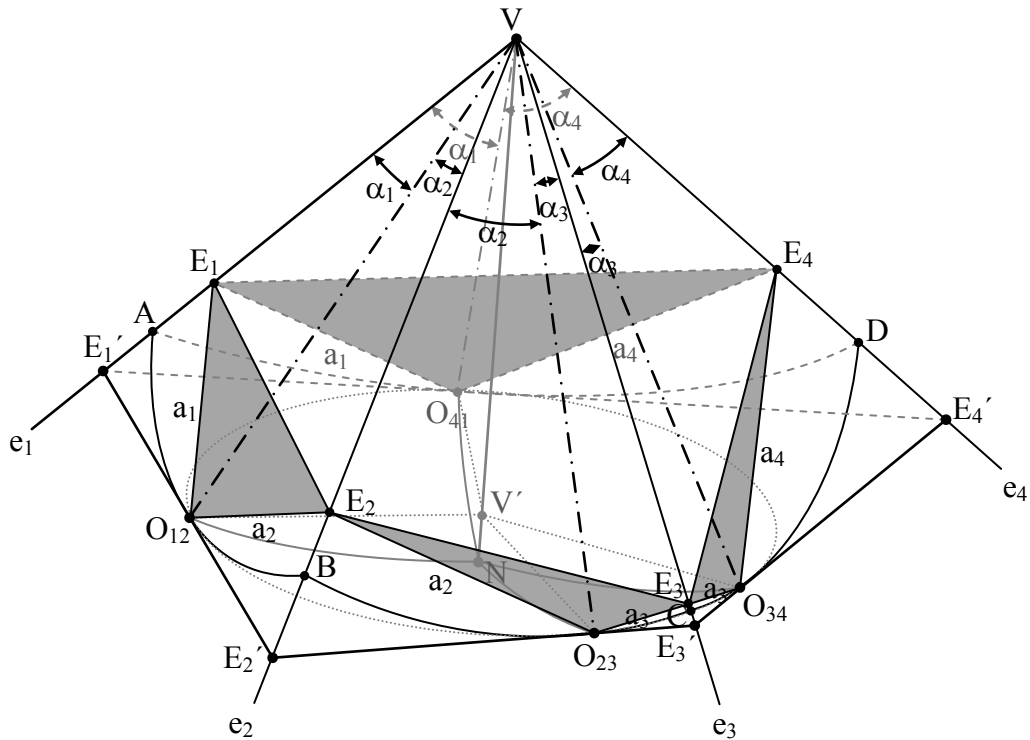


**Figure 6.17** A 4-valent vertex and associated parts of the polygonal links around the vertex

Consider a 4-valent vertex, summation of opposite plane angles of which are equal ( $\rho_{12} + \rho_{34} = \rho_{23} + \rho_{41}$ ) (Figure 6.17). Choose a point  $O_{12}$  on face 12 and locate its mirror images  $O_{41}$  and  $O_{23}$  along edges  $e_1$  and  $e_2$ , respectively. The mirror images of  $O_{23}$  and  $O_{41}$  along  $e_3$  and  $e_4$ , necessarily coincide due to the condition  $\rho_{12} + \rho_{34} = \alpha_1 + \alpha_2 + \alpha_3 + \alpha_4 = \rho_{23} + \rho_{41}$ . Let  $|VO_{12}| = |VO_{23}| =$



$|VO_{34}| = |VO_{41}| = r$ . Consider the sphere centered at V and passing through  $O_{12}$ ,  $O_{23}$ ,  $O_{34}$  and  $O_{41}$ . The intersection of this sphere with the faces is a spherical quadrilateral ABCD the side lengths of which are  $\widehat{AB} = r\rho_{12}$ ,  $\widehat{BC} = r\rho_{23}$ ,  $\widehat{CD} = r\rho_{34}$ , and  $\widehat{DA} = r\rho_{41}$ . This implies  $\widehat{AB} + \widehat{CD} = \widehat{AD} + \widehat{BC}$ .

At this point the following theorem can be deduced:

**Theorem 7:** a) If the summations of the opposite sides are equal in a spherical quadrilateral, then there exists an inscribing circle for this quadrilateral.

b) For such a spherical quadrilateral if four points  $O_{12}$ ,  $O_{23}$ ,  $O_{34}$  and  $O_{41}$  are chosen on sides such that they dissect the sides as  $\rho_{12} = \alpha_1 + \alpha_2$ ,  $\rho_{23} = \alpha_2 + \alpha_3$ ,  $\rho_{34} = \alpha_3 + \alpha_4$ ,  $\rho_{41} = \alpha_4 + \alpha_1$  as in Figure 6.15, these four points are coplanar, hence are on a circle.

**Proof:** a) To author's knowledge this side of the theorem is novel and hence is the proof. According to (Rosenfeld, 1988, pp. 33-34) the converse of the proposition is proved by I. A. Lexell in 1786.

Consider a spherical quadrilateral ABCD with sphere center V, sides of which satisfy  $\widehat{AB} + \widehat{CD} = \widehat{AD} + \widehat{BC}$  (Figure 6.17). There exist 4 circles tangent to arcs AB, BC and CD (M'cLelland & Preston, 1886, p. 1-2). Construct the tangent circle to these three arcs as follows: Locate point N by intersecting angle bisectors at B and C such that the bisectors are towards arc AD. Draw line NV and construct a right cone with this axis touching arcs AB, BC and CD. Let the circle center be V' and points of tangencies to arcs AB, BC and CD be E, F and G, respectively. Arcs NE, NF and NG are orthogonal to arcs AB, BC and CD and N is equidistant to the three sides, so NEBF and NFCG are spherical kites

with  $\widehat{EB} = \widehat{BF} = b$  and  $\widehat{FC} = \widehat{CG} = c$ . Also let  $\widehat{AE} = a$  and  $\widehat{GD} = d$ . By hypothesis  $\widehat{AD} = \widehat{AB} + \widehat{CD} - \widehat{BC} = a + d$ . Dissect arc AD at H, such that  $\widehat{HA} = a$  and  $\widehat{DH} = d$ . Let  $\angle DAB = \alpha$ ,  $\angle ABC = \beta$ ,  $\angle BCD = \gamma$ ,  $\angle CDA = \delta$  and assume spherical excesses of  $\alpha'$ ,  $\beta'$ ,  $\gamma'$  and  $\delta'$  for the spherical triangles HAE, EBF, FCG and GDH, respectively. Note that these four triangles are isosceles, hence  $\angle AHE = \angle AEH = (\pi + \alpha' - \alpha)/2$ ,  $\angle BEF = \angle BFE = (\pi + \beta' - \beta)/2$ ,  $\angle CFG = \angle CGF = (\pi + \gamma' - \gamma)/2$  and  $\angle DGH = \angle DHG = (\pi + \delta' - \delta)/2$ . So,  $\angle HEF = \pi - (\pi + \alpha' - \alpha)/2 - (\pi + \beta' - \beta)/2 = (\alpha + \beta - \alpha' - \beta')/2$ . Similarly  $\angle EFG = (\beta + \gamma - \beta' - \gamma')/2$ ,  $\angle FGH = (\gamma + \delta - \gamma' - \delta')/2$  and  $\angle GHE = (\delta + \alpha - \delta' - \alpha')/2$ . Then  $\angle HEF + \angle FGH = (\alpha + \beta + \gamma + \delta - \alpha' - \beta' - \gamma' - \delta')/2 = \angle EFG + \angle GHE$ , in which case the spherical quadrilateral EFGH is necessarily cyclic (M'cLelland & Preston, 1893, p. 32-33). Hence H is on the incircle with center V'. By side-side-side congruency of spherical triangles AEN and AHN, arcs NE and NH meet arcs AB and AD orthogonally, respectively, so the circle is tangent to arc AD. ■

b) Let points  $O_{12}$ ,  $O_{23}$ ,  $O_{34}$  and  $O_{41}$  be on arcs AB, BC, CD and DA, respectively, such that they dissect the sides as  $\rho_{12} = \alpha_1 + \alpha_2$ ,  $\rho_{23} = \alpha_2 + \alpha_3$ ,  $\rho_{34} = \alpha_3 + \alpha_4$ ,  $\rho_{41} = \alpha_4 + \alpha_1$ . Consider the tangency points E, F, G and H in part (a) and compare VE, VF, VG and VH with  $VO_{12}$ ,  $VO_{23}$ ,  $VO_{34}$  and  $VO_{41}$ . Because of the mirror symmetries, if the angle between VE &  $VO_{12}$  is  $\eta$ , the angles between VF &  $VO_{23}$ , VG &  $VO_{34}$  and VH &  $VO_{41}$  should be  $\eta$ , too. Then the distance of  $O_{12}$ ,  $O_{23}$ ,  $O_{34}$  and  $O_{41}$  to the plane defined by E, F, G and H are  $r(1 - \cos \eta)$ . If  $O_{12}$ ,  $O_{23}$ ,  $O_{34}$  and  $O_{41}$  are equidistant to this plane, they should be coplanar. Since  $O_{12}$ ,  $O_{23}$ ,  $O_{34}$  and  $O_{41}$  are on a sphere, they are on a circle. ■

So, Röschel's (2001) way of construction using circles is indeed the only way to obtain homothetic Jitterbug-like linkages when all the vertices are 4-valent, such as for an octahedron.

When vertex valence is greater than 4, the facial homothety centers  $O_{ij}$  around this vertex are not necessarily on a circle. Indeed the homothety centers around the 5-valent vertices of the snub disphenoidal linkage in Figure 6.8 are not on a circle.

#### **6.2.4.5 Degenerate Case: Coplanar Faces Around a Vertex**

Consider the special case where the faces around a vertex  $V$  are coplanar (polygon scaling problem). The problem breaks down into placing angulated elements  $E_i O_{ij} E_j$  along radial guides  $VE_i$  and  $VE_j$ . In this case, the ISAs are all parallel, hence they meet at the infinity. Then the reasoning in Section 6.2.2 is no longer valid and  $O_{ij}$  are not necessarily on a sphere (hence a circle in the plane). Therefore Theorems 2 and 3 do not hold in this degenerate case.

This planar case has already been worked out in (Kiper, Söylemez & Kişisel 2008) and Chapter 2. In these works, it is shown that if the fixed Cardan circles of all the angulated elements are to meet at a point, the supporting polygon needs to have an inscribing circle. Loosing this meet condition one can scale any kind of polygon (Chapter 2).

### 6.2.5 Open Problems

This chapter addressed the following questions: what are the conditions on the suitable polyhedra that can be used for homothetic linkages and how can one construct such linkages? The following questions remain in debate:

- Can one obtain homothetic linkages not satisfying Assumptions 1 and/or 2?
- Are these two assumptions unrelated or do they imply each other?

## CHAPTER 7

### MODIFICATIONS ON JITTERBUG-LIKE LINKAGES

Having defined Jitterbug-like linkages in Chapter 6, modifications on these linkages are issued in this chapter. New overconstrained linkages are obtained as a result of the modifications. Two different classes of modified linkages are presented in two sections.

#### 7.1 Addition of Links on the Faces of Jitterbug-Like Linkages<sup>1</sup>

It is already mentioned in Chapter 6 that the polygonal links of a Homothetic Jitterbug-like linkage go through Cardan motion with respect to a frame located at any of the corners of the associated supporting polygon. In this section, cranks are attached between centers of the fixed and moving centrodes to further constrain the already overconstrained linkages.

In this section, homothetic Jitterbug-like linkages are modified by adding  $n$ -ary links at the  $n$ -valent vertices and binary links in between these  $n$ -ary links and polygonal links. The additions are made such that the motion of the original links does not change. Then some link and joint groups are removed to obtain some new linkages.

---

<sup>1</sup> The main content of this section is published by Kiper and Söylemez (2010b).

### 7.1.1 The Cardan Motion Associated With the Polygonal Links

Consider a spatial  $2nR$  loop around an  $n$ -valent vertex  $V$  according to the definition in Chapter 6, like the one in Figure 7.1. The corners of a side  $AB$  of a polygonal link will be constrained to move on two adjacent edges of the corresponding supporting polygonal face. Since  $\angle VAB$  remains constant during the motion of a Jitterbug-like linkage, the motion of the segment  $AB$  on the associated face is equivalent to the coupler link of a double slider mechanism (Figure 7.2), coupler link of which has the Cardan motion as mentioned in Chapter 2.

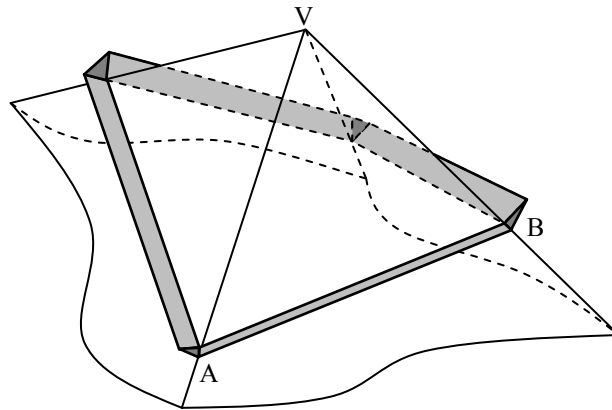


**Figure 7.1** An  $8R$  loop around a 4-valent vertex

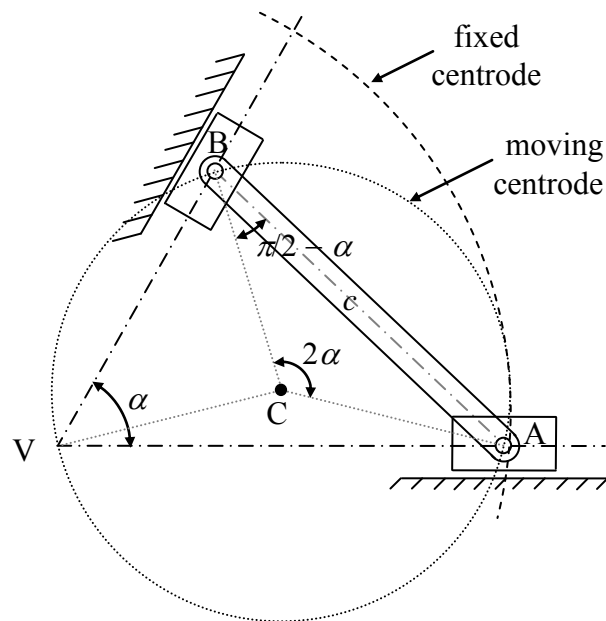


**Figure 7.2** A double slider mechanism

On the moving plane associated with the coupler link of the double slider mechanism there is a special point  $C$ , the center of the moving centrode, the trajectory of which is a circle. Given the plane angle  $\alpha$  and length  $c = |AB|$ , this point is located easily: Since points  $A$  and  $B$  have straight line trajectories, they are on the moving centrode. Also the center of the fixed centrode (point  $V$  in Figures 7.1 and 7.2) is on the moving centrode at all times, so the moving centrode is uniquely given by points  $V$ ,  $A$  and  $B$ . Then by inscribed angle theorem  $\angle BCA = 2\alpha$  and hence  $|CA| = |CB| = c/2\sin\alpha$ . This uniquely locates point  $C$ .

If for every side  $AB$  of the polygonal links of a homothetic Jitterbug-like linkage, a link  $VC$  is attached at the proper point  $C$ , then all such attached links

around a vertex can be connected to a common link without disturbing the original motion. In the next section, examples of such linkages are presented.

### **7.1.2 Attaching Links to Jitterbug-Like Linkages – Examples**

The first example shall be the Heureka Octahedron. By addition of the extra joints to the triangular links, the polygonal links of the Heureka Octahedron become regular hexagons. Some snapshots of the obtained mechanism is given in Figure 7.3.

Recall that the supporting polyhedron of the jitterbug is a regular octahedron. For the next two examples, the supporting polyhedra are the regular tetrahedron (Figure 7.4) and the cube (Figure 7.5). Note that for the tetrahedron and the cube the vertex valences are 3, so double polyhedra are used for them as was illustrated in Figure 6.1.

The examples given in Figures 7.3-7.5 turn out to be some special cases of linkages presented in (Kiper, Söylemez & Kışisel, 2008), where some polygonal linkages are introduced and used in the faces of polyhedral linkages. The cubic linkage in Figure 7.5 is also the subject of (Wei, Yao, Tian & Fang, 2006). What is not in (Kiper, Söylemez & Kışisel, 2008) are issued in the next section.



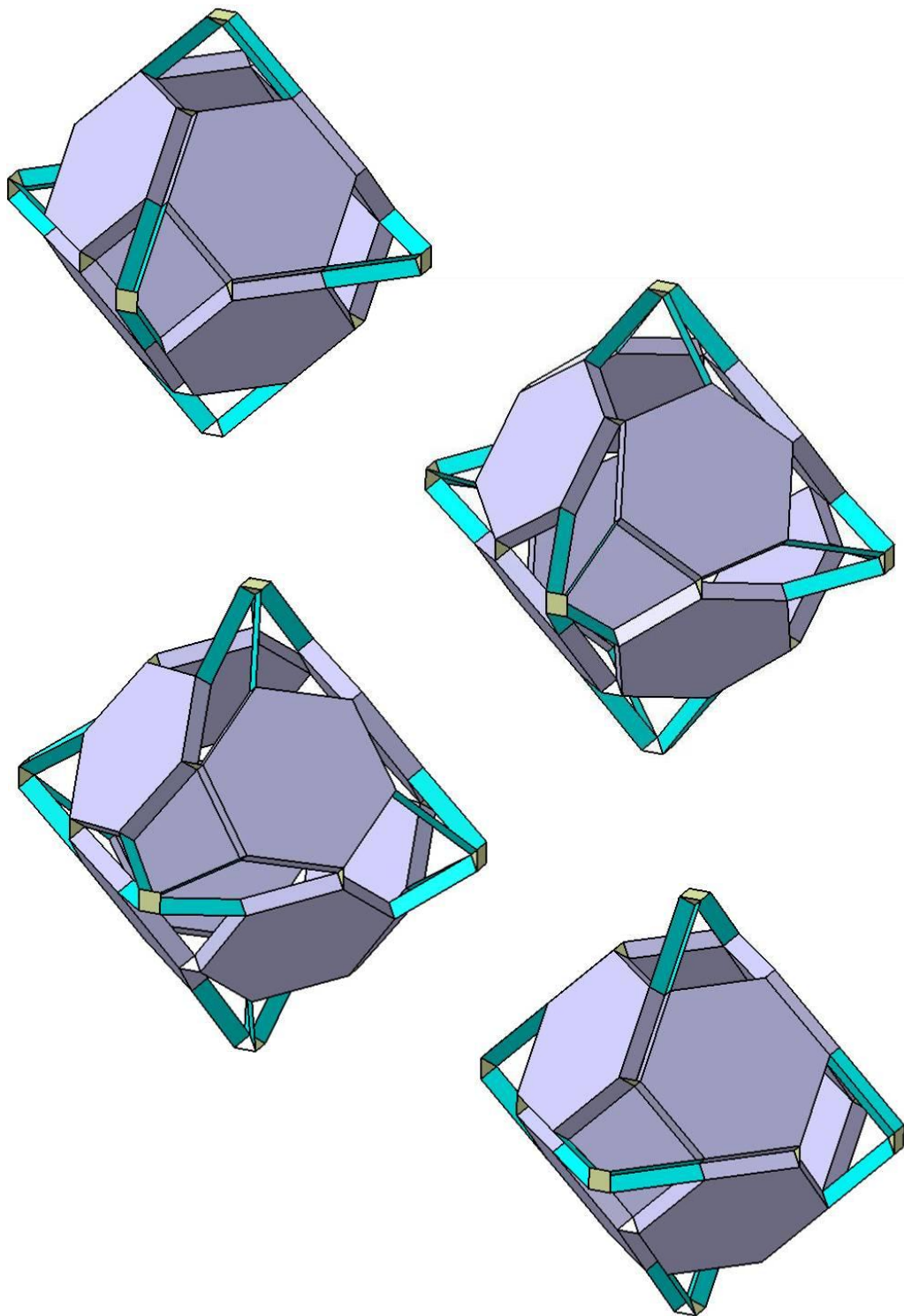


**Figure 7.3** The Heureka Octahedron with extra links

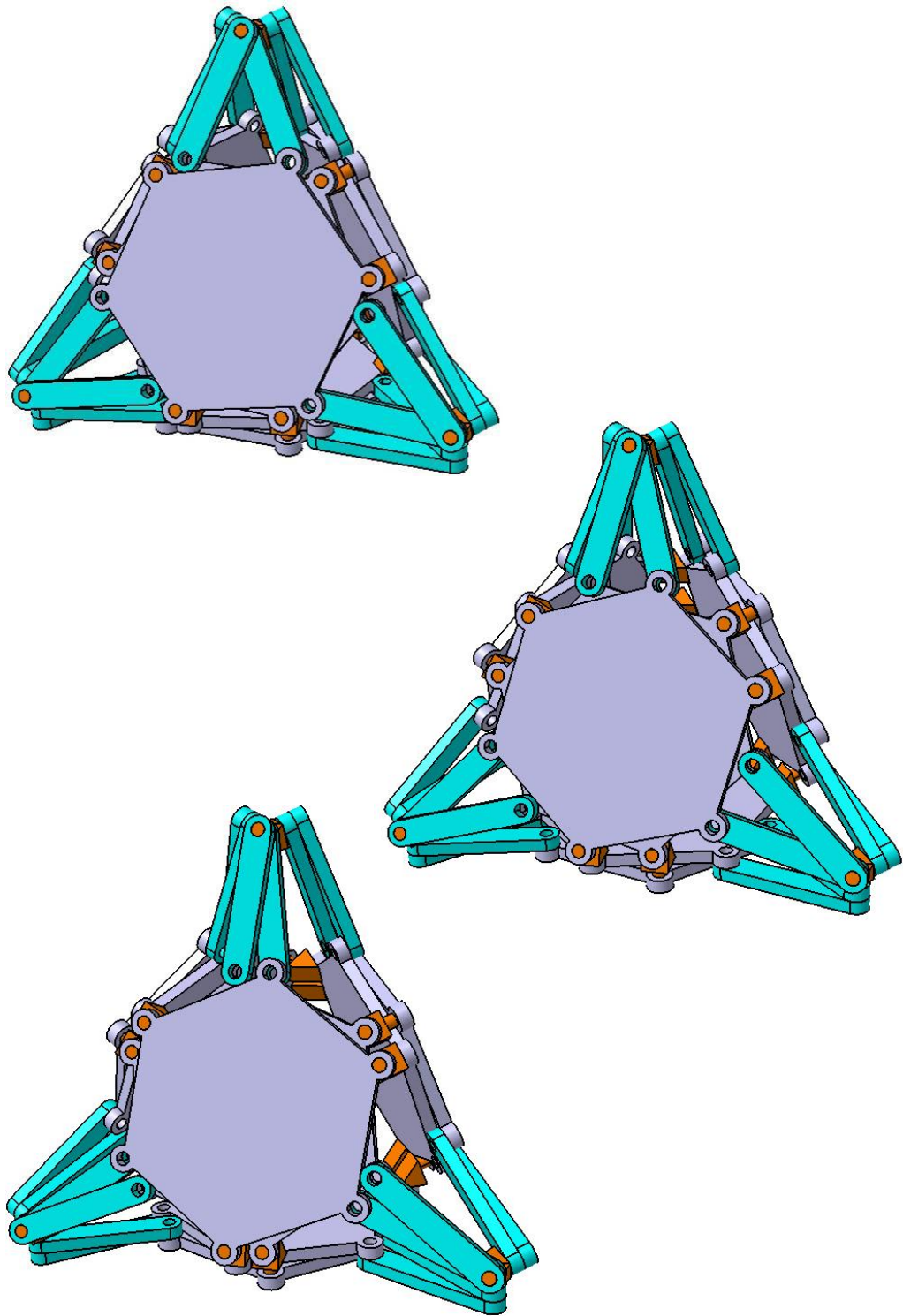


**Figure 7.4** Tetrahedral dipolygonid with extra links

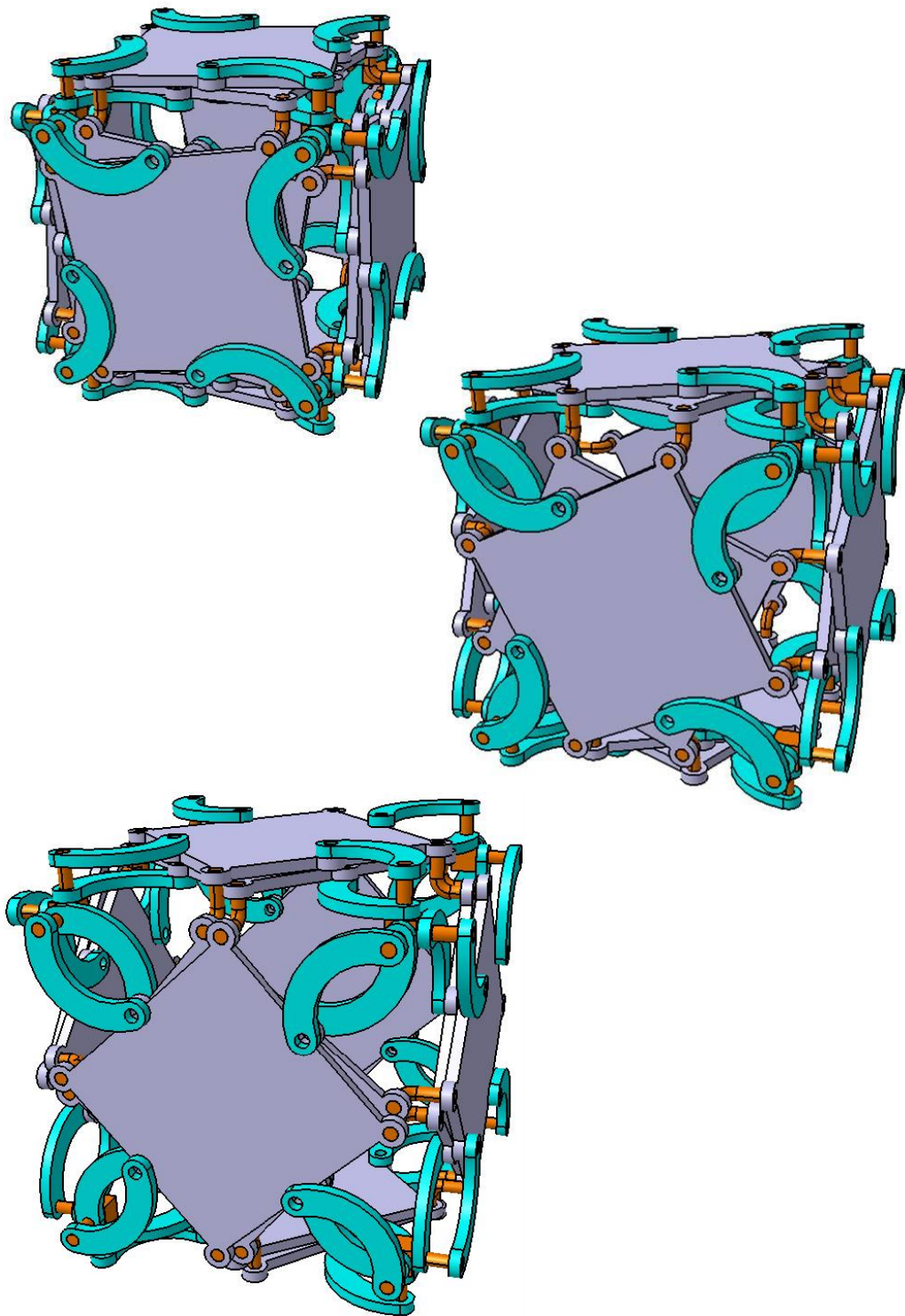


**Figure 7.5** Cubic dipolygonid with extra links

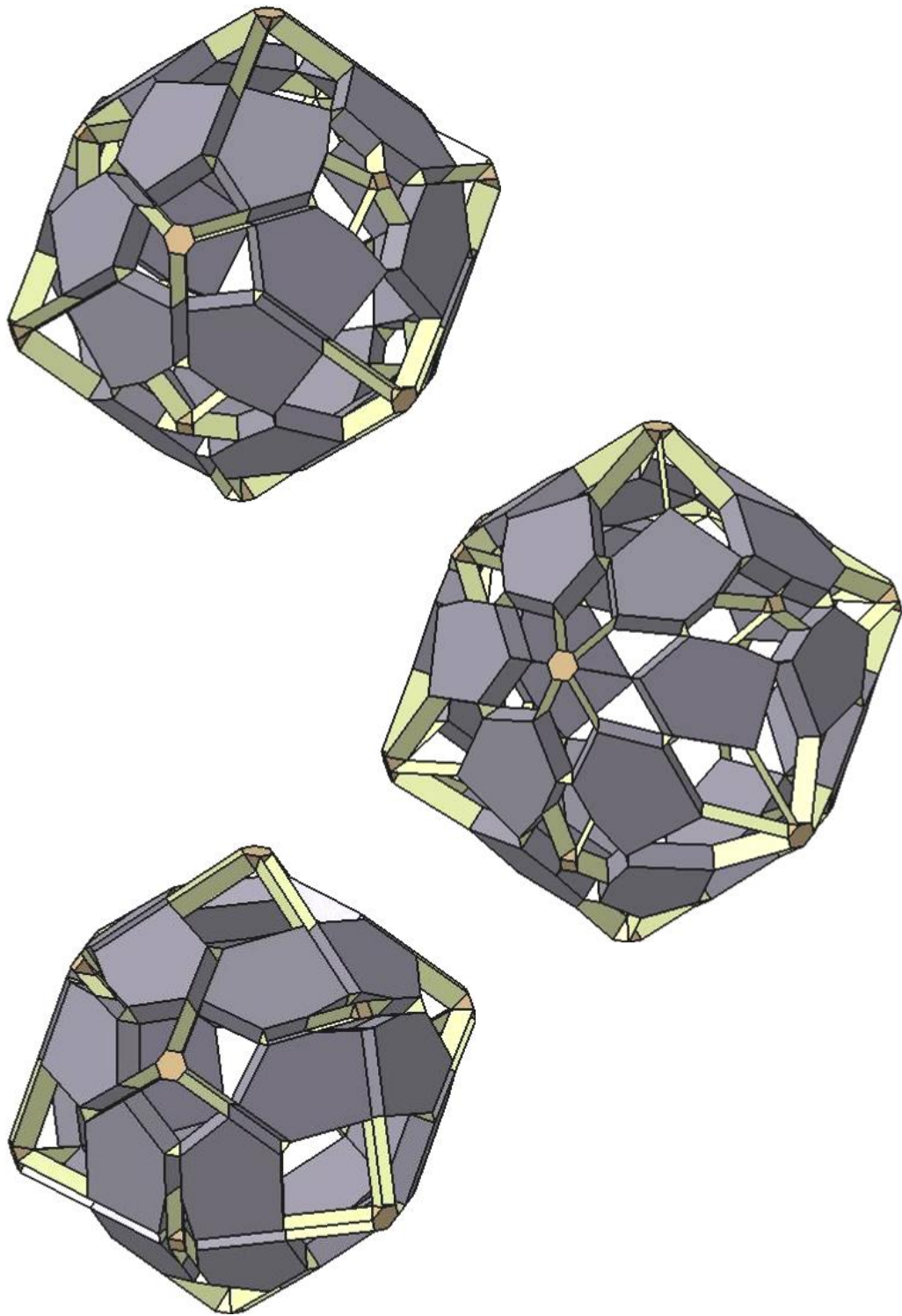


**Figure 7.6** Linkage obtained from a tetrakis hexahedron

Similarly, links can be added to the remaining two Platonic solids, i.e. the dodecahedron and the icosahedron. Among polyhedra with regular faces, the non-Platonic convex deltahedra (triangular dipyramid, pentagonal dipyramid, snub disphenoid, triaugmented triangular prism and gyroelongated square dipyramid) can also be used as supporting polyhedra. However, Archimedean solids are not suitable for the purpose because they cannot be used for homothetic linkages (See the paragraph after Corollary 2 in Section 6.2.2).

The Archimedean duals, i.e. the Catalan solids have insphere, so they can be used here. As an example, the linkage obtained from a tetrakis hexahedron is given in Figure 7.6. The tetrakis hexahedron is chosen due to its even-valent its vertices. Most Catalan solids have odd-valent vertices, so double polyhedra of them should be used to obtain a linkage (just like the tetrahedron and the cube).

An immediate advantage of these linkages over the original linkages is that the new linkages better represent their supporting polyhedra visually, because not only the faces and edges are represented by the polygonal and dip links, respectively, but also the vertices are represented by the new links.

### **7.1.3 Obtaining New Linkages by Removing Some Links and Joints**

Having obtained some further constrained overconstrained linkages in the previous section it is possible to obtain new linkages out of these linkages by properly removing some link groups.

Again the first example comes out of the Heureka Octahedron. Moving out two hexagonal links and the twelve binary links connected to these two polygonal

links of the linkage in Figure 7.3, the linkage in Figure 7.7 is obtained. The supporting polyhedron of this linkage is the rhombohedron.

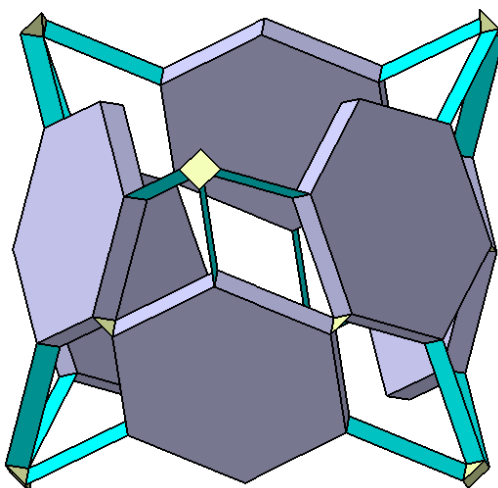


**Figure 7.7** A rhombohedral linkage

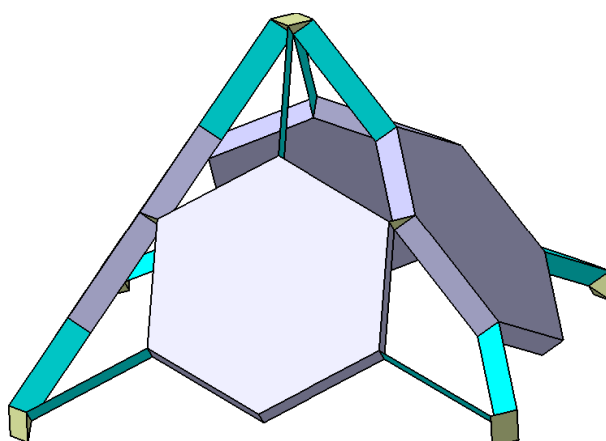


**Figure 7.8** A square pyramidal cap linkage



Another linkage can be obtained by keeping 4 adjacent hexagonal links meeting at a vertex and deleting the remaining four (Figure 7.8). In this case, a square pyramidal cap like geometry is obtained: the planes of the polygonal links do not bound a finite volume.

Next, consider the tetrahedral linkage of Figure 7.4. Deleting one of the polygonal links on each face one obtains the linkage in Figure 7.9. Note that there is no dap link in this linkage. This type of linkages was synthesized by Wohlhart (2001a).

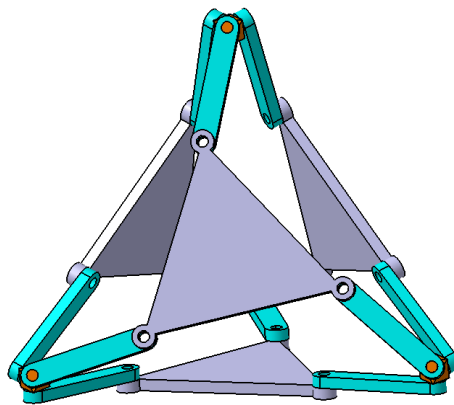


**Figure 7.9** A tetrahedral linkage

Alternatively one can remove a pair of polygonal links of a face. Furthermore, the binary links opposite to the removed polygonal links may be removed. The resulting linkage has still single dof (Figure 7.10). Also, three vertices of the tetrahedron may be chopped off to get the linkage in Figure 7.11.

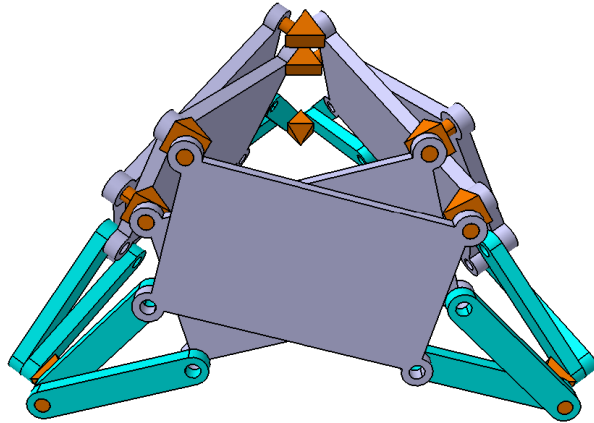


**Figure 7.10** A tetrahedral cap linkage

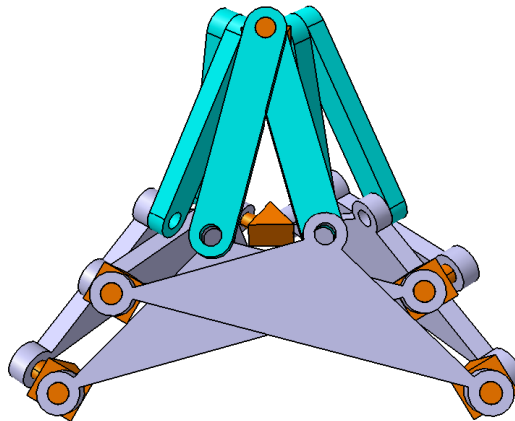


**Figure 7.11** Another tetrahedral cap linkage

Many other single dof linkages can be obtained using polyhedral shapes with inscribing spheres.



## 7.2 Addition of Links on Radial Planes of Jitterbug-Like Linkages<sup>2</sup>

Making use of the Cardan motion of the polygonal links of homothetic Jitterbug-like linkages, it is also possible to insert new links along radial planes passing through the global homothety center and edges of the supporting polyhedron.

### 7.2.1 An Observation

For a homothetic Jitterbug-like linkage consider the vicinity of two polygonal links around the common edge  $e$  the links meet on (Figure 7.12). Denote the meeting point by  $A$  and the ISA intersections on the faces by  $P$  and  $R$ . Let the global homothety center of the supporting polyhedron be  $O$ . By Assumption 2 of Chapter 6, initially  $PA$  and  $RA$  are perpendicular to  $e$ . As  $PA$ , and so  $RA$ , rotates by an angle  $\theta$ , the distance of the ISAs to the edge shortens by a ratio of  $\cos\theta$ , which is nothing but the dilation ratio. Initially let  $|P_1A_1| = |R_1A_1| = a$ ,  $|OA_1| = d$ . Consider a frame  $(O, x, y)$  in the plane defined by  $O$  and  $e$  such that positive  $x$  is in  $OA_1$  direction. Then for a rotation of the links by  $\theta$  the coordinates of  $A$  is  $(d \cdot \cos\theta, a \cdot \sin\theta)$ , so  $A$  tracks the ellipse  $X^2/d^2 + Y^2/a^2 = 1$ . Therefore for homothetic Jitterbug-like linkages ISAs of which meet at the homothety center, the joint intersections trace ellipses on planes defined by the homothety center and corresponding supporting polyhedron edge.

---

<sup>2</sup> The main content of this section is published by Kiper and Söylemez (2011a).

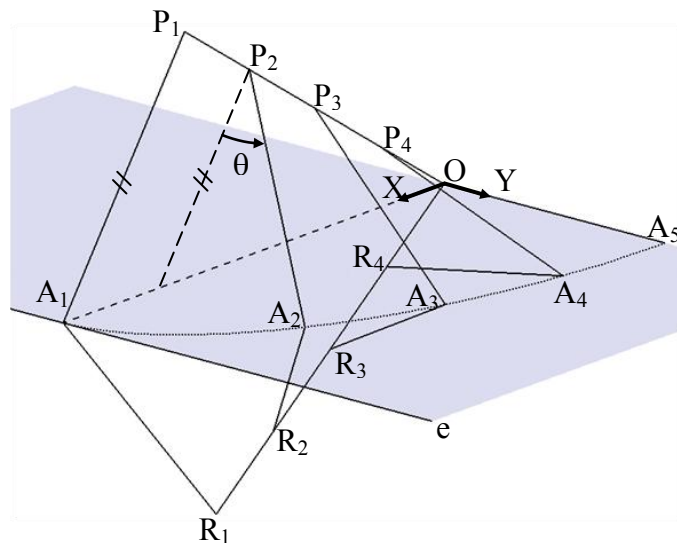


**Figure 7.12** The motion of relevant parts of two adjacent polygonal links

Another way to see the elliptical path of the joint intersections is as follows: The intersection point  $A$  moves in the intersection of two congruent cylinders with axes  $OP$  and  $OR$  and radius  $r$ . Cylinders with intersecting axes and equal radii intersect along ellipses (Verheyen, 1989, p. 208).

This observation is used in Section 7.2.2 for further constraining Jitterbug-like linkages by adding more links/joints while preserving the motion of the original links. The key point is the elliptical path of the joint intersections and the additional links will realize Cardan motion.

### 7.2.2 Relating the Cardan Motion With Elliptic Paths of Polygonal Links

For a moving frame located at the midpoint of the coupler link of a crank-attached double slider mechanism as in Figure 7.13, the transformation is

$$X = x \cos\phi + y \sin\phi + r \cos\phi \quad \text{and} \quad Y = -x \sin\phi + y \cos\phi + r \sin\phi$$

from which  $\phi$  can be eliminated to get

$$[(x - r)^2 + y^2]X^2 + [(x + r)^2 + y^2]Y^2 - 4ryXY = (x^2 + y^2 - r^2)^2 \quad (7.1)$$

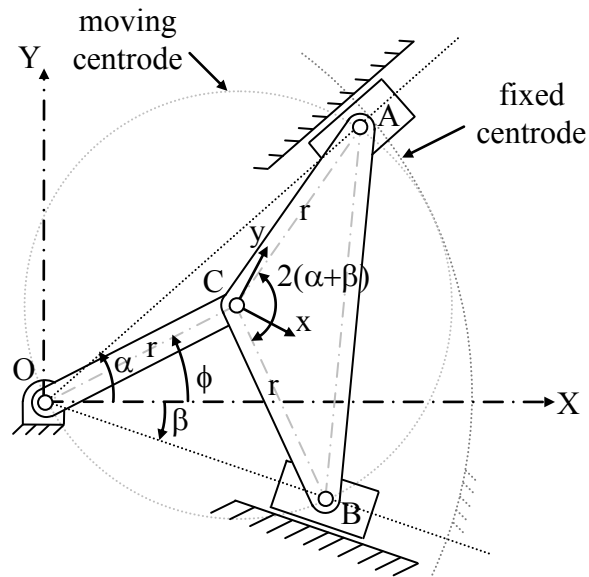


**Figure 7.13** A double slider mechanism with a crank attached

Note that this ellipse equation degenerates into a double straight line equation for a point  $(x = r \cdot \cos\psi, y = r \cdot \sin\psi)$  on the moving centrode.

Back to the polyhedral linkage problem, suppose that the following are given for an edge: (at maximal size), the distance of the homothety center to the edge,  $d$  and the distance of the neighboring ISAs to the edge,  $r$ . Observe from Figure 7.12 that  $|OA_1| = d$  for  $\theta = 0$  and  $|OA_5| = a$  for  $\theta = \pi/2$  are the semimajor and semiminor axes of the ellipse, respectively, hence to obtain this ellipse via a linkage as in Figure 7.13 the fixed frames  $(O, X, Y)$  in Figures 7.12 and 7.13 should coincide. Substituting  $A_1(d - r, 0)$  for  $(x, y)$  into (7.1) the moving Cardan circle radius to attain the ellipse  $X^2/d^2 + Y^2/a^2 = 1$  is determined as:

$$(d - 2r)^2 X^2 + d^2 Y^2 = d^2 (d - 2r)^2 \Rightarrow r = (d - a)/2 \quad (7.2)$$

The aim is to obtain linkages such that extra links can be joined at dap links, which slide along guides from the homothety center to the polyhedron vertices. It is necessary to find the conditions for which such neighboring links can share a common slider along their guides. The guides can then be removed.

Note that the faces of a tangential polyhedron are equidistant to the center of its insphere. Let the radius of the insphere of the tangential polyhedron be  $c$ . Referring to Figure 7.12,  $a^2 + c^2 = d^2$  for an edge. Then  $c^2 = (d + a)(d - a)$ . To couple the elliptical motions of the joint intersections, the same moving Cardan circle radius,  $r$ , should be used for all edges. Given a tangential polyhedron it is possible to choose  $r = (d - a)/2$  and  $d + a = c^2/2r$ , so  $d$  and  $r$  should be same for all edges. This means that the edges of the supporting polyhedron should be equidistant to the insphere center, i.e. there should be a midsphere (see Coxeter, 1948, p. 16) touching all of the edges of the supporting polyhedron. A polyhedron may have both a midsphere and an insphere, but these two spheres

may not be concentric (ex: a right pyramid with equilateral base that is not a regular tetrahedron), however, in the present case the supporting polyhedron has concentric midsphere and insphere. Such polyhedra have the following properties:

- If there is a midsphere, then the faces intersect the midsphere along a circle, i.e. the polygonal faces necessarily have incircles.

- $|OA_1|$  of Figure 7.12 would be the radius of the midsphere at the maximal configuration. Consider one of the faces, say  $F$ , of Figure 7.12 and let  $B_1, C_1, \dots$  be the closest points on the other sides to the global homothety center  $O$ . These points are all on the midsphere and hence are on the incircle of  $F$ . When a plane (on which  $F$  resides) cuts a sphere (the insphere) along a circle (the incircle), the sphere center and the circle of intersection define a right cone. The axis of the cone, which meets  $F$  perpendicularly is necessarily the ISA of the corresponding polygonal link on  $F$  due to the fixed-axis Darboux motion of the polygonal links, hence the center of the incircle is the homothety center on  $F$  ( $P_1$  in Figure 7.12). Hence the sides of a face  $F$  are equidistant to the facial homothety center. The requirement for homothetic Jitterbug-like linkages that the homothety centers of adjacent faces are equidistant to the edge at the meet of these faces (Theorem 2 of Chapter 6) demands that the incircles of adjacent polygonal faces, hence of all faces, are equivalent in size.

- Consider a vertex  $V$ , two homothety centers  $P$  and  $R$  on the two adjacent faces including  $V$  and the edge  $e$  common these faces. By Theorem 2 of Chapter 6, angles  $\angle PVe$  and  $\angle RVe$  are equal. Note that any homothety center on a face, i.e. the incenter of the tangential polygon is on the bisectors of the polygon angles. So the plane angles meeting at a vertex are all equal, i.e. all vertices are regular.

### 7.2.3 Polyhedral Linkages

The polyhedra of interest have concentric in sphere and midsphere, and also regular vertex figures. The polyhedra satisfying these conditions include the Platonic solids and the Catalan solids.

The Heureka Octahedron with extra coupler links and cranks is illustrated in Figure 7.14. Note that the Jitterbug motion is quite limited due to link collisions. The cranks can be removed to obtain a less limited motion (Figure 7.15).

Cardan circle radii can be calculated using (7.2) for all Platonic solids. The other four supporting polyhedra have odd-valent vertices, hence double polyhedra of them should be used. For the tetrahedron, the original linkage is the Heureka Octahedron H described by Stachel (1994) instead of a mere tetrahedron (Figure 7.16). Also the cubic linkage is presented in Figure 7.17. The link overlaps in the figures can be practically overcome by using very thin links. The dodecahedral and icosahedral linkages are not presented for conciseness. Note that the extra links remain inside the boundaries of the supporting polyhedron except for the octahedral case.

As an example of a Catalan solid, the modified linkage for the tetrakis icositetrahedron is presented in Figure 7.18. The 36 additional links of this linkage can be grouped into three which operate independently. If only the 12 additional links corresponding to the larger edges of the supporting polyhedron are used, the linkage in Figure 7.19 is obtained. This linkage can be compared with the “breathing ball” of Wohlhart (1995). The breathing ball and the linkage in Figure 7.19 have the same octahedral symmetry axes.

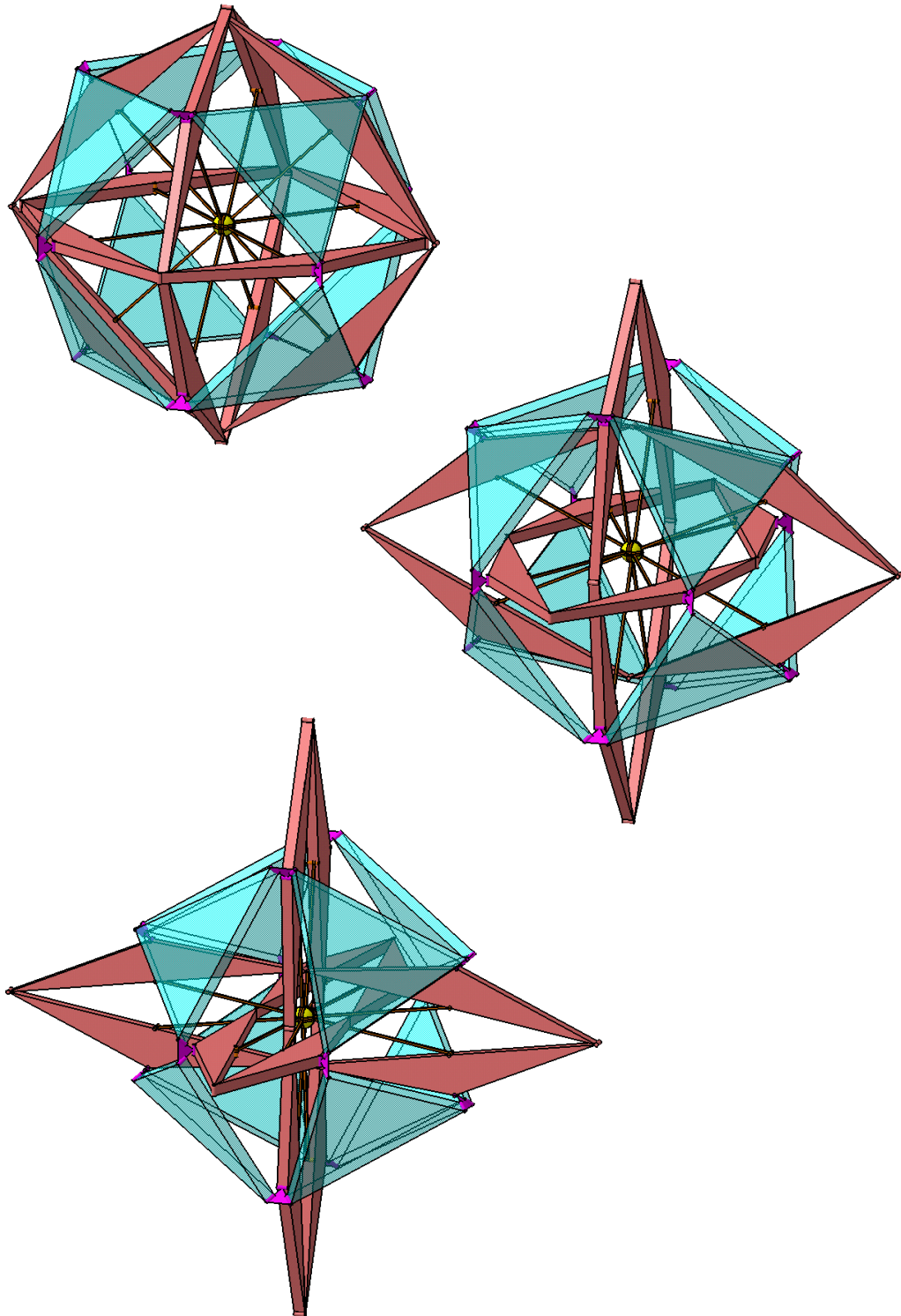


**Figure 7.14** The Heureka Octahedron with extra coupler links and cranks

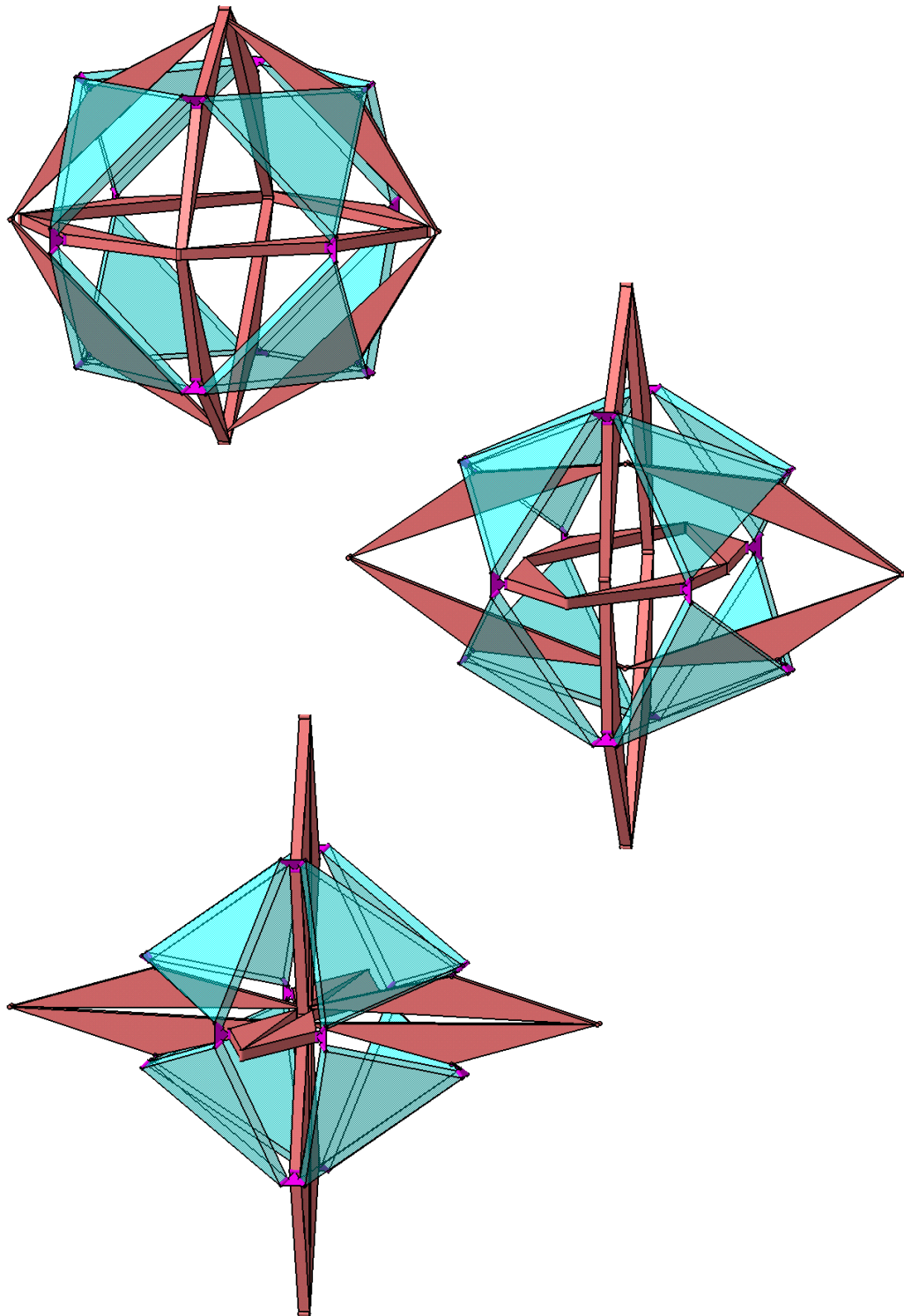


**Figure 7.15** The Heureka Octahedron with extra coupler links



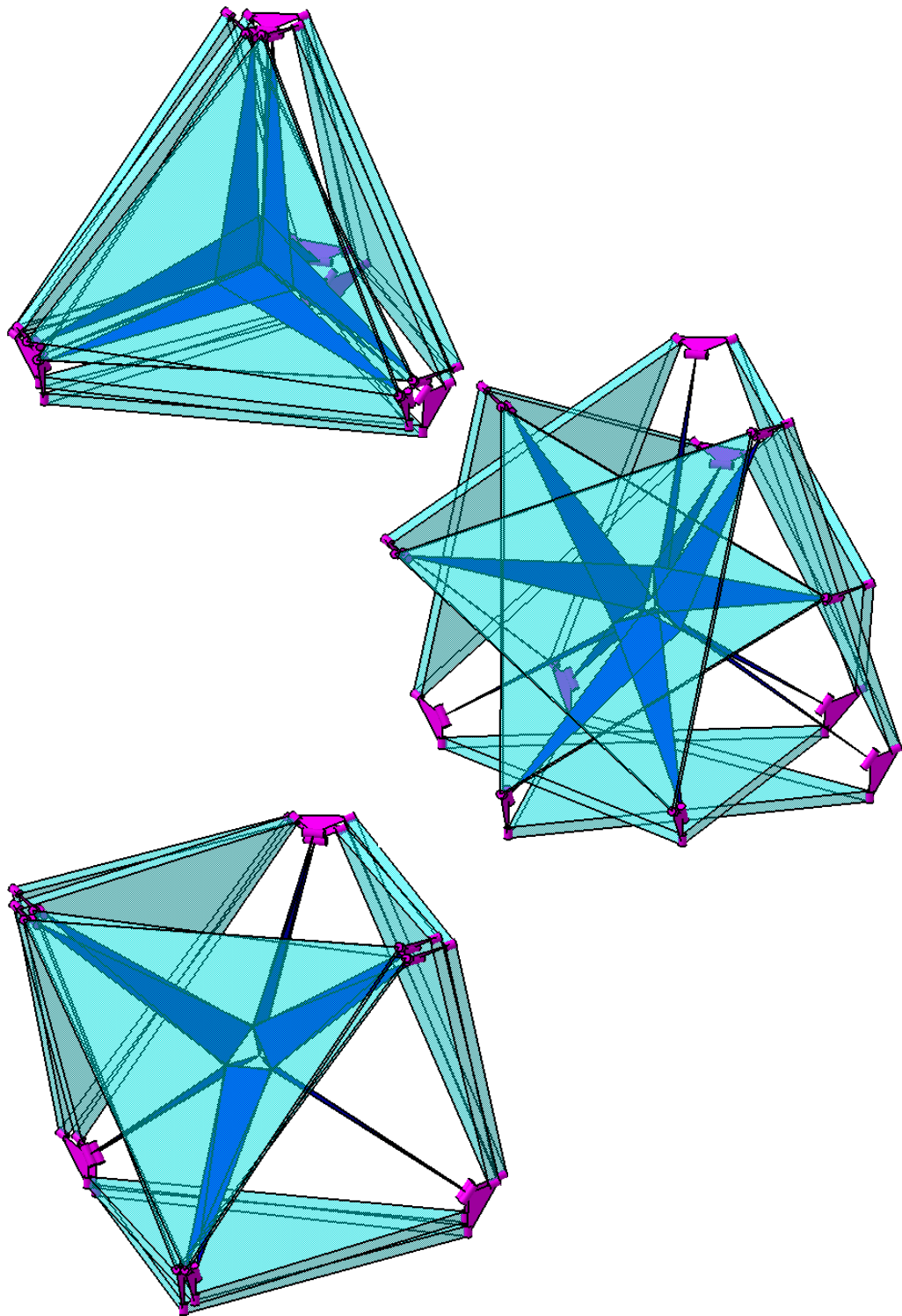


**Figure 7.16** Modified tetrahedral linkage

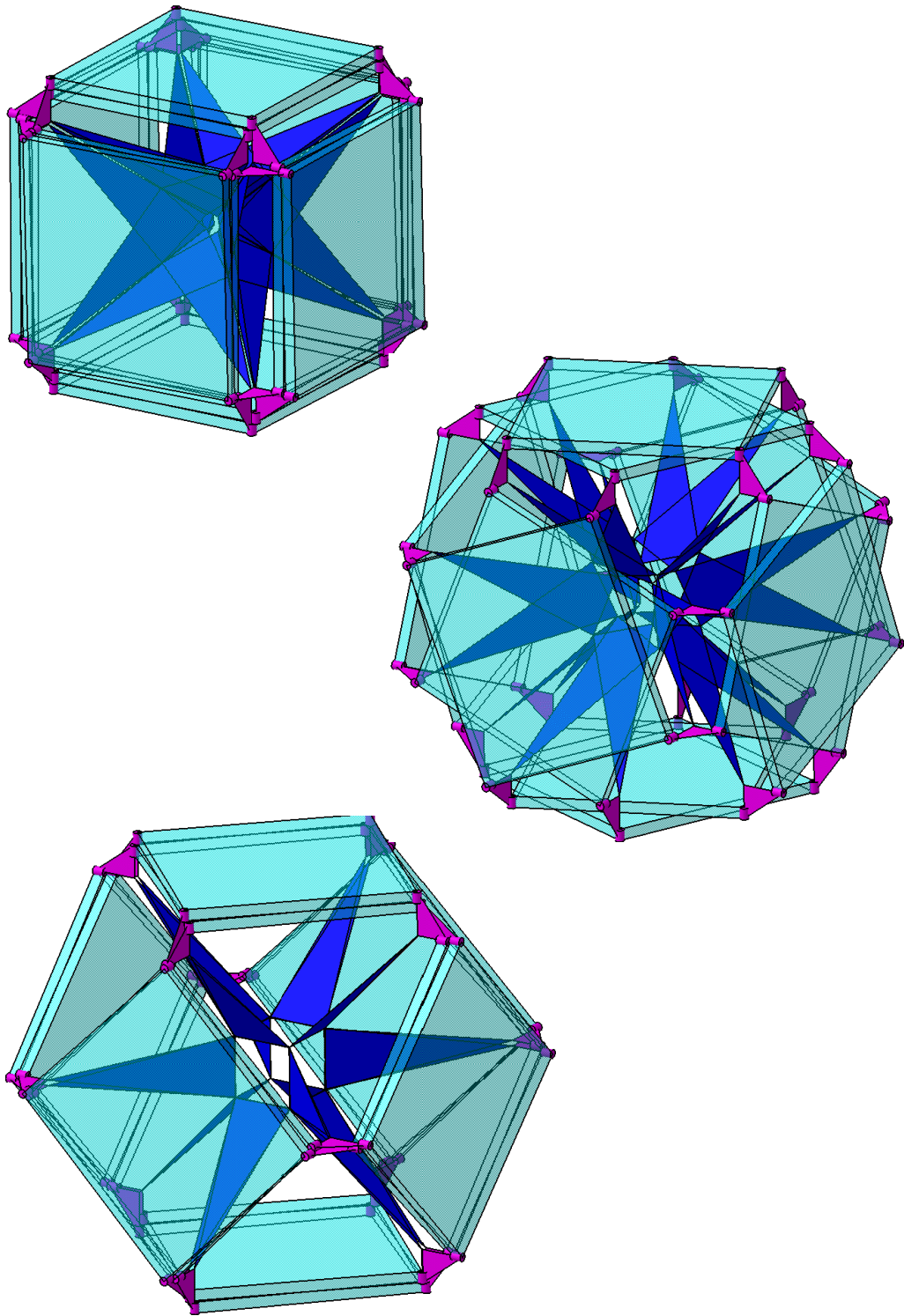


**Figure 7.17** Modified cubic linkage

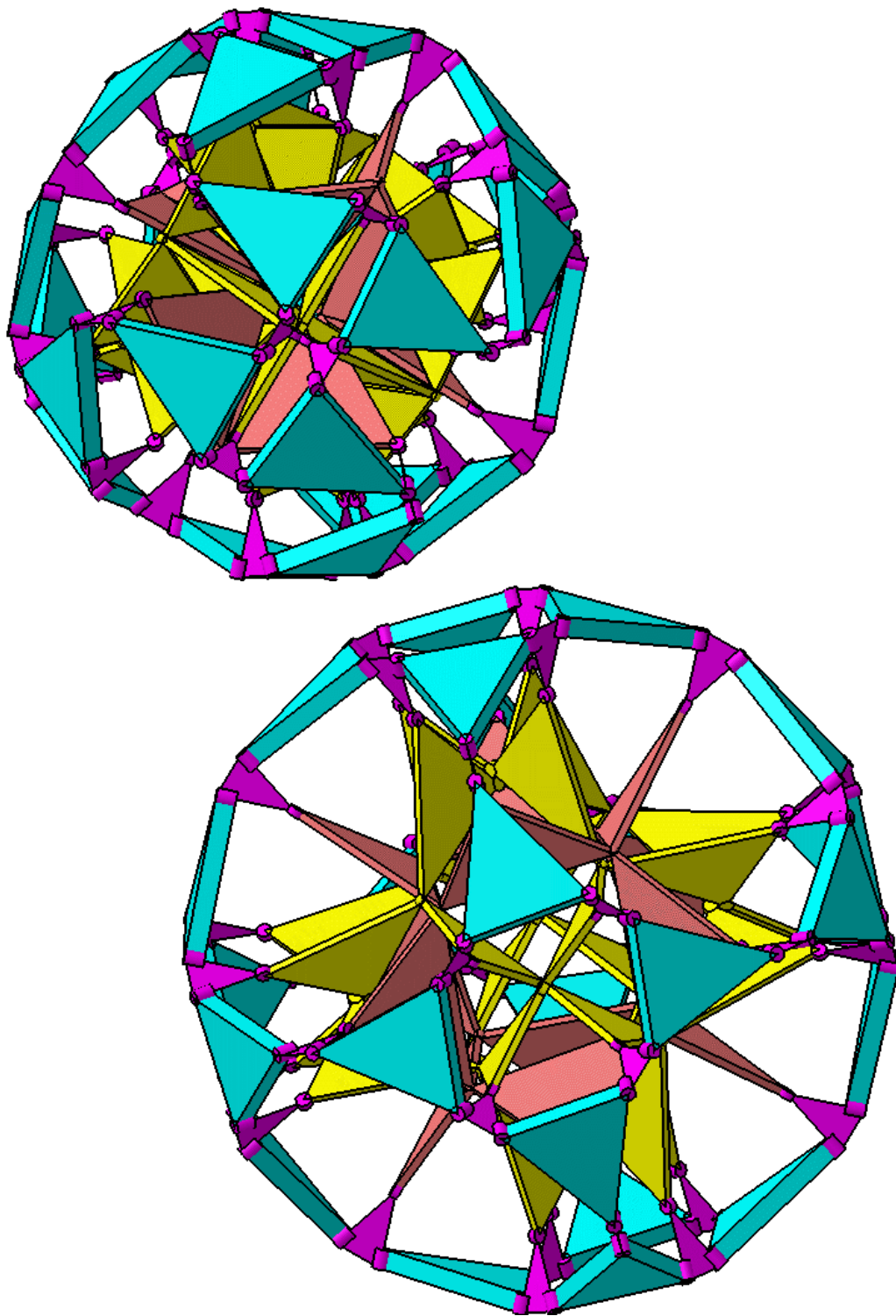


**Figure 7.18** Modified tetrakis icositetrahedral linkage

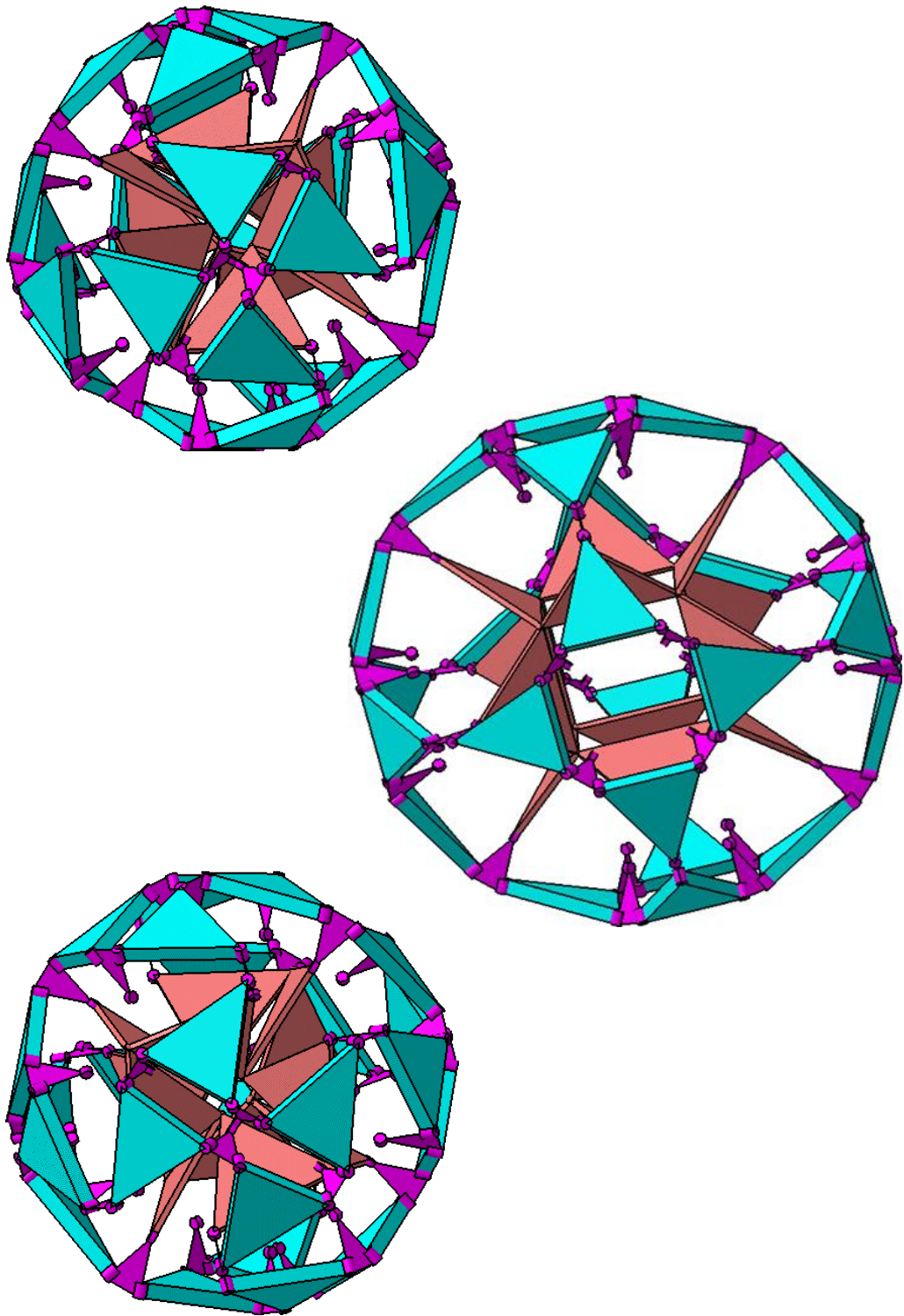


**Figure 7.19** Modified tetrakis icositetrahedral linkage with 24 links removed



## CHAPTER 8

### MODIFIED WREN PLATFORMS<sup>1</sup>

This chapter is unique in establishing a link between self-motions of parallel manipulators and Jitterbug-like polyhedral linkages. The resulting linkages have apparent applications.

#### 8.1 Self Motions of Parallel Manipulators and Wren Platforms

Husty et al. have published a series of papers regarding architecturally singular parallel manipulators which have the Borel-Bricard motion as a self-motion (Husty & Zsombor-Murray, 1994; Karger & Husty, 1998, Husty, 2000; Husty & Karger, 2000, 2002; Karger, 2001, 2008). A Borel–Bricard motion is a spatial motion, which has at least six spherical point trajectories (Karger, 2008). One specific mechanism, platform of which has this motion has a rather older history: the Wren platform as issued by Husty and Zsombor-Murray (1994) and Wohlhart (1996). Such a platform comprises at least five bars of equal length which connect to the base and the platform via spherical joints and the joint centers are on congruent circles (Wohlhart, 1996). For less than five limbs the mechanism has multi dof. This type of linkages has been used in design of pressure measuring devices (Brady, 1951), nozzles (Coleman, 1967),

---

<sup>1</sup> The main content of this section is published by Kiper and Söylemez (2011b).

rotary-to-linear/linear-to-rotary motion converters (Jacobsen, 1975; Mennito & Buehler, 1996) and deployable masts (Douglas, 1993).

Wohlhart (1996) has shown that the Wren platform has two modes where it possesses single or two dofs. Husty's studies and the applications mentioned above all relate to the single dof mode where the platform experiences the Borel-Bricard motion, more specifically in this case a line symmetric Schönflies motion (see Bottema & Roth, 1979, sec. 9.5) with respect to the base (Figure 8.1a). In this motion, the line of symmetry is the line joining the centers of the circles, on which the joint centers reside and the platform screws along this line during the motion. When the limbs become parallel (Figure 8.1b), this is the transition configuration of mobility and one can switch to the two-dof mode in which the platform has a pure translational freedom along spherical paths such that the platform remains parallel to the base (Figure 8.1c). The two-dof mode of the linkage can be seen as the spatial version of the planar parallelogram mechanism (see Figure 1.1).

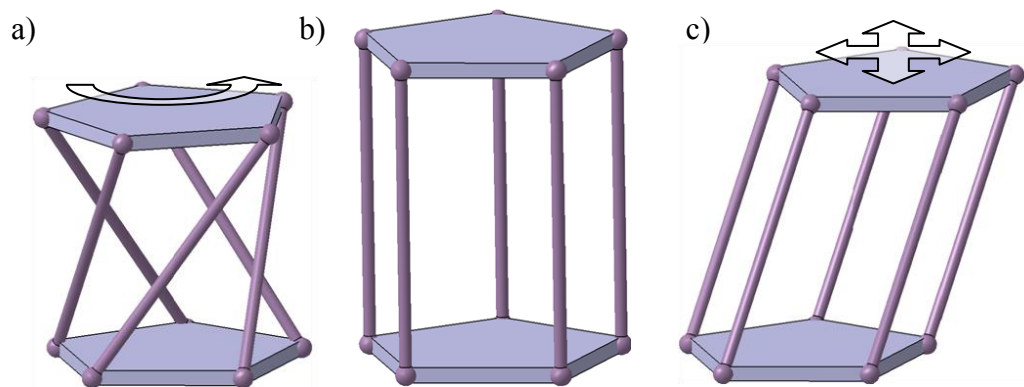


**Figure 8.1** a) Single dof mode b) Singular configuration c) Two-dof mode of a 5-leg Wren platform

Husty (2000) writes that when the joint centers of a Wren platform are chosen homologously on conic sections in the base and the platform, one can place the two systems in arbitrary positions relative to each other, link the corresponding points with rigid rods and the mechanism will be movable even when one adds infinitely many more rods. This fact is used in modification of the platforms.

## **8.2 3-UPU Parallel Manipulators**

As indicated by Tsai (1996), spherical joints are difficult to manufacture precisely at low cost, so it is not practical to design rigid link assemblies of the platform in Figure 8.1. Noticing that the rotations of the limbs along their axes are passive dof, it is natural to seek lower dof joint replacements without disturbing the platform motion. An immediate advantage of use of universal joints instead of spherical joints is that the motion of the platform can be obtained with three or four legs too. Indeed Tsai (1996) has applied this logic to devise a 3-UPU 3-dof manipulator. Many similar designs were proposed afterwards (Di Gregorio & Parenti Castelli, 1998; Karouia & Hervé, 2000, Wolf, Shoham & Park, 2002; Walter, Husty & Pfulner, 2009). These designs mainly differ by the arrangement of the revolute joints on the links. 3UU platforms are also used by Gao, Li, Jin and Zhao (2002) as a 2-dof composite kinematic pair. In this study a different leg configuration is presented in which the axes of the revolute joints on the base and the platform lie on a cylinder or a cone and the axes on the legs are parallel to each other. When the base surface is a cylinder, the substitute joints are universal joints, but in the case of a cone, the substitute joints are expected to be 2R joints with an acute angle between the intersecting revolute joint axes.

### 8.3 Jitterbug-Like Linkages

Jitterbug-like linkages are introduced in Chapter 6. Of these linkages, in this section the attention is on the class with two  $n$ -gonal links (base and platform) and  $n$  many digonal (binary) links (legs) which are connected to each other by the dihedral angle preserving (dap) joints. Verheyen (1989) investigates the case with equilateral polygonal links, identical digonal links and orthogonal dap joints, i.e. universal joints. The 3UU platform in Figure 8.2 is an example, but the number of limbs can be increased indefinitely.

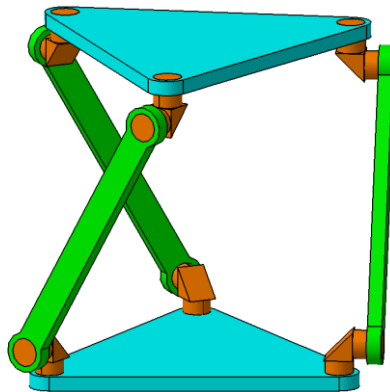


**Figure 8.2** One of Verheyen's (1989) dihedral dipolygonids

One immediately notices that this type of linkage is quite similar to a Wren platform. Indeed, the redundant rotations of the limbs about their axes are eliminated and the motion of the platform with respect to the base is the same



as a Wren platform. The algebraic characteristics of the single dof motion of this type of linkages are investigated by Röschel (1996b). Verheyen (1989) considers the single dof motion, but does not mention about the two-dof mode.

In the following sections such and similar platforms are investigated.

## **8.4 Modifications on the Verheyen Platform**

The modified platforms are classified according to joint axes arrangements.

### **8.4.1 Cylindrical Platforms**

Inspired from Husty (2000) one may expect that Verheyen's linkages may be modified for irregular cyclic polygonal platforms. Indeed to show that this is possible is quite simple. As Verheyen showed that  $n$ -UU platforms such as the one in Figure 8.2 are mobile for any equilateral  $n$ -gon and  $n$  can be increased indefinitely, suppose infinitely many legs for congruent circular base and platform. In this case the joint axes on the base/platform would define a full cylinder. The assembly is infinitely overconstrained and the platform motion does not alter if all the legs but  $m$  ( $m \geq 3$ ) of them are removed. The mobility of the resulting linkage is guaranteed, hence this way one can obtain any platform linkage with  $m$  legs arbitrarily located on a circle on congruent base and platform.

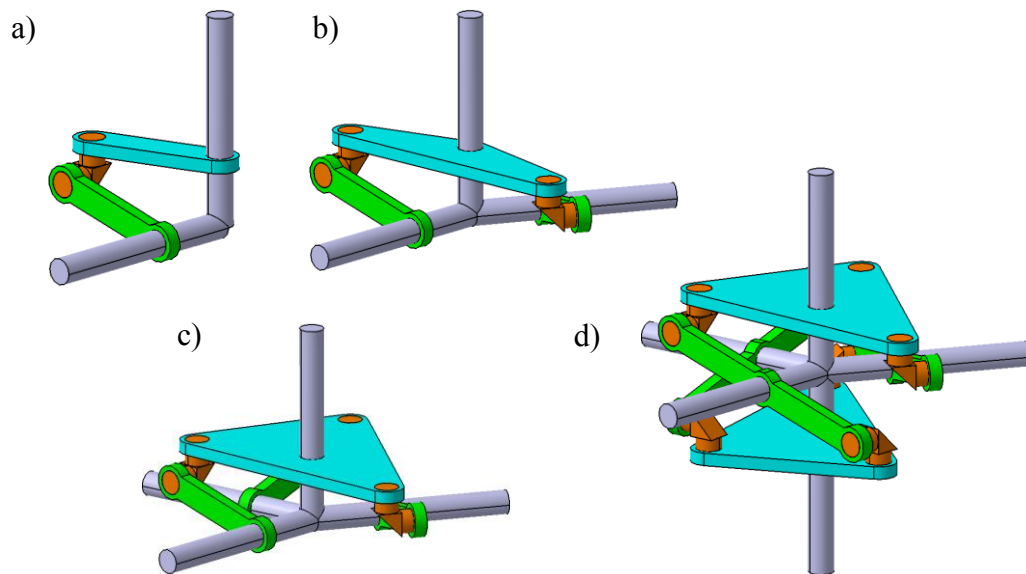


**Figure 8.3** Construction of a cylindrical platform with joint intersections on congruent circles

In (Verheyen, 1989) and (Röschel, 1996a) the main focus is in linkages for which there exists a fixed frame (centered at the midpoint of the centers of the circles of joint intersections) with respect to which ISAs of all links remain fixed. This is also the case for the ISAs of the cylindrical platforms in the single dof mode. Here is a constructional proof: It is known that an RCCR linkage is mobile with single dof if adjacent R (revolute) and C (cylindrical) joints have parallel axes (see Figure 6.9 and ex. [30]). Consider an RCCR loop for which nonparallel axes intersect orthogonally (Figure 8.3a). One can attach an identical loop to the first one such that one of the C axes and one of the links (triangular link in Figure 8.3b) is shared. One of these loops can drive the other one and the resulting 2-loop linkage is mobile. One can repeat these additions indefinitely about the same cylindrical joint axis (Figure 8.3c). Finally it is

possible to combine this multi-loop assembly with an anti-symmetric identical one to obtain a platform linkage (Figure 8.3d). In this assembly, the two polygonal links and all legs have fixed rotation axes and the axes can be removed to obtain the modified Verheyen platform described above.

When the universal joints are considered as links with two revolute joint connections these links have purely translatory motion with respect to each other and the spherical indicatrix of the assembly is immobile (Kiper, 2010a).

#### **8.4.2 General Parallel Leg Configuration**

Consider a more general case where all the joint axes on the base/platform are chosen parallel to each other. Axis offsets are arbitrary. The base and the platform joint axis locations should be congruent and the two are connected with equal size legs. In this case only the translational two-dof mode of the platform with respect to the base is obtained. A set of two independent rotation axes are illustrated in Figure 8.4a.

It is possible to add as many legs as desired as long as the platform/base joint axes are parallel. With this fact a spatial analog of the planar parallelogram mechanism is obtained.

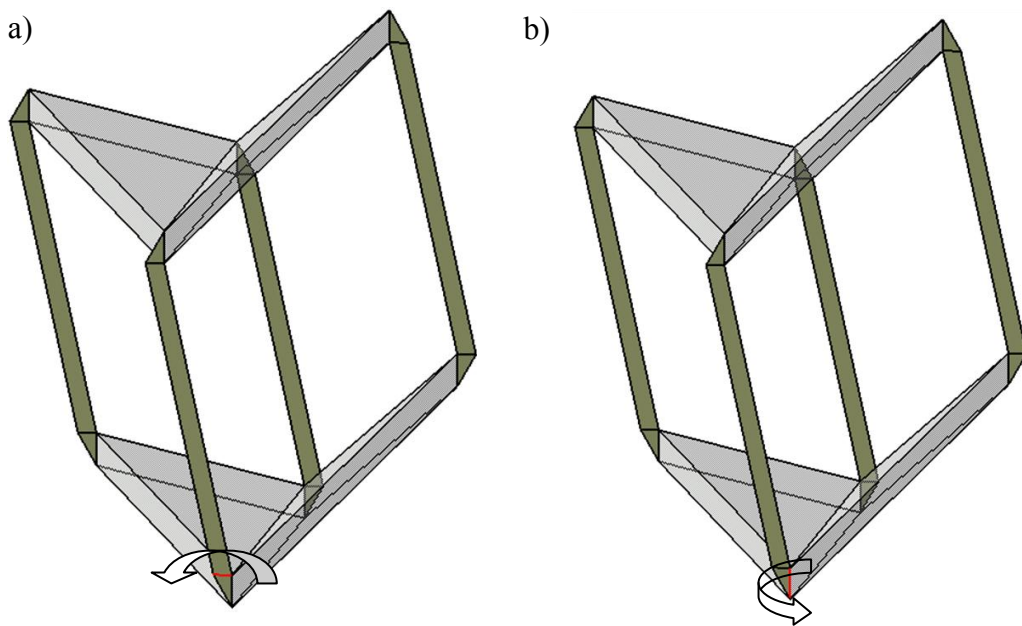


**Figure 8.4** The translatory motion of a spatial parallelogram mechanism (the joint axes on the platform/base are parallel to the view)

### 8.4.3 Conical Platforms

Again following Husty (2000) and also Karger (2001) platforms are sought for which the joint axes of the base/platform lie on a cone. The joint axes on the legs are again parallel to each other and perpendicular to the cone of platform axes. Joint axis intersections on the base/platform should be coplanar, hence are on circles of different size. This time, dap joints should be used instead of universal joints. When such an assembly is constructed one generically ends up with an immobile one, so further special geometrical conditions are needed. The results for homothetic Jitterbug-like linkages in Chapter 6 can be used. By Theorem 6 a sufficient condition to obtain such a mobile assembly realizing a

homothetic transformation is that the faces are all tangent to a sphere. When this condition is satisfied all the polygonal links have fixed ISAs, all meeting at the center of the above-mentioned sphere. In the present case the base, the platform and the diagonal legs should be equidistant to a central point. This point is necessarily on the symmetry axis of the cone (Figure 8.5).

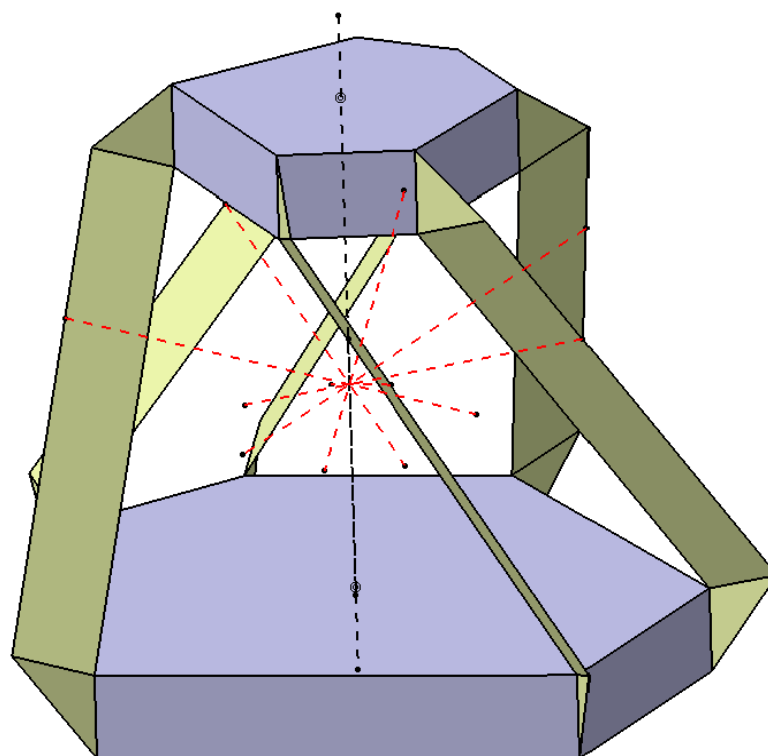


**Figure 8.5** A conical platform

#### **8.4.4 Other joint configurations**

A full classification of all possible platforms with UU or in general DD (D for dap) legs is not given here. Other possible joint configurations are subject to further studies.

#### **8.5 Use of Modified Wren Platforms as Deployable Structures**

It is already mentioned that Wren platforms or alike are used in various applications (Brady, 1951; Coleman, 1967; Jacobsen, 1975; Mennito & Buehler, 1996; Douglas, 1993). In this section the focus is on an obvious application – use of n-UU cylindrical platforms as uni-dimensional deployment applications. n-UU platforms are quite suitable for such a task especially if the leg lengths are chosen properly for more compact stowed position. When leg lengths are slightly bigger than the distance between joint axes on the polygonal links, serially connected platforms can be obtained for compact deployment. In Figure 8.6 an example with square platforms is illustrated. The problem in such a structure is actuation. n serial platforms totally have n dofs. However experiments on prototypes show that smooth deployment can be obtained if symmetric rotary inputs are applied on the platforms at the two ends.

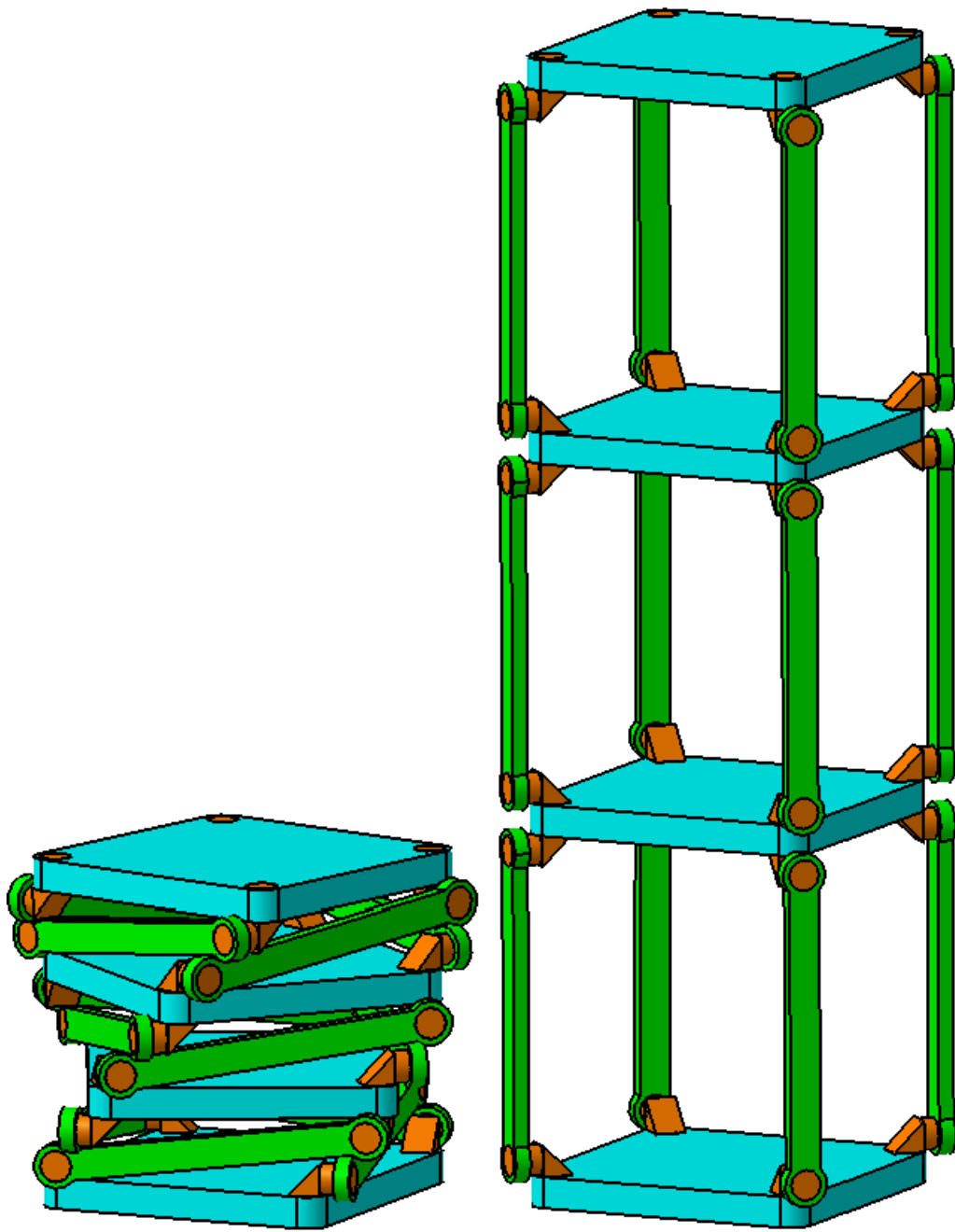


**Figure 8.6** A deployable mast with square polygonal links

## CHAPTER 9

### CONCLUSIONS

The following question is addressed in this thesis: What are the special geometric conditions to obtain homothetic deployable structures which comprise rigid links and revolute joints. Specifically polygonal and polyhedral geometries kept in focus.

In Chapter 2 angulated and regular scissor elements are used to deploy any kind of polygonal shape. The geometric conditions described in the chapter are not novel (see Liao & Li, 2005), yet the reasoning for these conditions were firmly established for the first time.

In Chapter 3 the planar linkages for regular polygonal shapes are assembled along intersecting planes to obtain star-like polyhedral linkages. Some existing linkages (Wohlhart, 1995; Hoberman, 2004a) were generalized.

In Chapters 4 Bennett loops are assembled to obtain polyhedral linkages. This chapter stands as an independent part in the thesis.

In Chapter 5 the polyhedral geometries of certain polyhedral linkages are deformed to obtain new ones. Though the method is applied to the Fulleroid (see Wohlhart, 1995) only, it is applicable for any kind of polyhedral linkage possessing symmetry.



Chapter 6 is the main contribution in this thesis. In this chapter Jitterbug-like linkages are introduced and some geometric conditions for these linkages are presented. First of all this chapter confirms the results of the previous studies and establishes a firm base for these results. As previous results (see Röschel, 1996a, 2001) mainly present necessary conditions, the theorems of Chapter 6 also contain sufficiency conditions. Furthermore this chapter involves new results such as  $\infty^2$  many Jitterbug-like linkages can be obtained for any homohedron. The analyses also relate to the linkages in Chapters 2 and 5 (see Sections 6.2.4.1, 6.2.4.5).

Chapter 7 is on modifications on the linkages introduced in Chapter 6. First type of modifications involves adding of links on the faces, while the second type involves adding links inside the supporting polyhedra.

Chapter 8 inherits its core material from Chapter 6, but relates to self motions of parallel manipulators. The content of this chapter is merely an introduction to design of a new class of kinematotropic parallel manipulators.

The author believes this thesis study enhances the state of the art regarding polygonal and polyhedral deployable structures, present some new methods to synthesize certain type of overconstrained linkages and finally emphasizes the relation of the subject with design of parallel manipulators - most popular area of research in machine theory science in the time this thesis is written.

## REFERENCES

- Agrawal, S. K., Kumar, S., & Yim, M. (2002). Polyhedral single degree-of-freedom expanding structures: design and prototypes. *Journal of Mechanical Design*, 124, 473-478.
- Akgün, Y., Gantes, C., Kalochairetis, K., & Kiper, G. (2010). A novel concept of convertible roofs with high transformability consisting of planar scissor-hinge structures, *Engineering Structures*, 32, 2873-2883.
- Altmann, F. G. (1954). Über räumliche sechsliedrige Koppelgetriebe, *Z V Deutscher Ingenieur*, 96, 245-249.
- Baker, J. E. (1978). Overconstrained 5-bars with parallel adjacent joint axes. *Mechanism and Machine theory*, 13, 213-218.
- Bennett, G. T. (1903). A new mechanism. *Engineering*, 76, 777-778.
- Bennett, G. T. (1911). Deformable octahedra. *Proceedings of the London Mathematical Society*, 2<sup>nd</sup> Series, 10, 309-343.
- Bennett, G. T. (1914). The skew isogram mechanism. *Proceedings of the London Mathematical Society*, 2<sup>nd</sup> Series, 13, 151-173.
- Bottema, O., & Roth, B. (1979). *Theoretical kinematics*, New York: North-Holland.
- Brady, J. M. (1951) *Pressure measuring device*, US patent 2564669.
- Bricard, R. (1897). Mémoire sur la théorie de l'octaèdre articulé. *The Journal des Mathématiques Pures et Appliquées*, 3, 113-150.
- Coleman, A. A. (1967). *Variable geometry nozzle*. US patent 3534908.
- Coxeter, H. S. L. (1946). *Regular polytopes*. London: Methuen & Co. Ltd.
- Coxeter, H. S. L., & Greitzer, S. M. (1967). *Geometry revisited*. Washington, DC: The Mathematical Association of America.
- Cromwell, P. R. (1997). *Polyhedra*. Cambridge: Cambridge University Press.

Delassus, E. (1900). Sur les systèmes articulés gauches, première partie. *Paris Annales Scientifiques de l'Ecole Normale Supérieures, 3<sup>rd</sup> Series, 17*, 455-499.

Delassus, E. (1902). Sur les systèmes articulés gauches, deuxième partie. *Paris Annales Scientifiques de l'Ecole Normale Supérieures, 3<sup>rd</sup> Series, 19*, 119-152.

Delassus, E. (1922) Les chaînes articulés fermées et déformables à quatre membres. *Bulletin des Sciences Mathématiques, 2<sup>nd</sup> Series, 46*, 283-304.

Denavit, J., & Hartenberg, R. S. (1955). A kinematic notation for lower-pair mechanisms based on matrices. *ASME Journal of Applied Mechanics, 22*, 215-221.

Di Gregorio, R., & Parenti-Castelli, V. (1998). A translational 3-dof parallel manipulator. In: Lenarčič, J., & Wenger, P. (Eds.): *Advances in robot kinematics: Analysis and control*, Dordrecht: Kluwer Academic Publishers, 49-58.

Dietmaier, P. (1995). A new 6R space mechanism. *Proc. 9<sup>th</sup> world congress on the theory of machines and mechanisms, 1*, Milano, 52-56.

Dijkman, E. A. (1976). *Motion geometry of mechanisms*. Cambridge: Cambridge University Press.

Dimentberg, F. M., & Yoslovich, I. V. (1966) A spatial four link mechanism having two prismatic pairs. *Journal of Mechanisms, 4*, 101-114.

Douglas, M. V. (1993). *Module for an articulated stowable and deployable mast*, US patent 5267424.

Dörrie, H. (1965). *100 Great problems of elementary mathematics: their history and solutions*, New York: Dover.

Edge, W. L. (1931). *The theory of ruled surfaces*. London: Cambridge University Press.

Edmondson, A. C. (2007). *A Fuller explanarion – the synergetic geometry of R. Buckminster Fuller*. Pueblo: EmergentWorld.

Fang, Y., & Tsai, L. W. (2004). Enumeration of a class of overconstrained mechanisms using the theory of reciprocal screws. *Mechanism and Machine Theory, 39*, 1175-1187.

- Fuller, R. B. (1975). *Synergetics: explorations in the geometry of thinking*. New York: Macmillan, Section 460.
- Fuller, R. B., Krausse, J., & Lichtenstein, C. (1999). *Your private sky: R. Buckminster Fuller, the art of design science*. Baden: Lars Müller.
- Galiliunas, P., & Sharp, J. (2005). Duality of polyhedra. *International Journal of Mathematical Education in Science and Technology*, 36, 617-642.
- Gantes, C. J., & Konitopoulou, E. (2004). Geometric design of arbitrarily curved bi-stable deployable arches with discrete joint size. *International Journal of Solids and Structures*, 41, 5517-5540.
- Gao, F., Li, W., Zhao, X., Jin, Z., & Zhao, H. (2002). New kinematic structures for 2-, 3-, 4-, and 5-dof parallel manipulator designs. *Mechanism and Machine Theory*, 37, 1395-1411.
- Goldberg, M. (1942). Polyhedral linkages. *National Mathematics Magazine*, 16, 323-332.
- Goldberg, M. (1943). New five-bar and six-bar linkages in three dimensions. *Transactions of the ASME*, 65, 649-661.
- Gogu, G. (2008). *Structural synthesis of parallel robots: Part 1 – Methodology*. Dordrecht: Springer.
- Gosselin, C. M., & Gagnon-Lachance, D. (2006). Expandable polyhedral mechanisms based on polygonal one-degree-of-freedom faces. *Proceedings of the Institution of Mechanical Engineers - Part C: Mechanical Engineering Science*, 220, 1011-1018.
- Hervé, J. M. (1978). Analyse structurelle des mécanismes par groupe des déplacements. *Mechanism and Machine Theory*, 23, 171-183.
- Hilbert, D., & Cohn-Vossen, S. (1990). *Geometry and the imagination* (2<sup>nd</sup> ed.) (P. Nemenyi, Trans.). New York: Chelsea Publishing Company. (Original work published 1952)
- Hoberman, C. (1990). *Reversibly expandable doubly-curved truss structure*, US patent 4942700.
- Hoberman, C. (1995). *Hoberman Associates – transformable design – Hoberman sphere (product)*. Retrieved January 20, 2011, from

[http://www.hoberman.com/portfolio/hobermansphere-toy.php?rev=0&onEnterFrame=\[type+Function\]&myNum=12&category=&projectname=Hoberman+Sphere+\(product\)](http://www.hoberman.com/portfolio/hobermansphere-toy.php?rev=0&onEnterFrame=[type+Function]&myNum=12&category=&projectname=Hoberman+Sphere+(product))

Hoberman, C. (2004a). *Geared expanding structures*, US patent 7464503.

Hoberman, C. (2004b). *Hoberman Associates – transformable design - switch pitch*. Retrieved January 20, 2011, from <http://www.hoberman.com/portfolio/switchpitch.php?projectname=Switch%20Pitch>.

Hunt, K. H. (1978). *Kinematic geometry of mechanisms*. Oxford: Clarendon Press.

Husty, M. L., & Zsombor-Murray, P. (1994). A Special Type of Singular Stewart Gough Platform. In: Lenarčič, J., & Ravani, B. (Eds.): *Advances in robot kinematics and computational geometry*, Dordrecht: Kluwer Academic Publishers, 439-449.

Husty, M. L. (2000). E. Borel's and R. Bricard's papers on displacements with spherical paths and their relevance to self-motions of parallel manipulators. In: *Proceedings of the international symposium on history of machines and mechanisms*, Dordrecht: Kluwer Academic Publishers, 163-172.

Husty, M.L., & Karger, A. (2000). Architecture singular parallel manipulators and their self motions. In: Lenarčič, J., & Stanišić, M. M. (Eds.): *Advances in robot kinematics*, Dordrecht: Kluwer Academic Publishers, 355-364.

Husty, M.L., & Karger, A. (2002). Self motions of Stewart-Gough platforms – An overview. *Proceedings of workshop on fundamental issues and future research directions for parallel mechanisms and manipulators*, Quebec City, 131-141.

Jacobsen, S. C. (1975). *Rotary-to-linear and linear-to-rotary motion converters*, US patent 3864983.

Karger, A., & Husty, M. L. (1998). Classification of all self-motions of the original Stewart-Gough platform. *Computer Aided Design*, 30, 205-215.

Karger, A. (2001). Singularities and self motions of equiform platforms. *Mechanism and Machine Theory*, 36, 801-815.

Karger, A. (2008). Self-motions of Stewart-Gough platforms. *Computer Aided Geometric Design*, 25, 775-783.

- Karouia, M., & Hervé, J. M. (2000). A three-dof tripod for generating spherical rotation. In: Lenarčič, J., & Stanišić, M. M. (Eds.): *Advances in robot kinematics*, Dordrecht: Kluwer Academic Publishers, 395-402.
- Kempe, A. B. (1878). On conjugate four-piece linkages, *Proceedings of the London Mathematical Society, 1<sup>st</sup> Series*, 9, 133-147.
- Kiper, G. (2006). *New design methods for polyhedral linkages*, Master of Science Thesis, Ankara: Middle East Technical University.
- Kiper, G., Söylemez, E., & Kişisel, A. U. Ö. (2007). Polyhedral linkages synthesized using Cardan motion along radial axes. In: *Proceedings of the 12<sup>th</sup> IFToMM world congress* (CD), Besançon.
- Kiper, G., Söylemez, E., & Kişisel, A. U. Ö. (2008). A family of deployable polygons and polyhedra. *Mechanism and Machine Theory*, 43, 627-640.
- Kiper, G. (2009a). Fulleroid-like linkages. In: Ceccarelli, M. (Ed.): *Proceedings of EUCOMES 08*, Dordrecht: Springer, 423-430.
- Kiper, G., & Söylemez, E. (2009b). Regular polygonal and regular spherical polyhedral linkages comprising Bennett loops, In: Kecskeméthy, A., & Müller, A (Eds.): *Computational kinematics*, Dordrecht: Springer, 249-256.
- Kiper, G. (2010a). Some properties of Jitterbug-like polyhedral linkages. In: Pisla, D., Ceccarelli, M., Husty, M., & Corves, B. (Eds.): *New trends in mechanism science: analysis and design*, Dordrecht: Springer, 137-145.
- Kiper, G., & Söylemez, E. (2010b). Obtaining new linkages from Jitterbug-like polyhedral linkages. In: *Proceedings of the AzC IFToMM 2010 international symposium of mechanism and machine science*, İzmir, 137-143.
- Kiper, G., & Söylemez, E. (2010c). Irregular polygonal and polyhedral linkages comprising scissor and angulated elements. In: *Proceedings of the 1<sup>st</sup> IFToMM Asian conference on mechanism and machine science* (CD), Taipei.
- Kiper, G., & Söylemez, E. (2011a). Some new overconstrained linkages obtained from homothetic Jitterbug-like linkages. In: *Proceedings of the 13<sup>th</sup> IFToMM world congress* (CD), Guanajuato.
- Kiper, G., & Söylemez, E. (2011b). Modified Wren platforms. In: *Proceedings of the 13<sup>th</sup> IFToMM world congress* (CD), Guanajuato.

- Kokawa, T. (1997). Cable scissors arch-marionettic structure. In: Chilton, J. C. (Ed.): *Structural morphology: Towards the new millennium*. Nottingham: University of Nottingham Press, 107-114.
- Kovács, F., Tarnai, T., Fowler, P. W., & Guest, S. D. (2004a). A class of expandable polyhedral structures. *International Journal of Solids and Structures*, *41*, 1119-1137.
- Kovács, F., Tarnai, T., Guest, S. D., & Fowler, P. W. (2004b), Double-link expandohedra: a mechanical model for expansion of a virus. *Proceedings of the Royal Society: Mathematical, Physical & Engineering Sciences*, *461*(2051), 3191-3202.
- Langbecker, T. (1999). Kinematic analysis of deployable bar structures, *International Journal of Space Structures*, *14*, 1–16.
- Liao, Q., & Li, D. (2005) Mechanisms for scaling planar graphs. *Chinese Journal of Mechanical Engineering*, *41*, 140-143.
- Mao, D., Luo, Y., & You, Z. (2009). Planar closed loop double chain linkages. *Mechanisms and Machine Theory*, *44*, 850-859.
- Mavroidis, C., & Roth, B. (1995). New and revised overconstrained mechanisms. *Transactions of the ASME, Journal of Mechanical Design*, *117*, 75-82.
- M’cLelland, W.J., & Preston, T. (1886). *A treatise on spherical trigonometry with applications to spherical geometry and numerous examples - Part II*, London: Macmillan.
- M’cLelland, W.J., & Preston, T. (1893). *A treatise on spherical trigonometry with applications to spherical geometry and numerous examples - Part I* (4th ed.), London: Macmillan.
- Mennitto, G., & Buehler, M. (1996). CARL: A compliant articulated robot leg for dynamic locomotion. *Robotics and Automation Systems*, *18*, 337-344.
- Myard, F. E. (1931). Contribution à la géométrie des systèmes articulés. *Bulletin de la Société Mathématique de France*, *59*, 183-210.
- Olshevsky, G. (2006). *Multidimensional glossary*. Retrieved February 01, 2011, from [http://gluon.softcafe.net/gravity/reprints/ref\\_thesis/Olshevsk-2001\\_GlossaryForHyperspace.htm](http://gluon.softcafe.net/gravity/reprints/ref_thesis/Olshevsk-2001_GlossaryForHyperspace.htm).

Patel, J., & Ananthasuresh, G. K. (2007). A kinematic theory for radially foldable planar linkages. *International Journal of Solids and Structures*, 44, 6279-6298.

Pfurner, M. (2009). A new family of overconstrained 6R-mechanisms, In: Ceccarelli, M. (Ed.): *Proceedings of EUCOMES 08*, Dordrecht: Springer, 117-124.

Rico, J. M., & Ravani, B. (2007). On calculating the degrees of freedom or mobility of overconstrained linkages: single-loop exceptional linkages. *Journal of Mechanical Design*, 129, 301-311.

Rosenfeld, B.A. (1988). *A History of non-Euclidean geometry - evolution of the concept of a geometric space*, (A. Shenitzer, Trans.). New York: Springer-Verlag. (Original work published 1976)

Röschel, O. (1995). Zwangläufig bewegliche Polyedermodelle I. *Mathematica Pannonica*, 6, 267-284.

Röschel, O. (1996a). Zwangläufig bewegliche Polyedermodelle II. *Studia Scientiarum Mathematicarum Hungarica*, 32, 383-393.

Röschel, O. (1996b). Linked Darboux motions, *Mathematica Pannonica*, 7, 291-301.

Röschel, O. (2001). Zwangläufig bewegliche Polyedermodelle III. *Mathematica Pannonica*, 12, 55-68.

Röschel, O. (2010). The self-motions of a Fulleroid-like mechanism. *Proceedings of the 14<sup>th</sup> international conference on geometry and graphics*, Kyoto, 1-7.

Sarrus, P. T. (1853). Note sur la transformation des mouvements rectilignes alternatifs, en mouvements circulaires; et réciproquement. *Académie des Sciences, Comptes rendus hebdomadaires des séances, Paris*, 36, 1036-1038.

Schatz, P. (1975). *Rhythmusforschung und Technik*, Stuttgart: Freies Geistesleben.

Stachel, H. (1994). The Heureka polyhedron. In: Fejes Tóth, G. (Ed.): *Intuitive Geometry*. Coll. Math. Soc. J. Bolyai, 63, Amsterdam: North-Holland, 447-459.



Tsai, L. W. (1996). Kinematics of a three-dof platform with three extensible limbs. In: Lenarčič, J., & Parenti-Castelli, V. (Eds.): *Recent Advances in robot kinematics*, Dordrecht: Kluwer Academic Publishers, 401-410.

Verheyen, H. F. (1989). The complete set of Jitterbug transformers and the analysis of their motion. *The International Journal of Computers and Mathematics With Applications*, 17, 203-250.

Waldron, K. J. (1967). A family of overconstrained linkages. *Journal of Mechanisms*, 2, 201-211.

Waldron, K. J. (1968). Hybrid overconstrained linkages. *Journal of Mechanisms*, 3, 73-78.

Waldron, K. J. (1969). Symmetric overconstrained linkages. *Transactions of the ASME, Journal of Engineering for Industry*, 91, 158-162.

Waldron, K. J. (1979). Overconstrained linkages. *Environment and Planning B*, 6, 393-402.

Waldron, K. J., & Kinzel, G. L. (2004). *Kinematics, dynamics, and design of machinery* (2<sup>nd</sup> ed.). New York: John Wiley & Sons, Inc.

Walter, D. R., Husty, M. L., & Pfurner, M. (2009). A complete kinematic analysis of the SNU 3-UPU parallel robot. In: Bates, D. J., Besana, G. M., Di Rocco, S., & Wampler, C. (Eds.): *Interactions of Classical and Numerical Algebraic Geometry, Contemporary Mathematics 496*, 331-346.

Wei, X. Z., Yao, Y. A., Tian, Y. B., & Fang, R. (2006). A new method of creating expandable structure for spatial objects. *Proceedings of the Institution of Mechanical Engineers - Part C: Mechanical Engineering Science*, 220, 1813-1818.

Weisstein, E. W. (n.d.). *MathWorld – A Wolfram web source*. Retrieved January 20, 2011, from <http://mathworld.wolfram.com>.

Wikipedia Foundation, Inc. (n.d.). *Wikipedia – the free encyclopedia*. Retrieved January 20, 2011, from <http://en.wikipedia.org>.

Wohlhart, K. (1987). A new 6R space mechanism. *Proceedings of the 7<sup>th</sup> world congress of the theory of machines and mechanisms*, 1, 193-198.

Wohlhart, K. (1991). Merging two general Goldberg 5R linkages to obtain a new 6R space mechanism. *Mechanism and Machine Theory*, 26, 659-668.

Wohlhart, K. (1993). Heureka octahedron and Brussels folding cube as special cases of the turning tower. *Proceedings of the 6<sup>th</sup> IFToMM international symposium on linkages and computer aided design methods*, Bucharest, 325-332.

Wohlhart, K. (1994). The screwtower, an overconstrained multi-loop space mechanism. *Proceedings of the international conference on spatial mechanisms and high-class mechanisms, 1*, Almaty, 38-45.

Wohlhart, K. (1995). New Overconstrained spheroidal linkages. *Proceedings of the 9<sup>th</sup> world congress on the theory of the machines and mechanisms*, Milano, 149-155.

Wohlhart, K. (1996). Kinematotropic Linkages. In: Lenarčič, J., & Parenti-Castelli, V. (Eds.): *Recent advances in robot kinematics*, Dordrecht: Kluwer Academic Publishers, 359-368.

Wohlhart, K. (1997). Kinematics and Dynamics of the Fulleroid. *Multibody System Dynamics, 1*, 241-258.

Wohlhart, K. (1998). The Kinematics of Röschel Polyhedra. In: Lenarčič, J., & Husty, M. L. (Eds.): *Advances in robot kinematics*, Dordrecht: Kluwer Academic Publishers, 277-286.

Wohlhart, K. (1999). Deformable cages. *Proceedings of the 10<sup>th</sup> world congress on theory of machines and mechanisms, 2*, Oulu, 683-688.

Wohlhart, K. (2000). Double-chain mechanisms, In: Pellegrino, S. & Guest, S. D. (Eds.): *Proceedings of the IUTAM-IASS symposium on deployable structures: theory and applications*, Dordrecht: Kluwer Academic Publisher, 457-466.

Wohlhart, K. (2001a). Regular polyhedral linkages, *Proceedings of the 2<sup>nd</sup> workshop on computational kinematics*, Seoul, 239-248.

Wohlhart, K. (2001b). New regular polyhedral linkages. *Proceedings of the SYROM 2001*, Bucharest, 365-370..

Wohlhart, K.. (2004a). Irregular polyhedral linkages, *Proceedings of the 11<sup>th</sup> world congress in mechanism and machine Sciences*, Tianjin, 1083-1087.

Wohlhart, K. (2004b). Polyhedral zig-zag linkages. In: Lenarčič, J., & Galletti, C. (Eds.): *On advances in robot kinematics*, Dordrecht: Kluwer Academic Publishers, 351-360.

Wohlhart, K. (2005). Double pyramidal linkages. *Proceedings of the 11<sup>th</sup> international symposium on theory of machines and mechanisms, 1*, Bucharest, 293-300.

Wohlhart, K. (2008). Double-ring polyhedral linkages. *Proceedings of the conference on interdisciplinary applications of kinematics*, Lima, 1-17.

Wolf, A., Shoham, M. & Park, F. C. (2002). Investigation of singularities and self-motions of the 3-UPU parallel robot. In: Lenarčič, J., & Thomas, F (Eds.): *Advances in robot kinematics: theory and applications*, Dordrecht: Kluwer Academic Publishers, 401-410.

You, Z., & Pellegrino, S. (1997). Foldable Bar Structures. *International Journal of Solids and Structures*, 34, 1825-1847.

## APPENDIX A

### Glossary

Meanings of some terms which are thought to be unfamiliar to the reader are listed below.

**Apex:** (geometry) A descriptive label for a visual singular highest or most distant point or vertex in an isosceles triangle, pyramid or cone, usually contrasting with the opposite side called the base (Wikipedia, n.d.)

**Antiprism:** A polyhedron composed of two parallel copies of some particular polygon, connected by an alternating band of triangles (Wikipedia, n.d.)

**Archimedean (semiregular) solids:** Convex polyhedra that have a similar arrangement of nonintersecting regular convex polygons of two or more different types arranged in the same way about each vertex with all sides the same length – There are 13 such solids (Weisstein, n.d.). The duals of the Archimedean solids are called as the Catalan solids.

**Catalan solids:** Dual polyhedra of the Archimedean solids (Wikipedia, n.d.)

**Concave:** Curving in or hollowed inward, as opposed to convex (Wikipedia, n.d.)

**Conformal transformation:** A transformation which preserves angles (Wikipedia, n.d.)

**Convex:** Curving out or bulging outward, as opposed to concave (Wikipedia, n.d.)

**Cuboctahedron:** A polyhedron with eight triangular faces and six square faces – It has 12 identical vertices, with two triangles and two squares meeting at each, and 24 identical edges, each separating a triangle from a square. It is an Archimedean solid (Wikipedia, n.d.).

**Cumulation:** The operation which replaces the faces of a polyhedron with pyramids of height  $h$  (where  $h$  may be positive, zero, or negative) having the face as the base (Weisstein, n.d.)

**Cupola:** A solid formed by joining two polygons, one (the base) with twice as many edges as the other, by an alternating band of triangles and rectangles (Wikipedia, n.d.)

**Deltahedron:** A polyhedron whose faces are congruent equilateral triangles – There are 8 convex deltahedra, 3 of which are Platonic (tetrahedron, octahedron and icosahedron) and the remaining 5 of which are Johnson solids (triangular dipyramid, pentagonal dipyramid, snub disphenoid, truncated triangular prism and gyroelongated square dipyramid) (Weisstein, n.d.).

**Dihedral angle:** The angle between two adjacent faces of a polyhedron (Cromwell, 1997, p. 13)

**Dilation:** See “homothety”

**Dipolygon:** A pair of regular polygons with a common vertex, the axes of symmetries of which intersect each other (Verheyen, 1989)

**Dipolygonid:** A polyhedral linkage generated by a dipolygon under the two group actions given by the cyclic symmetry groups of the two regular polygons of the dipolygon (Verheyen, 1989)

**Dipyramid (bipyramid):** A polyhedron formed by joining a pyramid and its mirror image base-to-base (Wikipedia, n.d.)

**Dodecahedron:** A polyhedron with twelve flat faces (Wikipedia, n.d.). Unless otherwise indicated, “dodecahedron” is used for the regular dodecahedron, which is convex and has equilateral pentagonal faces.

**Edge:** A line segment along which two faces come together (Cromwell, 1997, p. 13) – To avoid confusion the term “side” is used for polygons and “edge” is used for polyhedra

**Equiform transformation (or similarity):** A transformation that preserves angles and changes all distances in the same ratio, called the ratio of magnification - can also be defined as a transformation that preserves ratios of distances (Weisstein, n.d.)

**Euler characteristic:** a topological invariant  $\chi$ , a number that describes a topological space's shape or structure regardless of the way it is bent – for polyhedra  $\chi = V - E + F = 2 - 2g$ , where  $g$  is the genus of the polyhedral surface, so  $\chi \leq 2$  (Wikipedia, n.d.)

**Face:** Each polygon of a polyhedron (Cromwell, 1997, p. 13)

**Genus:** A topologically invariant property of a surface defined as the largest number of nonintersecting simple closed curves that can be drawn on the surface without separating it - roughly speaking, the number of holes in a surface (Weisstein, n.d.)

**Gyroelongated square dipyramid:** One of the eight convex deltahedra built up from 16 equilateral triangles - It consists of two oppositely faced square pyramids rotated  $45^\circ$  to each other and separated by a 4-antiprism. It is Johnson solid  $J_{17}$  (Weisstein, n.d.).

**Hexahedron:** A polyhedron with six faces (Wikipedia, n.d.)

**Homohedron:** A polyhedron all of whose faces are congruent (Olshevsky, 2006)

**Homothety (homothecy, dilation):** A similarity transformation which preserves orientation, also called a homothety (Weisstein, n.d.)

**Icosahedron:** A 20-faced polyhedron (Weisstein, n.d.) - Unless otherwise indicated, "icosahedron" is used for the regular icosahedron, which is convex and has equilateral triangular faces.

**Icositetrahedron:** A 24-faced polyhedron (Weisstein, n.d.)

**Isohedron (face-transitive polyhedron):** A polyhedron for which any pair of faces there is a symmetry of the polyhedron which carries the first face onto the second – Physically this means that the polyhedron looks the same when viewed face on, no matter which face is presented to the eye (Cromwell, 1997, p. 367)

**Johnson solids:** Convex polyhedra having regular faces and equal edge lengths (with the exception of the completely regular Platonic solids, the "semiregular" Archimedean solids, and the two infinite families of prisms and antiprisms) – There are 92 Johnson solids in all (Weisstein, n.d.)

**Kite (deltoid or trapezoid):** A planar convex quadrilateral consisting of two adjacent sides of length  $a$  and the other two sides of length  $b$  (Weisstein, n.d.)

**Octahedron:** A polyhedron with eight faces (Wikipedia, n.d.) - Unless otherwise indicated, “octahedron” is used for the regular octahedron, which is convex and has equilateral triangular faces.

**Plane angle:** The angle in the corner of a polygonal face of a polyhedron (Cromwell, 1997, p. 13)

**Platonic (regular) solids:** Convex polyhedra with equivalent faces composed of congruent convex regular polygons - There are exactly five such solids: the cube, dodecahedron, icosahedron, octahedron and tetrahedron (Weisstein, n.d.)

**Rhombic Dodecahedron:** A convex polyhedron with 12 rhombic faces (Wikipedia, n.d.)

**Rhombohedron:** Three-dimensional figure like a cube, except that its faces are not squares but rhombi (Wikipedia, n.d.)

**Ruled surface:** A surface formed by a singly infinite system of straight lines (Edge, 1931, p. 7) – If a line moves continuously, it generates a ruled surface (Bottema & Roth, 1979, p. 55).

**Similarity:** See “equiform transformation”

**Solid angle:** The region of a solid polyhedron near a vertex (Cromwell, 1997, p. 13) - It used to be used instead of “vertex”.

**Snub disphenoid (Siamese dodecahedron):** The 12-faced convex deltahedron which is also Johnson solid  $J_{84}$  (Weisstein, n.d.)

**Spherical excess:** The amount by which the sum of the angles of a spherical n-gon exceeds the sum of the angles of a planar n-gon (Wikipedia, n.d.)

**Stella octangula:** The only stellation of the octahedron (Weisstein, n.d.)



**Stellation:** the process of constructing polyhedra by extending the facial planes past the polyhedron edges of a given polyhedron until they intersect (Weisstein, n.d.)

**Tetrahedron:** A polyhedron composed of four triangular faces, three of which meet at each vertex (Wikipedia, n.d.) - Unless there is an indication of irregularity, “tetrahedron” is used for the regular tetrahedron, which has equilateral triangular faces.

**Tetrakis hexahedron (disdyakis cube):** A non-regular icositetrahedron that can be constructed as a positive cumulation of regular cube (Weisstein, n.d.)

**Trapezohedron (antipyramid or deltohedron):** The dual polyhedron of an n-gonal antiprism - Its  $2n$  faces are congruent kites (Weisstein, n.d.).

**Triaugmented triangular prism:** One of the the convex deltahedra - It is composed of 14 equilateral triangles, and is Johnson solid  $J_{51}$  (Weisstein, n.d.).

**Truncation (of a polyhedron vertex):** The process of cutting all the vertices in a symmetric fashion (Cromwell, 1997, p. 80) – Truncation of an n-valent vertex results in a new n-gonal face, n new edges and n-1 new 3-valent vertices.

**Valency (of a vertex):** A vertex is said to have valence n, or to be n-valent, if it is the meeting point of n edges and, therefore is surrounded by n faces (Cromwell, 1997, p. 192)

**Vertex:** A point where several edges and faces of a polyhedron come together (Cromwell, 1997, p. 77) – To avoid confusion the term “corner” is used for polygons and “vertex” is used for polyhedra.

**Vertex Figure:** 1. The spherical polygon formed by the intersection of the faces surrounding a vertex with a small sphere centered on that vertex (Cromwell, 1997, p. 77), 2. The polygon you see after slicing off a pyramid about a vertex of a polyhedron in a way that removes the same amount of each edge (Cromwell, 1997, p. 77). 3. Can be used interchangeably with solid angle

## CURRICULUM VITAE

### PERSONAL INFORMATION

Surname, Name: Kiper, Gokhan  
Nationality: Turkish (TC)  
Date and Place of Birth: 07 March 1982, Ezine  
Marital Status: Single  
Phone: +905334526821  
Email Address: kiper@gmail.com

### EDUCATION

Degree	Institution	Year of Graduation
MS	METU Mechanical Engineering Dept.	2006
BS	METU Mathematics Dept.	2004
BS	METU Mechanical Engineering Dept.	2004
High School	İzmir High School of Science	2000

### WORK EXPERIENCE

Year	Place	Enrollment
2005-Present	METU Mechanical Engineering Dept.	Research Assistant
2010 April-August	Advanced Highway Maintenance and Construction Technology Research Center, University of California, Davis	Temporary Affiliate
2003-2004	Çankaya Municipality Arman Talay Sports Center, Ankara	Assistant Karate Do Trainer
2003 August	HİDROMEK	Intern Student
2003-2004	METU Mechanical Engineering Dept.	Student Assistant
2002 August	ASELSAN	Intern Student

### FOREIGN LANGUAGES

Fluent English, Elementary German

### SELECTED PUBLICATIONS

Akgün, Y., Gantes, C.J., Kalochairetis, K.E. and Kiper, G., A novel concept of convertible roofs with high transformability consisting of planar scissor-hinge structures, *Engineering Structures*, 32(9), 2010, 2873-2883.

Kiper, G., Söylemez, E., and Kişisel, A.U.Ö., A family of deployable polygons and polyhedra, *Mechanism and Machine Theory*, 43(5), 2008, 627-640.